Preparation and application of RTIL membranes

Song, Ting

Publication date:
2019

Document Version
Publisher's PDF, also known as Version of record

Preparation and application of RTIL membranes

Ting Song
PhD Thesis
2019

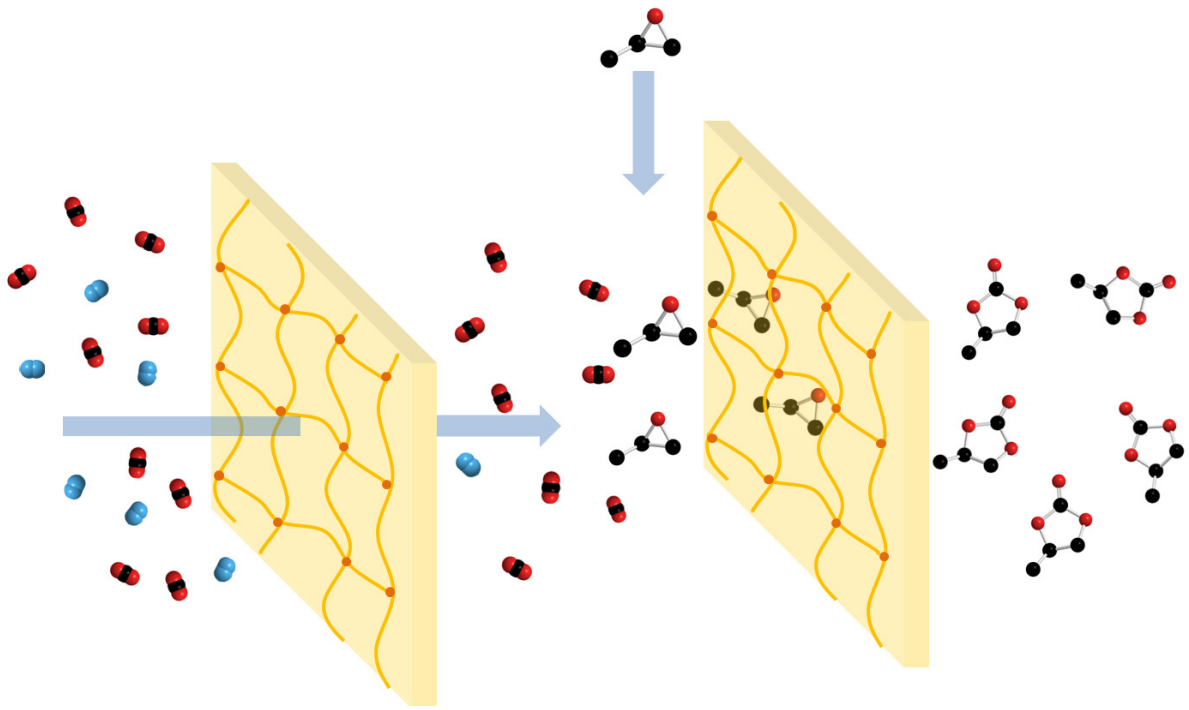

DTU Chemical Engineering
Technical University of Denmark

Preparation and application of RTIL membranes

Ting Song

Supervisors:

Assoc. Prof. Peter Szabo

Assoc. Prof. Anders E. Daugaard

Prof. Suojiang Zhang

Prof. Xiangping Zhang

PhD thesis

Jan. 2019

PhD Thesis

2019

Published by: DTU, Department of Chemical and Biochemical Engineering, Søltofts Plads, Building 229, 2800 Kgs. Lyngby Denmark

www.kt.dtu.dk

Preface

This thesis is the result of my PhD project conducted at the Danish Polymer Centre (DPC), Department of Chemical and Biochemical Engineering (KT), Technical University of Denmark (DTU) and Institute of Process Engineering (IPE), Chinese Academy of Sciences, between November 2015 and January 2019. This project was financed by both DTU and IPE.

First of all, I would like to thank my supervisors, Associate Prof. Peter Szabo and Prof. Suojiang Zhang (IPE), for giving me the chance to play a role in the great cooperation between KT and IPE. Meanwhile, I highly appreciate supervisors Anders E. Daugaard and Prof. Xiangping Zhang for giving me so much guidance, advice, support and patience, which made my PhD life much easier. Anders, thank you for standing by my side throughout – you really helped me a lot.

Additionally, I would link to thank Prof. Liyuan Deng, who gave me a chance to work in her group for one month at Department of Chemical Engineering, Norwegian University of Science and Technology (NTNU), thus helping me to get my manuscript published successfully.

I would like to thank my cooperators, PhD student Xianglei Meng and Zhibo Zhang, for supporting and encouraging me. We did nice work together.

I am also highly grateful to my colleagues at DPC for the positive working environment and their company. It was tough to begin a new life in a country with which I was completely unfamiliar, but because of you I was very happy. It was my pleasure to be with you, and especially Liyun Yu and Peter Jeppe Madsen are thanked for their help with the sample characterisation.

Finally, I would like to thank my parents for their love and support. I would also like to thank the members of student union of IPE at KT for their company and encouragement. A special thank you goes to my boyfriend, Zhanjun Xia, for his love, sustenance, patience and understanding.

Ting Song

January 2019

Kgs. Lyngby, Denmark

Abstract

The massive emission of CO_2 makes it extremely important to improve technology relating to CO_2 capture and usage (CCU). Among the numerous CO_2 capture methods, membrane technology is one of the most attractive, because of its easy operation, low price, low energy consumption and small footprint. Room temperature ionic liquids (RTILs), as outstanding CO_2 absorbents, were combined in this thesis with membrane technology, including mixed matrix membranes (MMMs), poly(RTIL) modified commercial PSf membranes and free-standing cross-linked poly(vinylimidazole-co-butyl acrylate) (poly(VIm-co-BuA)) membranes.

First, magnetic porous particles, ZIF-8@SiO_2@Fe_3O_4, were prepared to form MMMs under magnetic field conditions. It was expected that the ordered porosity and space between the polymer and particles would induce an improvement in CO_2 separation performance. Meanwhile, neat polyvinylidene fluorid (PVDF) membranes were cast with different methods, and RTIL monomers were synthesised in order to prepare poly(RTIL) membranes. However, both PVDF and poly(RTIL) membranes could not be formed, so free-standing poly(RTIL) membranes were prepared thereafter and used for CO_2 separation in this thesis.

Second, the commercially available polysulfone (PSf) ultrafiltration membrane was modified with poly(RTILs) via surface initiated atom transfer radical polymerisation (SI-ATRP), which gave a range of membranes used for CO_2 separation and water treatment. The water flux of a series of modified membranes was tested instead of CO_2 separation, since the modified membranes were unsuitable for gas separation. The results showed that the water flux of PSf membranes increased 1.8-3.5 times after modification, which made them great candidates for water treatment. The protein rejection performance of modified PSf membranes was investigated, which showed that the modified PSf membrane showed good potential for use as a protein rejection membrane.

Third, in order to prepare a free-standing poly(RTIL) membrane, vinylimidazole and butyl acrylate were copolymerised as a poly(VIm-co-BuA) series with different VIm and BuA ratios of 63:37, 48:52 and 24:76. Free-standing poly(RTIL) membranes were formed by cross-linking poly(VIm-co-BuA) (24:76) with 1, 6-dibromohexane in one-pot reactions. Additionally, the poly(RTIL) membranes with different cross-linking degrees were obtained by ranging the ratio of cross-linker 1, 6-dibromohexane and blocking agent 1-bromobutane. The CO_2 separation performance of the series

of poly(VIm-co-BuA)-based poly(RTIL) membranes was measured with a single gas setup and showed improvement compared to analogous neat poly(RTIL) membranes.

Finally, since poly(RTILs) are used in many fields, it was attempted to extend the application of poly(VIm-co-BuA)-based poly(RTIL) membranes to catalytic systems for CO_2 conversion. The swelling property and CO_2 affinity of cross-linked poly(VIm-co-BuA) membranes made them excellent heterogeneous catalysts for CO_2 insertion to epoxides. The catalytic activity of these novel catalysts was therefore evaluated, and the reaction conditions were optimised in the last part of the thesis.

Resumé

Den massive udledning af CO_2 gør det meget vigtigt at forbedre teknologien for CO_2-fangst og -brug (CCU). Blandt de mange CO_2-indfangningsmetoder er membranteknologi en af de mest attraktive teknologier, fordi den er let at anvende, har en lav pris, et lavt energiforbrug og et lille fodaftryk. I denne afhandling blev rumtemperatur-ioniske væsker (RTILs) som udmærkede CO_2-absorberende stoffer kombineret med membranteknologi, herunder blandede matrixmembraner (MMMs), poly (RTILs) modificerede kommercielle PSf-membraner og fritstående tværbundne poly (vinylimidazol-cobutyl-acrylat) (poly (VIm-co-BuA)) membraner.

For det første blev magnetiske porøse partikler ZIF-8@SiO_2@Fe_3O_4 fremstillet til dannelse af MMM'er under magnetfelt. Det var forventet, at den ordnede porøsitet og mellemrummet mellem polymer og partikler kunne lede til en forbedring af CO_2-separationsydelsen. Endvidere blev rene polyvinylidenfluorid (PVDF) membraner støbt med forskellige metoder, og RTIL-monomerer blev syntetiseret til fremstilling af poly (RTIL) membraner. Imidlertid kunne både PVDF- og poly (RTIL) membraner ikke dannes. Derfor blev fritstående poly(RTIL) membraner fremstillet efterfølgende og anvendt til CO_2-separation i denne afhandling.

For det andet blev kommercielt tilgængelige polysulfon (PSf) ultrafiltreringsmembraner modificeret med poly (RTILs) via overfladeinduceret atomoverføringsradikalpolymerisation (SI-ATRP), som resulterede i en række membraner som blev anvendt til CO_2-separation og vandbehandling. Vandstrømningen gennem serier af modificerede membraner blev testet i stedet for CO_2-adskillelse, da de modificerede membraner ikke var egnede til gasadskillelse. Resultaterne viste, at vandfluxen af PSf-membraner steg 1,8-3,5 gange efter modifikation, hvilket gjorde dem til gode kandidater til vandbehandling. Proteinafstødningsydelsen af modificerede PSf-membraner blev undersøgt, hvilket viste at den modificerede PSf-membran havde potentiale til anvendelse som proteinafstødningsmembran.

For det tredje blev vinylimidazol og butylacrylat copolymeriseret som en serie af poly (VIm-co-BuA) med forskellige VIm- og BuA-forhold på 63:37, 48:52 og 24:76 for at fremstille fritstående poly (RTILs) membraner. Fristående poly (RTIL) membraner blev dannet ved tværbinding af poly (VIm-co-BuA) (24:76) med 1,6-dibromhexan i "one-pot" reaktioner. Derudover blev poly (RTIL) membraner med forskellige tværbindingsgrader opnået ved at justere forholdet mellem tværbinder 1, 6-dibromhexan og blokeringsmiddel 1-brombutan. CO_2-separationsydelsen af serien af poly (VIm-

co-BuA) -baserede poly (RTIL) membraner blev målt med en enkeltgasopsætning og viste forbedring sammenlignet med analoge fine poly (RTIL) membraner.

Endelig, da poly (RTILs) anvendes på mange felter, blev det forsøgt at udvide anvendelsen af poly (VIm-co-BuA) -baserede poly (RTIL) membraner til katalytiske systemer til omdannelse af CO_2. Svulmeegenskaben og CO_2-affiniteten af tværbundne poly (VIm-co-BuA) membraner gjorde dem til fremragende heterogene katalysatorer for CO_2-cykloaddition til epoxider. Den katalytiske aktivitet af disse nye katalysatorer blev derfor evalueret, og reaktionsbetingelserne blev optimeret i den sidste del af afhandlingen.

.

Contents

Abbreviations and symbols

^{1}H NMR	^{1}H Nuclear magnetic resonance
AIBN	2,2´-azobis(isobutyronitrile)
ATRP	Atom transfer radical polymerisation
BET	Brunauer emmett teller
BSA	Bovine serum albumin
BuA	Butyl acrylate
BMIM	1-butyl-3-methylimidazolium
CCS	CO_2 capture and storage
CCU	Carbon capture and usage
CF	Conventional filtration
CRP	Controlled radical polymerisation
DMF	N,N-dimethyl formamide
DMSO	Dimethyl sulfoxide
DSC	Differential scanning calorimetry
FTIR	Fourier transform infrared
GC	Gas chromatography
GPC	Gel permeation chromatography
MF	Microfiltration
MMMs	Mixed matrix membranes
MOFs	Metal organic frameworks
M_w	Weight average molecular weight
M_n	Number average molecular weight
n-BuLi	n-butyllithium
NF	Nanofiltration
Pebax	poly (amide-6-b-ethylene oxide)
PEG	Poly (ethylene glycol)
Poly(RTILs)	Poly(room temperature ionic liquids)
PSf	Polysulfone
PVDF	Polyvinylidene fluoride
RO	Reverse osmosis

RTILs	Room temperature ionic liquids
SLMs	Support liquid membranes
SILMs	Support ionic liquid membranes
SI-ATRP	Surface initiated atom transfer radical polymerisation
TEM	Transmission electron microscope
TEOS	Tetraethoxysilane
Tf_2N	Bis(trifluoromethanesulfonyl)imide
T_g	Glass transition temperature
TGA	Thermo gravimetric analysis
TSILs	Task-specific ionic liquids
UF	Ultrafiltration
VIm	N-vinylimidazole
WCA	Water contact angle
XPS	X-ray photoelectron spectroscopy
XRD	X-ray diffraction
ZIF	Zeolitic imidazolate frameworks

1 Objectives and outline

1.1 Objectives

CO_2 emissions hit 35 billion tons worldwide in 2014, and this figure has continued to rise ever since. CO_2 concentration in the air sat at around 410 ppm in 2018, whereas it was 310 ppm in 1960. CO_2 is considered as one of the strongest contributors to environment sustainability, and so it is necessary to improve the technology employed for its capture and usage (CCU). For the case of CO_2 separation over the past few decades, the methods used in industrial applications include pressure swing adsorption, amine absorption and cryogenic distillation; however, they all suffer from high energy consumption. On the contrary, membrane technology possesses unique properties, including easy operation, economy, a small footprint and low energy consumption. According to previous investigations, room temperature ionic liquids (RTILs) possess excellent CO_2 affinity, which makes them great candidates as absorbents. In order to overcome the shortcomings of RTILs, such as high viscosity and price, they have been combined with membrane technology since the beginning of this century. RTIL gas separation membranes have been developed from supported ionic liquid membranes (SILMs) to poly(room temperature ionic liquids) (poly(RTILs)) membranes, and then mixed matrix membranes (MMMs). At the same time, CO_2 is also the most abundant, nontoxic and renewable carbon resource, which makes it worthwhile expending effort to invest in its utilisation. For instance, it has been used as feedstock to produce a range of valuable chemicals, among which the synthesis of cyclic carbonate has been commercially applied through CO_2 insertion to epoxides. To date, RTIL- and poly(RTIL)-based materials have been used widely as catalysts in CO_2 reactions, to get rid of metal coupling catalysts and co-catalysts. Inspired by the versatile application of RTILs, the main objective of this thesis is to prepare RTIL-based materials that can be used for both CO_2 separation and conversion.

1.2 Outline

RTILs, the importance of CO_2 capture and the background to gas separation membranes are introduced in *Chapter 2*.

Several kinds of membranes were prepared in this thesis, including mixed matrix membranes (MMMs), poly(RTILs) modified commercial PSf membranes and free-standing poly(RTIL) membranes. MMMs are investigated in *Chapter 3*, where magnetic ZIF-8 was prepared for

introduction in polymer matrix, such as PVDF and poly(RTILs), so that tunable channels of porous particles could be formed under a magnetic field.

The commercial polysulfone (PSf) membrane was modified with poly(vinylimidazole) (poly(VIm)) and imidazole-based poly(RTILs), as presented in *Chapter 4*. The water flux and protein rejection capability of both original and modified PSf membranes were tested instead of CO_2 separation performance.

Generally, imidazole-based poly(RTIL) are too brittle to form free-standing membranes. In order to get rid of the porous supporting membrane, the copolymer of VIm and butyl acrylate (BuA) poly(VIm-co-BuA) was cross-linked with 1, 6-dibromohexane via a one-pot reaction to form free-standing poly(RTIL) membranes, as described in *Chapter 5*, and the CO_2 separation performance of the prepared free-standing membranes was evaluated accordingly.

In *Chapter 6*, different kinds of cross-linked poly(VIm-co-BuA) membranes were prepared and ground into small particles, following which they were used as catalysts for the CO_2 insertion epoxide reaction that made the poly(RTIL) membranes into bifunctional materials. The reaction conditions were optimised as well.

The overall conclusion and outlook can be found in *Chapter 7* and *Chapter 8*, respectively. Whereas *Chapter 9* contains the experimental details of the unpublished work.

The work presented in this thesis is based on the following publication:

Publication 1 (see Appendix 1)

Song, T.; Deng, J.; Deng, L.; Bai, L.; Zhang, X.; Zhang, S.; Szabo, P.; Daugaard, A. E. Poly(Vinylimidazole-Co-Butyl Acrylate) Membranes for CO_2 Separation. *Polymer*. **2019**, *160*, 223–230.

Additionally, the work included in this thesis was presented at different conferences, including:

1) Song, T.; Zhang, X.; Zhang, S.; Szabo, P.; Daugaard, A. E. The study of the preparation and CO_2 separation performance of ionic liquid-based membranes. Annual Polymer Day, Kgs. Lyngby, Denmark, November 2016 (Talk)

2) Song, T.; Zhang, X.; Zhang, S.; Szabo, P.; Daugaard, A. E. The modification of PSf membranes with ionic liquids used for CO_2 separation. DTU Kemiteknik-Research Day, Kgs. Lyngby, Denmark, August 2017 (Poster)

3) Song, T.; Zhang, X.; Zhang, S.; Szabo, P.; Daugaard, A. E. Synthesis of poly(RTIL) membranes for CO_2 separation. Annual Polymer Day, Kgs. Lyngby, Demmark, November 2017 (Talk)

4) Song, T.; Zhang, X.; Zhang, S.; Szabo, P.; Daugaard, A. E. Poly(ionic liquid) membranes for CO_2 separation from N_2. Nordic Polymer Days, Copenhagen, Denmark, May 2018 (Poster)

5) Song, T.; Zhang, X.; Zhang, S.; Szabo, P.; Daugaard, A. E. Poly(Vinylimidazole-Co-Butyl Acrylate) Membranes for CO_2 Separation. DTU Kemiteknik-Research Day, Kgs. Lyngby, Demmark, August 2018 (Video)

6) Song, T.; Deng, J.; Deng, L.; Bai, L.; Zhang, X.; Zhang, S.; Szabo, P.; Daugaard, A. E. Poly(Vinylimidazole-Co-Butyl Acrylate) Membranes for CO_2 Separation. DPC seminar, Kgs. Lyngby, Demmark, December 2018 (Talk)

2 Background

2.1 Room temperature ionic liquids

Room temperature ionic liquids (RTILs), which contain large and nonsymmetrical organic cations and organic or inorganic anions, are molten salts at temperatures below 100 °C.[1] RTILs emerged at the end of the last century, and they attracted more and more interest in the following years due to their excellent chemical, thermal and electrochemical stability, non-flammability and negligible volatility.[2][3] Initially, RTILs were used as solvents to overcome the disadvantages of common solvents, which have a relatively narrow liquidus region.[4] In the past two decades, RTILs have become popular in many fields, such as for batteries[5], in extractions[6], as catalysts[7] and for separation[8]. The common cations of RTILs include imidazolium (Fig. 2-1 a), ammonium (Fig. 2-1 b), pyrrolidinium (Fig. 2-1 c), pyridinium (Fig. 2-1 d) and tetra alkylphosphonium (Fig. 2-1 e). Task-specific ionic liquids (TSILs) can be obtained by ranging the R group equipped with different functional groups. Additionally, anions (X^-) can range from inorganic to organic groups, such as halides, mineral acid anions, bis(trifluoromethanesulfonyl)imide (Tf_2N^-), etc. The large selection of possible counterions, being cationic or anionic as well as hydrophilic/hydrophobic, endows RTILs with tunable properties to match different applications.

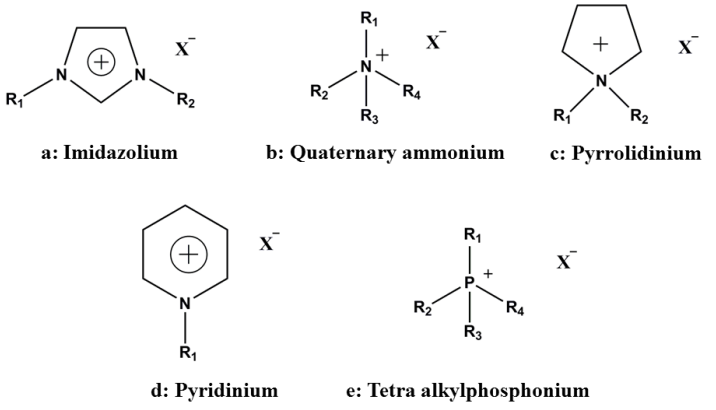

Fig. 2-1 The main classification of ionic liquid.

It was found for the first time in 2001 that RTILs have good affinity to CO_2, which makes them promising candidates as absorbents.[9][10] Since then, more and more researchers have paid attention to investigating RTILs used for CO_2 separation (as shown in Fig. 2-2). It has been proven

that both cations and anions have an influence on the solubility of CO_2 in RTILs, and RTILs with imidazole as a cation have an outstanding ability to grab CO_2 rather than other gases, such as CH_4 and N_2.[11][12] Nevertheless, the alkyl chain length of RTILs is also a main factor affecting CO_2 solubility, which increases in line with increasing alkyl chain length.[13][11] Furthermore, the solubility of CO_2 in typical RTILs can be increased by introducing functional moieties, such as amine[14] and ether groups[15][16], to form TSILs. In the case of the influence of anions, it has been investigated that they possess stronger effects than those of cations.[12][17][18] Apart from the halogen alternative, anions commonly used for CO_2 capture are known as Tf_2N^-, BF_4^- and PF_6^-.[19][20][21] However, the industrial application of RTILs has been limited, due to their high viscosity, price and liquid morphology.[22]

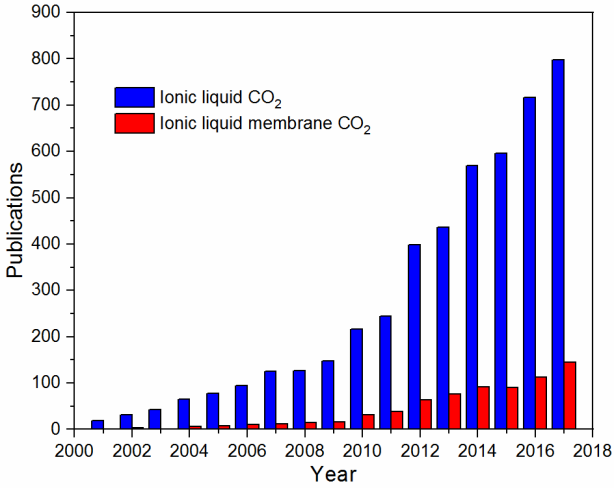

Fig. 2-2 Publication numbers per year from year 2001 to 2017.

2.2 CO_2 separation

As we all know, CO_2 is the largest contributor to global warming, and so it is highly important to make efforts to counter climate change, such as by improving power efficiency, using clean energy and developing CO_2 capture and usage (CCU) technologies. In the case of capturing CO_2 (emission from fuel combustion), the main method can be divided into three classifications, namely 1) pre-combustion, 2) oxyfuel combustion and 3) post-combustion. Nowadays, CO_2 separation technology is considered as a potential method to reduce the emission of CO_2, which is commonly found in natural gas streams (pre-combustion), biogas (pre-combustion), flue gas (post-combustion) and products related to coal gasification (post-combustion).[23] The main methods employed to

separate CO_2 include absorption, adsorption, cryogenic distillation and membrane separation.[24] Among them, membrane separation technology has potential, due to its unique properties. It has developed over the past 40 years and been spread widely across many fields, including gas separation[25], catalysts[26], batteries[27] and water treatment[28]. Membranes are potential materials because of their easy operation, favourable cost, small footprint and low energy consumption.[29] There are numerous categories of membranes for different applications, ranging from inorganic membranes to organic membranes, but they are also combined with other kinds of materials (such as MOFs, graphene and nanotubes) or compounds (such as RTILs) to improve their performance.

In this thesis, RTILs and membrane technology were combined and used for CO_2 separation from N_2 and CH_4. Considering both the advantages and the disadvantages of membranes and RTILs, their combination has drawn more and more attention recently. Table 2-1 provides information on the three main types of RTIL membranes used for CO_2 separation: SILMs (supported ionic liquid membranes), poly(RTIL) membranes and MMMs (mixed matrix membranes).

Table 2-1 Comparison of different membrane classifications used for CO_2 separation.

Classification	Composition commonly	Preparation	Drawbacks	Benefits
SILMs	Porous polymer membranes (usually commercial) + RTILs	Impregnation	Unstable under high pressure	High gas permeability
Poly(RTIL) membranes	RTILS monomer + free RTILs	RTILs monomer directly as membrane	Brittle to form freestanding membrane	Immobilised RTILs, stable; Free RTILs improve performance
MMMs	Polymer + RTILs + inorganic fillers	Dissolve all the components together and cast	Dense membrane with lower gas permeability	More stable than SILMs, easily prepared

2.2.1 Supported ionic liquid membrane

Initially, RTILs were used in supported liquid membranes (SLMs), where commercially available porous membranes were filled with a range of liquids by weak capillary forces. The liquid-phase absorbents in traditional SLM membranes used for CO_2 separation were amine-based aqueous solvents (such as diethylenetriamine (DETA), triethylene glycol (TEG), diaminoethane (DAE) and diglycolamine (DGA), and these were used as industrial CO_2 absorbents.[30] However, traditional SLMs suffered from liquid-phase loss, mainly because of the evaporation of aqueous solvents. Due to the non-evaporating feature and CO_2 absorption capacity of RTILs, they were chosen as potential candidates to replace volatiles to form SILMs, which in turn had good CO_2 separation performance

with ideal CO_2 permeabilities of more than 2,000 Barrers and CO_2/N_2 permselectivity of more than 20.[31] After all, the loss of RTILs through leakage from the membrane support at high pressures still cannot be ignored,[32] since RTILs were immobilised in porous membranes with weak capillary forces. This instability of SILMs has limited their industrial application, even though they have shown promising CO_2 separation performance.[21]

2.2.2 Poly(room temperature ionic liquids) membranes

Poly(room temperature ionic liquids) (Poly(RTILs)), which consist of a polymer backbone and ionic liquid as repeat units, were synthesised to immobilise RTILs. Poly(RTILs) not only combine both polymer and RTIL properties, but they also provide new properties and possibilities,[10] thus making them a new class of polymeric material. Therefore, poly(RTILs) extend the application space of RTILs; for instance, they are potential candidates as heterogeneous catalysts.[7] In another example, poly(RTILs) as solid polyelectrolytes avoid the disadvantages associated with liquid electrolytes, which are difficult to shape and leak easily in battery and fuel cell areas.[11]

In order to overcome the shortcomings of SILMs, Noble et al.[21][33] polymerised RTIL monomers with acrylic-, styrenic- or vinyl imidazole-based backbones on porous support membranes to form stable poly(RTIL) membranes for gas separation. These membranes possess mechanical stability and efficiently immobilise RTILs in contrast to SILMs, albeit they do exhibit much lower gas permeability and diffusivity, which is attributed to a lower fractional free volume of the dense poly(RTIL) compared to that of free RTILs.[22] Combinations of poly(RTILs) and RTILs in composite membranes improved CO_2 permeability by 400% relative to neat poly(RTIL) membranes, due to the introduction of free RTILs. Commonly, the introduction of RTILs influences diffusivity more than solubility, since the added free RTIL acts as a plasticiser, which subsequently greatly decreases T_g and enhances chain mobility at the same time. Furthermore, RTILs and poly(RTIL) matrixes are combined by strong ion-ion attractive interactions, which makes the poly(RTIL)-RTIL composite membranes stable enough to withstand high temperatures.[34]

Imidazole-based poly(RTILs) are generally too brittle to form free-standing membranes and therefore need the support of porous polymer membranes. Recently, new types of poly(RTIL) membranes have been reported. Poly(RTILs) have been combined with polymers, which possess excellent mechanical properties, such as polyimides,[35][36] polybenzimidazoles,[37][38] polyesters,[39] polyethersulfones[40] and polyurethane,[41] to form novel and flexible poly(RTIL) membranes through condensation polymerisation or polymer modification.[42]

2.2.3 Mixed matrix membranes

As well as poly(RTILs), RTILs have also been combined with other kinds of polymers, such as the commercially available polymers poly(ethylene glycol) (PEG) [43], Pebax[44], polyvinylidene fluorid (PVDF) [45] and so on, or specially synthesised copolymers. Generally, the introduction of RTILs in polymers offers a means of improving the gas separation performance of neat polymeric membranes, due to the CO_2 affinity of RTILs. In addition, the introduction of porous materials and nanoparticles, such as MOFs[46], zeolites[47], carbon nanotubes[48] and graphene oxide,[48] is also an efficacious way to increase gas permeability.[17][49] Systems with inorganic filler in mixed matrix membranes (MMMs) possesses relatively higher gas diffusion coefficients compared to polymers.[50] The gap between the polymer matrix and inorganic filler provides space for gas to pass through; however, the void not only increases CO_2 permeability, but it also decreases gas pair selectivity. To overcome such problems, as well as modifying the inorganic filler, researchers have also introduced RTILs into the polymer matrix as well as on the surface of solid fillers. On the one hand, the introduced RTILs increase CO_2 solubility in the polymer matrix, whilst on the other hand, RTILs on the surface of inorganic particles fill up the interfacial void between the polymer matrix and inorganic fillers.[51] For instance, Noble RD and his coauthors [52] introduced both zeolite SAPO-34 and RTILs [emim][Tf_2N] into the poly(RTIL) membranes, which increased CO_2 permeability from 13.9 Barrers of poly(RTIL) membrane with zeolite to 72 Barrers of poly(RTIL) membrane, with both zeolite and RTILs and CO_2/N_2 selectivity, from 35 to 40.

For MMMs, there are three variables, namely a polymer matrix, solid fillers and RTILs, that can be chosen to improve gas separation performance further. Additionally, each of them possesses a large tunable space.

2.2.4 Polymeric membrane gas transportation mechanism

The mechanism for transporting gas through polymer membranes is known to follow a solution-diffusion model, which is commonly used to describe the transportation of gas, vapour, ion or liquid in dense membranes.[53][54] The premise behind this model is that there are no pores in membranes, and so the realisation of separation is due to the different levels of solubility and diffusivity of a variety of species in the membrane.[48] In the case of gas separation, first, gas molecules upstream of membranes dissolve in the membrane; second, gas molecules diffuse through the membrane and then desorb from the membrane downstream.

2.2.5 Gas separation performance evaluation

There are two kinds of equipment available to evaluate gas separation performance: one of them is used for testing solitary gas (single gas set-up), which was used in this thesis, and the other one is used for testing mixed gas (mixed gas set-up). The testing mechanism for both options is actually the same, but the analysis method is different. The single gas set-up is shown in Fig. 2-3. In detail, gases are fed separately into a membrane cell (containing membrane) at a desired pressure, gas molecules are then subsequently dissolved and diffused in the membrane, and then the membrane is disposed of downstream, which was vacuumed at the beginning. The pressure of gas in the downstream can be tested with a pressure meter, and then gas permeability, P (Barrer=10^{-10} cm^3 (STP) cm s^{-1} cm^{-2} cm Hg^{-1}), can be calculated by equation 2-1):

$$P = \frac{dp}{dt} \times \frac{V}{A} \times \frac{T_0}{p_0 T} \times \frac{l}{p_1 - p_2} \quad (2\text{-}1)$$

where dp/dt (Pa s^{-1}) is the steady-state pressure increase in time t, V (cm^3) is downstream volume, A (cm^2) represents the effective membrane area, T (K) is the temperature, l (cm) refers to the thickness of a membrane and T_0 and p_0 are the temperature and pressure in standard conditions, i.e. 273.15 K and 1.0133 ×10^5 Pa, respectively.

The relationship between the P, D (cm^2 s^{-1}) and solubility (S) (cm^3 (STP) cm^{-3} cm Hg^{-1}) of the gas in the polymer membrane is described in eq. 2-2): [33]

$$P = S \times D \quad (2\text{-}2)$$

The single gas diffusivity coefficient can be calculated from eq. 2-3), in which "θ" represents "time-lag":

$$D = \frac{l^2}{6\theta} \quad (2\text{-}3)$$

The ideal level of selectivity, $\alpha_{i/j}$, was calculated by the ratio of species permeability, shown as eq. 2-4):

$$\alpha_{i/j} = \frac{P_i}{P_j} \quad (2\text{-}4)$$

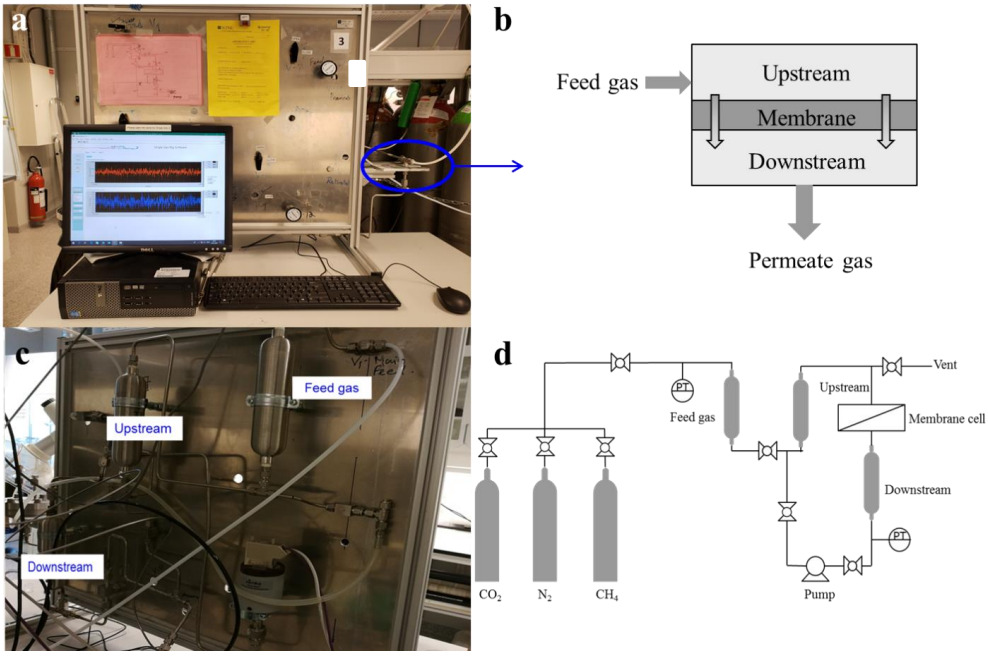

Fig. 2-3 Schematic diagram of the experimental rig set-up used in this project: set-up appearance (a), membrane cell detail (b) and pipeline detail (c and d).

The gas separation process involved in the mixed gas set-up can be described thus: replace the pure feed gas with a mixed gas containing a target gas pair with a specific component, following which gas chromatography (GC) is used to analyse the composition of the permeate gas.

2.2.6 Robeson upper bounds

To improve membrane separation technology, it is significant to use and develop polymers with high permeability in terms of more permeable gas (P_i) and high gas pair selectivity ($\alpha_{i/j}$).[55] For polymeric membranes, it has been found that an increase in P_i usually leads to a decrease in $\alpha_{i/j}$ based on numerous previous investigations. In 1991, Robeson derived Robeson upper bounds, plotted as log $\alpha_{i/j}$ versus log P_i, which showed for the first time the limitations of $\alpha_{i/j}$ for the corresponding P_i according to data from more than 300 references. The 1991 Robeson upper bounds illustrate the trade-off relationship between gas pairs, including H_2/N_2, H_2/CH_4, CO_2/CH_4, He/H_2, He/CH_4, He/O_2, H_2/O_2, He/N_2 and O_2/N_2.[55] In the following decades, many new membrane materials were investigated and found to reach and exceed the empirical Robeson upper bound. Therefore, Robeson revised an upper bound in 2008.[56] Another significant gas pair,

CO_2/N_2, was also included in the 2008 Robeson upper bound. Fig. 2-4 shows the 2008 Robeson upper bounds of CO_2/N_2 and CO_2/CH_4 as well as the corresponding performance of RTIL-based membranes.

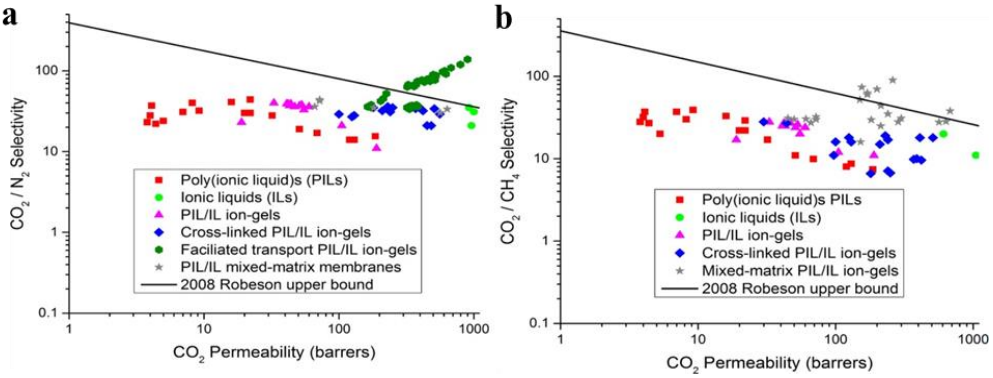

Fig. 2-4 The 2008 Robeson upper bound for the CO_2/N_2 gas pair (a) and CO_2/CH_4 gas pair (b). [57] (Reproduced with permission of ACS Inc. and further permissions related to the material excerpted should be directed to the ACS.)

The 2008 Robeson upper bounds are therefore used as a reference to evaluate the comprehensive performance of polymeric gas separation membranes. The target of the gas separation field is to move beyond the limitation of the 2008 Robeson upper bounds, thereby increasing opportunities for industrialisation.

3 Mixed matrix membranes for CO_2 separation

As mentioned, mixed matrix membranes (MMMs) are one of the main kinds of RTIL-based CO_2 separation membranes, and they usually consist of polymer, inorganic or organic porous filler and RTILs. Furthermore, they possess a number of advantages, such as ease of fabrication, tunability and excellent gas separation properties. Briefly, MMMs can be prepared by solution-casting a mix of polymer, filler and free RTILs, which is why they were investigated at the beginning of this PhD study. The porosity and the space between polymers and porous nanoparticles provide more space for gas transportation; hence, the idea of this chapter is to order the magnetic nanoparticle filler in the membrane with the help of a magnetic field, so that gas permeability will be improved further. This chapter is based on unpublished experiments, and the experimental details can be found in Chapter 9.

3.1 Preparing the magnetic filler

The addition of porous fillers is an efficient way to improve the gas permeability of membranes. A magnetic porous filler was chosen in this study, since we expected that it could be ordered under a magnetic field while the membrane was being formed. Such ordered porous fillers would provide a fractional free-volume channel, which is known to be beneficial for gas transportation[58] and thus improve gas permeability further.

Among the numerous kinds of porous particles, ZIF-8, which is one of the more well-known metal organic frameworks (MOFs) used widely in gas separation membranes, was selected as the base structure of the magnetic filler. Ji et al. (2015) reported the synthesis of a new magnetic material named ZIF-8@SiO_2@Fe_3O_4 (shown in Fig. 3-1),[59] the particles of which were synthesised by encapsulating SiO_2@Fe_3O_4 particles, which provided the magnetic property, into ZIF-8. It was then used as the catalyst for a Knoevenagel reaction of p-chlorobenzaldehyde. The magnetic and porous properties of ZIF-8@SiO_2@Fe_3O_4 attracted our attention, and its particles were synthesised following the published procedure.

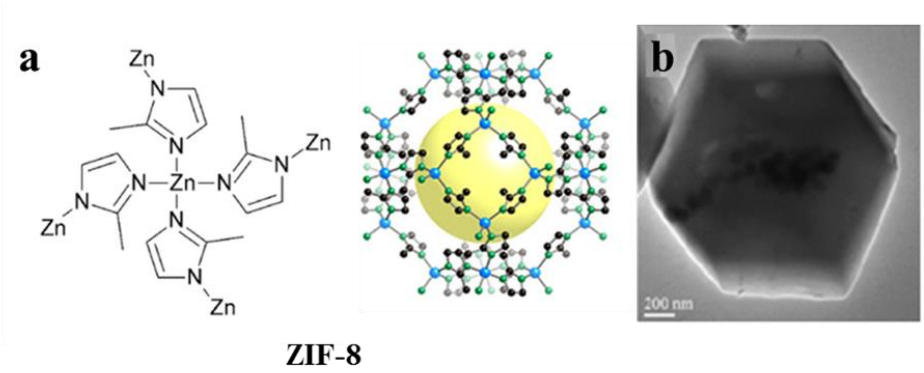

Fig. 3-1 Chemical structure of ZIF-8 (a) [60] (Reproduced with permission of Elsevier B.V, Inc.) [48] (Reproduced with permission of ACS Inc. and further permissions related to the material excerpted should be directed to the ACS.); The ZIF-8@SiO_2@Fe_3O_4 as synthesised in the literature (b).[59] (Reproduced with permission of Elsevier B.V, Inc.)

First of all, ZIF-8 (as shown in Fig. 3-1a) was synthesised and characterised with TEM, FT-IR, N_2 adsorption measurements and XRD. The morphology of synthesised ZIF-8 is shown in Fig. 3-2 a, which shows that it is approximately 80 nm in size. Fig. 3-3 exhibits the FT-IR spectrum of ZIF-8, C=C-H stretching vibration at 3131 cm^{-1} and peaks at 1582 cm^{-1}, 1458 cm^{-1} and 1414 cm^{-1}, representing the C=N stretching vibration. Plane vibration of the imidazole ring is shown at 1306 cm^{-1} and 1178 cm^{-1}. The N_2 adsorption/desorption measurement was tested, and the adsorption/desorption curve, which is shown in Fig. 3-4, exhibited type-I adsorption behaviour. According to the measurement, the BET surface area is 1623.46 m^2/g and the Langmuir surface area is 2242.06 m^2/g. What is more, the pore diameter and volume of ZIF-8 are 25.6 nm and 0.72 cm^3/g, respectively.

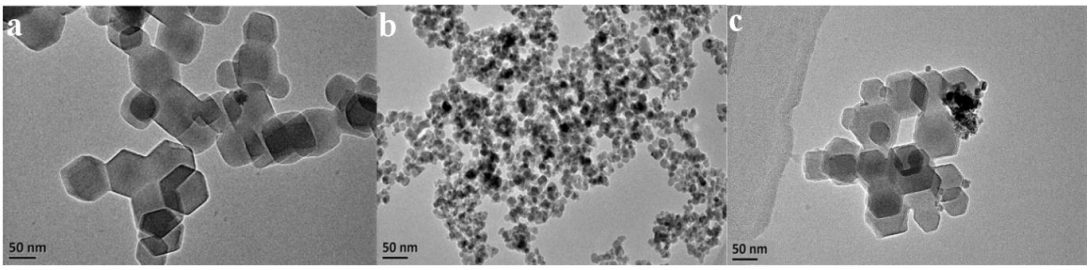

Fig. 3-2 TEM image of synthesised ZIF-8 (a), SiO_2@Fe_3O_4 (b) and ZIF-8@SiO_2@Fe_3O_4 (c).

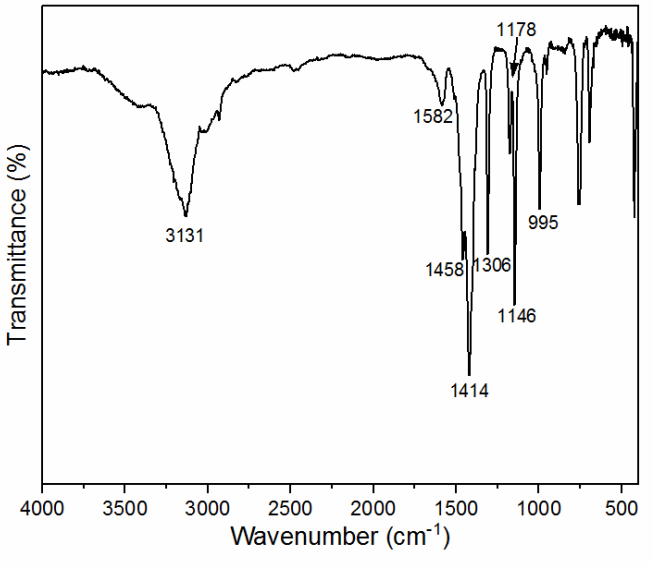

Fig. 3-3 FTIR spectrum of synthesised ZIF-8.

The crystal structure of the prepared ZIF-8, SiO_2@Fe_3O_4 and ZIF-8@SiO_2@Fe_3O_4 was confirmed with powder X-ray diffraction (XRD) (shown in Fig.3-5). There are obvious diffraction peaks of pure ZIF-8 at 2θ = 7.42 (011), 10.39 (002), 12.79 (112), 14.75 (022), 16.51 (013) and 18.08 (222), which is consistent with reported literature data,[60] thereby indicating the crystal structure of ZIF-8.

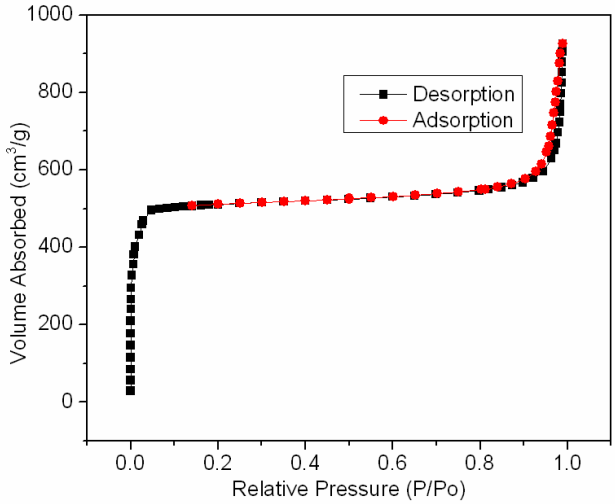

Fig. 3-4 N_2 adsorption/desorption isotherms of ZIF-8.

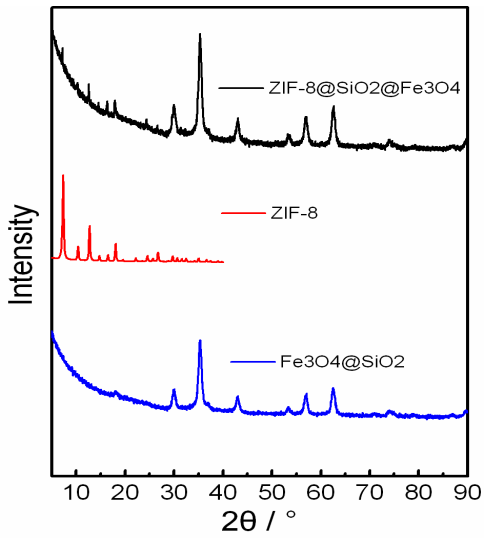

Fig. 3-5 XRD of prepared ZIF-8, SiO_2@Fe_3O_4 and ZIF-8@SiO_2@Fe_3O_4.

SiO_2@Fe_3O_4 and ZIF-8@SiO_2@Fe_3O_4 were prepared according to Ji et al. (2015)'s work.[59] TEM images of SiO_2@Fe_3O_4 and ZIF-8@SiO_2@Fe_3O_4 are shown in Fig. 3-2 b and c, and it is clearly evident that the ZIF-8@SiO_2 particles are not encapsulated in ZIF-8, albeit the XRD spectrums of SiO_2@Fe_3O_4 and ZIF-8@SiO_2@Fe_3O_4 are consistent with the reported literature.

3.2 Polymer membrane preparation

3.2.1 Commercial polymer

Numerous kinds of commercially available polymers have been used as matrices for gas separation membranes, such as poly(vinylidene fluoride) (PVDF),[61] polyethylenimine (PEI),[62] polyimide (PI),[63] Pebax[64] and so on. PVDF was chosen as the membrane matrix in this study, because of its mechanical properties and CO_2 affinity. Furthermore, very few studies have reported on PVDF combined with RTILs and porous fillers used as CO_2 separation membranes, which therefore seemed attractive for this study.

The neat PVDF membranes were prepared via two different methods: solution casting (as shown in Fig. 3-6a) and knife coating (as shown in Fig. 3-6c). Briefly, the procedure for solution casting involves pouring the polymer solution into a glass mould with a certain size, following which the solvent evaporates at a constant temperature; knife coating is conducted by pouring the polymer solution onto the end of a glass plate with a desired width, then drawing the solution across the plate

with a height-tunable knife and then subsequently letting the solvent evaporate. Membranes prepared by solution casting are shown in Fig. 3-1b; it should be noted here that it was very difficult to obtain membranes with a nice appearance, even though the concentration of polymer solution was in the range of published methods. In contrast, the membranes obtained from the knife coating method look much more homogeneous and flatter, as illustrated in Fig. 3-6d. The gas permeability properties of membranes prepared by both methods were tested with a single gas set-up. Unfortunately, it transpired that the gas permeability of all of the membranes prepared in this study was too high, even though the membranes appear dense and homogeneous.

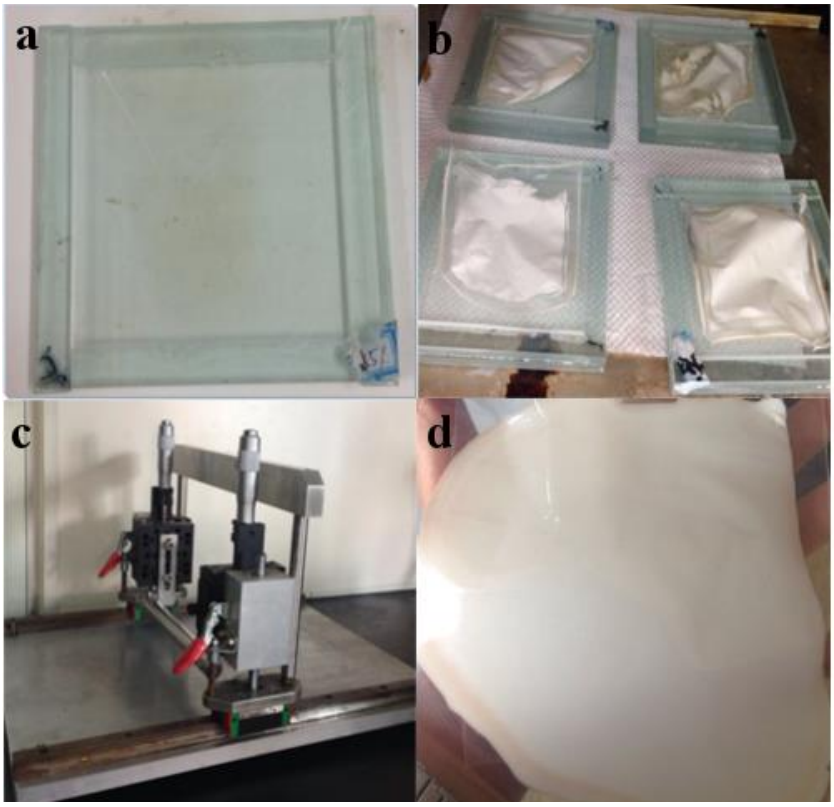

Fig. 3-6 Membrane casting mode (a); membrane obtained from solution casting (b); Membrane knife (c); membrane obtained from knife coating (d).

3.2.2 Synthesis of poly(room temperature ionic liquid)

As mentioned in Chapter 2, poly(RTIL) membranes have been investigated as gas separation membranes that can immobilise RTILs. Therefore, poly(RTILs) were treated as an alternative

polymer to PVDF in this study. Vinylimidazole-based RTILs monomers "a" and "b", the structures of which are shown in Fig. 3-1, were synthesised. Fig. 3-7 shows the ^{1}H NMR spectrum of the RTIL monomer "a".

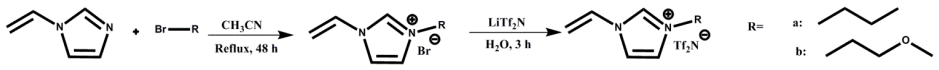

Scheme 3-1 The structures of the synthesised ionic monomers.

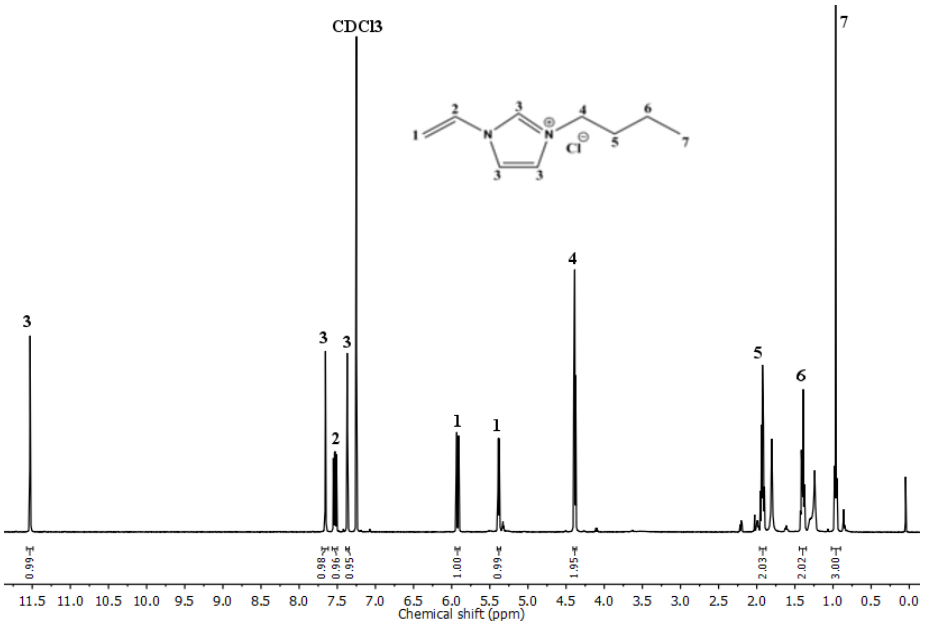

Fig. 3-7 ^{1}H NMR spectrum of RTIL monomer "a".

Usually, poly(RTIL) membranes are obtained by UV polymerisation of RTIL monomers on a porous matrix. The same method was employed in an attempt to prepare poly(RTIL) membrane with monomer "a" (as shown in Fig 3-7), but it failed due to lack of experience.

3.3 Concluding remarks

In order to improve further gas separation performance, we aimed at preparing novel MMM under a magnetic field, with the intention of providing ordered fractional free-volume channels. Porous ZIF-8@SiO_2@Fe_3O_4 particles with magnetic properties were prepared according to previous reports and then characterised accordingly. Unfortunately, ZIF-8@SiO_2@Fe_3O_4 particles could not be obtained in this instance. PVDF was expected to be a good candidate as a polymer matrix; however, neat

PVDF membranes prepared by different casting methods possess too high a level of permeability to be used as gas separation membranes. As a type of immobilised RTIL, Poly(RTILs) were also taken into consideration, and two kinds of RTIL monomers were synthesised. However, poly(RTIL) membranes could not be obtained by UV polymerisation.

4 Polysulfone membrane modification used for anti-fouling

The prepared PVDF membrane was not useful for gas separation, due to its extremely high gas permeability. Therefore, it was decided to use a commercial alternative for testing surface-bound poly(RTILs). It was expected that such membranes could be obtained from commercial membranes by chemical modification. Thus, poly(RTILs) were grafted onto the surface of a commercially available polysulfone (PSf) membrane via atom transfer radical polymerisation (ATRP). It was found that such modified membranes failed as gas separation membranes, and so the water flux of the initial PSf membrane and modified PSf membranes was tested in this study. The adapted membranes were considered for use as protein rejection membranes. This chapter is based on unpublished work, and the experimental details can be found in Chapter 9's experimental section.

4.1 Background

4.1.1 Introduction to the PSf membrane

PSf is an attractive polymer for forming membranes because of its outstanding properties, such as physical, chemical, thermal and mechanical stability.[65] Numerous PSf membranes have been prepared for gas and liquid separation, water treatment and fuel cell applications,[66][67] and many of them have already been commercialised, not only because of the pre-mentioned properties, but also due to their reasonable price. Fig 4-1 shows the sizes of common solutes and their corresponding filtration membranes, which include reverse osmosis (RO), nanofiltration (NF), ultrafiltration (UF), microfiltration (MF) and conventional filtration (CF). In this context, PSf is usually made into UF membranes, used for water treatment and as enzyme biocatalytic reactors. The example used in this study is a PSf UF membrane with a molecular weight cut off (MWCO) of 100 kDa as a skin layer, and a porous polypropylene as a support layer. However, PSf membranes still suffer from the disadvantage of their hydrophobic nature, which leads to low water flux and heavy surface fouling.[68] Therefore, the key to improving these membranes' properties is to increase the hydrophilicity of their surfaces. It has been proven that membrane surface modification is a successful way of overcoming this shortcoming in PSf membranes.[68]

One such membrane surface modification method is surface coating. It has been reported that several hydrophilic polymers have been coated onto the surface of PSf membranes, such as poly(ethylene glycol) (PEG), poly(vinyl alcohol) (PVA), poly(vinyl pyrrolidone) (PVP) and their

derivative polymers.[69] Covalent grafting is another efficient pathway to realise surface modification. The most commonly used strategies for covalent grafting include photo-induced grafting, plasma-induced grafting, radiation-induced grafting and surface-initiated atom transfer radical polymerisation (SI-ATRP).[70] Among these surface modification techniques, SI-ATRP, which is suitable for a variety of monomers and achieves well-controlled polymer chain growth, has garnered the most attention.[68][71]

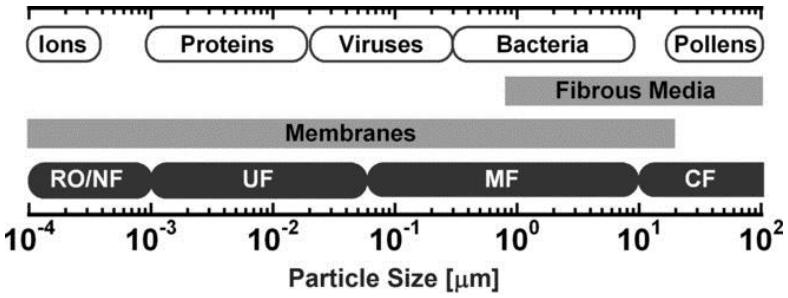

Fig. 4-1 Illustration of a porous membrane classification according to the size of the removal particles. [72] (Reproduced with permission, John Wiley & Sons, Inc.)

4.1.2 Atom transfer radical polymerisation

Atom transfer radical polymerisation (ATRP) as a branch of controlled radical polymerisation (CRP) is one of the most advanced polymerisation methods available.[73][74] ATRP is widely used for the synthesis of, for example, linear or architectural branched polymers and copolymers, graft copolymers and surface modifications.[73] Scheme 4-1 depicts the equilibrium mechanism of ATRP. Typically, the halogen of the dormant species (P_n-X) transfers to the transition metal complex (M^m/L), which acts as a catalyst by forming propagating radicals (P_n*), while the metal complex reaches a higher oxidation state through the rate of K_{act}, which is presented as X-M^{m+1}/L. The transfer of the halogen atom defines this polymerisation procedure as ATRP. Polymer chains grow by adding monomer to the intermittently generated P_n* with the rate constant of propagation (k_p). The reaction of P_n-X and Mt^m/L is reversible, whereby P_n* reacts with X-Mt^{m+1}/L through the rate of K_{deact}. Additionally, P_n* terminates with rate constant of termination (k_t).[75]

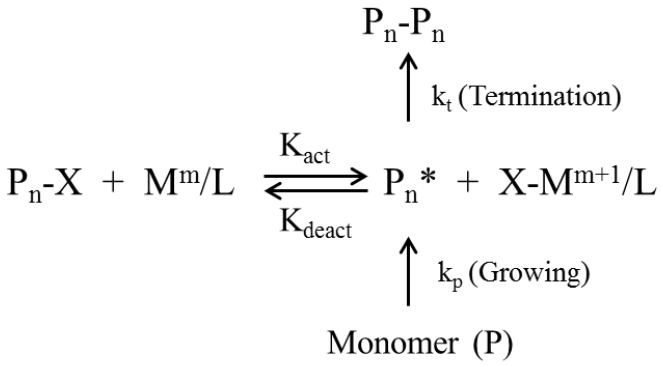

Scheme 4-1 The ATRP equilibrium.

4.2 PSf membrane modification

4.2.1 Chlorination of the PSf membrane

In this study, SI-ATRP was used to modify PSf membranes. Initially, the commercial PSf membrane was pretreated with ethanol to remove the protective glycerol layer. Subsequently, the PSf membrane was heterogeneously lithiated with n-butyllithium (n-BuLi) in diethyl ether at room temperature (as shown in Scheme 4-2). Usually, the lithiate process requires a low temperature due to the reactivity of n-BuLi and the degradation of the reacting solvent.[76][77] However, a low temperature will lead to the formation of fissures on the skin layer of PSf membranes. The reaction condition was optimised in previous investigations made by our group,[77] and it turned out that the lithiation of PSf membranes can be conducted at room temperature with diethyl ether as a solvent. The lithiated PSf membrane was then reacted with 4-(Chloromethyl)benzoyl Chloride at 0°C (as shown in Scheme 4-2). The reaction was confirmed by FT-IR, as shown in Fig. 4-2, and the two extra peaks at 1762 and 762 cm^{-1} that show up after the chlorination reaction represent carbonyl and C-Cl vibration, respectively.

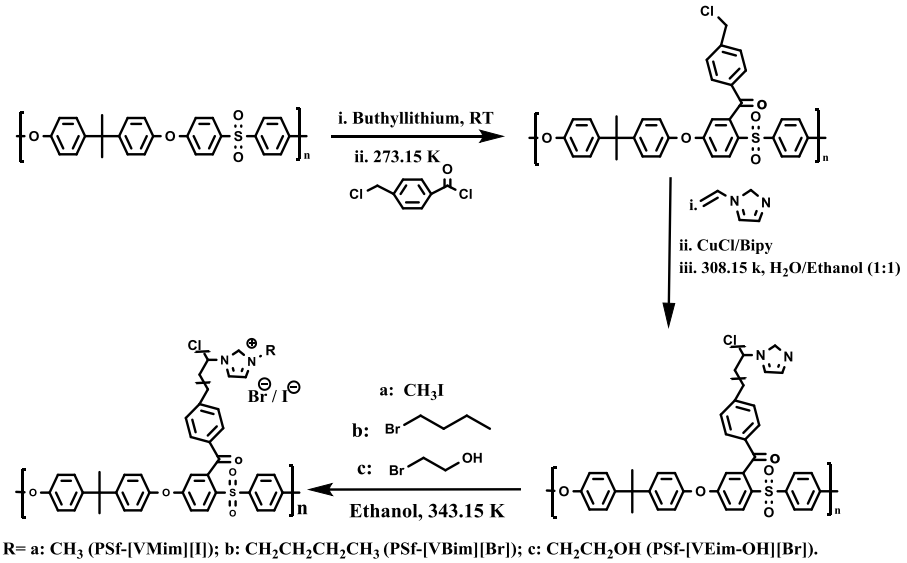

Scheme 4-2: Preparation of the modified PSf membrane.

4.2.2 PSf membrane modified with Vinylimidazole via ATRP

To increase the hydrophilicity of PSf, the hydrophilic monomer vinylimidazole (VIm) was selected to graft onto the surface of the PSf membrane (named PSf-[VIm]). The chloride atom on the surface of the chlorinated PSf membrane acts as an initiator and permits VIm polymerisation via ATRP with CuCl and 2,2'-bipyridine as catalyst, as shown in Scheme 4-2. The FT-TR spectrum of both the reference and PSf-[VIm] are shown in Fig. 4-2, which demonstrates no obvious difference between the FT-IR spectrum of the chlorinated PSf membrane and that of the VIm grafted membrane, since the characteristic vibration peaks of the imidazole ring, such as C-H stretching in the imidazole ring at around 3111 cm^{-1} and C=N stretching at around 1660 cm^{-1}, and C-C in the imidazole ring stretching at around 1494 cm^{-1}, overlap with the original peaks of the chlorinated PSf membrane. The broad peaks between 3700 and 3000 cm^{-1} of the PSf and PSf-[VIm] membranes belong to glycerol and water, respectively. Glycerol was used to protect the pores in the commercial PSf membrane; on the other hand, the existence of water in PSf-[VIm] is because of the hygroscopic nature of poly(VIm). The experimental procedure followed previous investigations, in which the modified membranes were tested and confirmed by XPS analysis.[77] Thus, we suppose VIm was polymerised successfully on the surface of the chlorinated PSf membrane in this study. ATRP is a well-controllable polymerisation approach, and its reaction time is one of the key parameters in controlling the degree of polymerisation. Therefore, we prepared PSf-[VIm] with

ATRP reaction times of 5 min and 45 min, following which different polymer chain lengths were obtained, with the 45-min grafted membranes being longer than the 5-min grafted membranes.

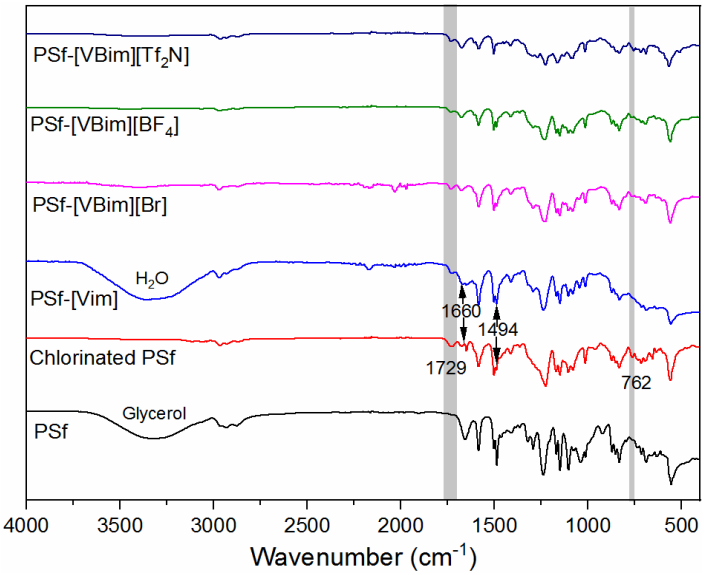

Fig. 4-2 FT-IR spectrum of pure and modified PSf membranes.

4.2.3 Poly(RTILs) modified PSf membrane

As mentioned, RTILs are attractive salts that possess special properties. Therefore, it is worthwhile converting poly(vinylimidazole) (poly(VIm)) on the surface of PSf membrane into poly(RTILs). In this project, a range of PSf membranes with poly(RTILs) were formed by quaternising poly(VIm) on the surface of PSf membranes with iodomethane, 1-bromobutane and 1-bromoethanol, which were named PSf-[VMim][I], PSf-[VBim][Br] and PSf-[VEim-OH][Br], respectively (as shown in Scheme 4-2).

It is well known that the counterions of RTILs affect the latter's properties,[78] one of which is hydrophilicity. In order to investigate the influence of counterions on the poly(RTIL) modified PSf membrane, the counterion of PSf-[VBim][Br] was changed into [BF_4] and [Tf_2N], named as PSf-[VBim][BF_4] and PSf-[VBim][Tf_2N], respectively. The FT-IR spectrum of PSf-[VBim][BF_4] and PSf-[VBim][Tf_2N] are shown in Fig. 4-2. However, there is no obvious difference compared to of PSf-[VBim][Br], so the water contact angle of membranes with different counterions was therefore tested.

4.3 Water contact angle

Fig. 4-3 shows the dynamic water contact angles of PSf-[VIm], PSf-[VBim][Br], PSf-[VBim][BF_4] and PSf-[VBim][Tf_2N]. As can be seen, it was possible to obtain advancing contact angles on the membranes, but the reducing contact angles could not be obtained, because the high porosity of PSf membranes led to rapid penetration of water into the membrane during the measurement. The changes of the surface properties of the membranes due to different counterions were determined preliminarily according to the advancing contact angles. The advancing contact angle of PSf-[VIm] decreased after quaternisation into PSf-[VBim][Br], which is interpretated as an increase in hydrophilicity. Similarly, the hydrophilicity of PSf-[VBim][BF_4] and PSf-[VBim][Tf_2N] does not increase in comparison to PSf-[VBim][Br], and especially for PSf-[VBim][BF_4], an increase in the contact angle was observed, indicating an increase in hydrophobicity, though this did not surpass the original PSf membrane. Therefore, no further water treatment investigation was carried out related to counterion exchange.

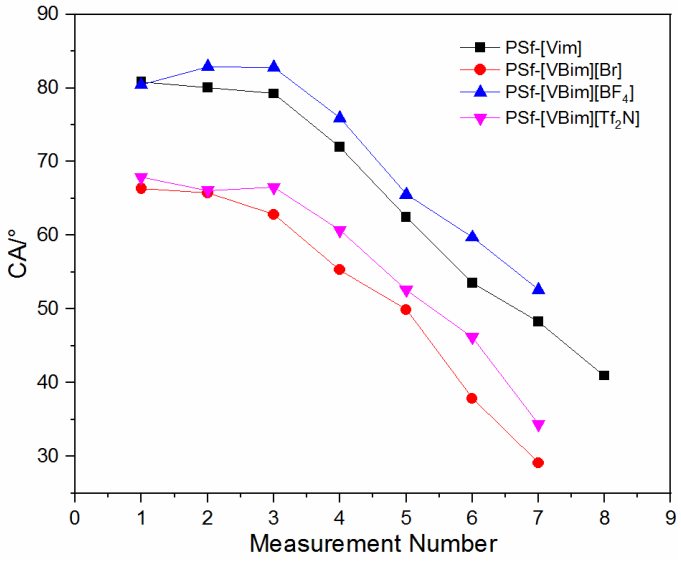

Fig. 4-3 Water contact angles of PSf-[VIm], PSf-[VBim][Br], PSf-[VBim][BF_4] and PSf-[VBim][Tf_2N].

4.4 Water treatment evaluation of the modified membranes

In this thesis, we aimed at preparing membranes used for CO_2 separation, and so we expected that the modified PSf membranes could be used as CO_2 separation membranes. However, the VIm grafted and post polymerisation modified membranes were too brittle when completely dry to be

used in this regard. The brittle nature of poly(VIm) and the corresponding RTILs requires that membranes must be kept wet after modification. It is well known that PSf membranes are also widely used for water treatment, which inspired us to use modified membranes in this particular application. Therefore, the water flux of the modified membranes was tested, and the results are shown in Table 4-1. The water flux of original PSf membrane was tested as a reference, and it transpired that the water flux of the modified membrane increases 1.8-3.5 times compared to the original PSf membrane, which is 179 L/m^2 h bar. Generally, the water flux of membranes decreases in line with an increased ATRP reaction time, from 5 min to 45 min, which means that the longer polymer chain hinders water flux to a certain extent and that ATRP reaction time plays a critical role. Poly(VIm) is a hydrophilic polymer, which causes the water permeability of PSf-[VIm] to increase to 559.7 and 422.1 L/m^2 h bar for the 5 and 45 min grafted membranes, respectively. In order to investigate the function of poly(RTILs), the water flux of PSf-[VMim][I], PSf-[VBim][Br] and PSf-[VEim-OH][Br] was tested. According to the results, the water permeability of PSf membranes with poly(RTILs) was generally higher than for PSf-[VIm], which illustrated that poly(RTILs) are potential candidates for increasing the hydrophilicity of a membrane. The increase in the water flux of PSf-[VBim][Br] compared to PSf-[VIm] is in agreement with the results seen for the water contact angle, as illustrated in Fig. 4-3. Compared to the results for PSf-[VMim][I] and PSf-[VBim][Br], it turns out that the length of the carbon chain on poly(RTILs) has no obvious influence over the 5-min reaction time ATRP membrane. On the contrary, for the membranes with a 45-min reaction time, the water permeability of PSf-[VBim][Br], which possess longer carbon chains, is lower than that of PSf-[VMim][I], due possibly to the longer carbon chain blocking the pores in the membrane even further. The water flux of PSf-[VEim-OH][Br] improved from around 600 L/m^2 h bar to 622.4 L/m^2 h bar for the 5-min ATRP membranes, and from 506.0 L/m^2 h bar of PSf-[VMim][I] to 562.7 L/m^2 h bar for the 45-min membranes. This indicates that the introduction of the PSf-[VEim-OH][Br] hydroxyl improves water flux further. After all, the widely tunable property of RTILs provides many more possibilities for membrane surface modifications, and different functional groups can be introduced, to target different applications.

Table 4-1 The water flux of pure and modified PSf membranes.

Membrane	J_1 (L/m^2 h bar)		
	No reaction	ATRP -5 min	ATRP - 45 min
PSf (reference)	179.0	-	-
PSf-[VIm]	-	559.7	422.1
PSf-[VMim][I]	-	598.5	506.0
PSf-[VBim][Br]	-	600.0	334.3
PSf-[VEim-OH][Br]	-	622.4	562.7

J_1: Water flux

Encouraged by the substantial improvement in water flux, the protein rejection performance of modified PSf membranes was investigated (as shown in Table 4-2). The water flux of the PSf membrane increased from 268.65 L / m^2 h bar to 1047 L / m^2 h after pretreatment, which was conducted in order to remove the protective glycerol layer. It is well known that solvents (ethanol and ether herein) have the ability to change the pore structure and size of a membrane during the pretreatment. The water flux of the modified membranes was around 600 L / m^2 h, which is lower than that for the pretreated membranes but still more than two times that of the original PSf membrane. After measuring the water flux, the protein solution, i.e. BSA (bovine serum albumin) solution at a concentration (C_f) of 150 mg/L, flux was tested. Compared to water flux, the BSA solution flux had different degrees of reduction. For the modified PSF membranes this was greater than that of the neat PSf membranes. BSA concentration in the permeate (C_p) of both PSf and pretreated PSf membranes was equal to C_f, which meant PSf and the pretreated PSf membranes had no BSA rejection property (Rejection=0). On the contrary, the modified PSf membranes, PSf-[VIm] and PSf-[VEim-OH][Br], showed BSA rejection capability, especially since rejecting PSf-[VIm] reached 78.6%. We supposed that the rejection capability of PSf-[VIm] and PSf-[VEim-OH][Br] was attributed to the interaction of the imidazole group and BSA. Moreover, the quarternisation of vinylimidazole hindered the interaction at some point. Therefore, compared to PSf-[VIm], PSf-[VEim-OH][Br] showed slightly lower rejection of BSA. Due of time limitations, this part of the study could not be continued, but the results showed the potential of poly(RTIL) modified PSf membranes for use as protein rejection membranes.

Table 4-2 The water flux and BSA rejection performance of pure and modified PSf membranes.

Membrane	J_1 (L / m^2 h bar)	J_2 (L / m^2 h bar)	C_f (mg / L)	C_p (mg / L)	Rejection (1-C_p/C_f)%
PSf (reference)	268.65	237.31	150	150	0
Pretreated PSf	1047	756.71	150	150	0
PSf-[VIm]	608.95	181.34	150	32	78.67
PSf-[VEim-OH][Br]	600	111.94	150	92	38.67

ATRP reaction time: 45 min; J_1: Water flux; J_2: Water flux of protein solution; C_p: BSA concentration in permeate; C_f: BSA concentration in feed solution; Pretreatment: Immersed in ethanol for 2 h, and then in ether for 30 mins.

4.5 Concluding remarks

Commercial PSf membranes were modified in this chapter with poly(VIm) and poly(RTILs), namely PSf-[VIm], PSf-[VMim][I], PSf-[VBim][Br], PSf-[VBim][BF_4], PSf-[VBim][Tf_2N] and PSf-[VEim-OH][Br], via ATRP. However, these modified membranes were too brittle to be used for gas separation. In this context, the water flux of initial and modified PSf membranes PSf-[VIm], PSf-[VMim][I], PSf-[VBim][Br] and PSf-[VEim-OH][Br] was tested. It turns out that the water flux increased 1.8-3.5 times after modification. Membranes with a shorter ATRP reaction time, with lower polymerisation, possess higher water flux. The water flux of the membranes modified with poly(RTILs) is generally higher than that of poly(VIm) modified membranes. Especially PSf-[VMim-OH][Br] with hydroxyl and a 5-min ATRP reaction time has the highest water flux, which reached 622.4 L/m^2 h bar, which is 3.5 times that of the original PSf membrane. The modified PSf membrane showed potential for useage as a protein rejection membrane. The rejection of BSA increased from 0 for neat PSf membranes to 78.67% for PSf-[VIm] and 38.67 % for PSf-[VEim-OH][Br]. This tunable property of RTILs provides many more possibilities for membrane surface modifications in different applications and is considered an interesting field to pursue further.

5 Poly(Vinylimidazole-co-butyl acrylate) membranes for CO_2 separation

As mentioned previously, poly(RTIL) membranes are widely used as gas separation membranes, especially imidazole-based poly(RTIL) membranes. However, imidazole-based poly(RTILs) are generally too brittle to form free-standing membranes and need porous polymer counterparts as support. The objective of this chapter is to prepare a free-standing poly(RTIL) membrane. Therefore, a relatively soft monomer, butyl acrylate, was copolymerised together with vinylimidazole in free radical polymerisations. The copolymer poly(VIm-co-BuA) was quarternised and cross-linked to form a free-standing poly(RTIL) membrane under mild conditions. The whole process for membrane preparation is shown in Scheme 5-1. This work has been published in publication 1 (see Appendix 1).

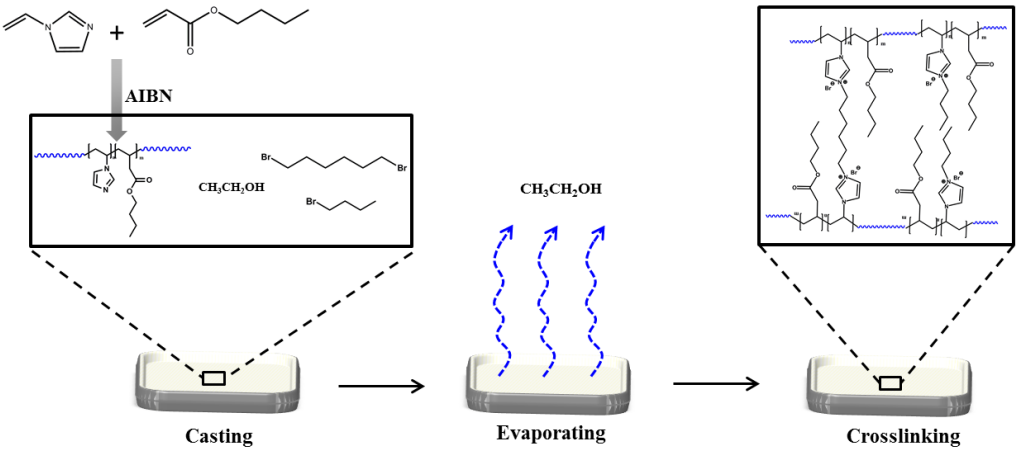

Scheme 5-1 Copolymer preparation and one-pot casting and cross-linking of membranes.

5.1 Synthesis of poly(VIm-co-BuA)

Imidazoles are popular for preparing RTILs, since they are easily converted into a range of RTILs through reaction with a broad selection of alkyl halides. Correspondingly, poly(RTILs) can be prepared easily by using VIm-based RTIL monomer, which polymerises through free radical and controlled radical conditions. Poly(VIm) is a semi-crystalline, extremely brittle polymer, which limits its application in many fields. It is also not possible to form free-standing membranes consisting solely of poly(VIm), due to this brittleness. It was recently shown that direct 3D printing

of VIm and BuA mixtures results in a material with significantly reduced brittleness[79]. Poly(VIm-co-BuA) with different ratios was synthesised in this work (as shown in Table 5-1), and the exact ratio of the polymers was calculated from ^{1}H NMR spectrum. The structure of the prepared polymers was confirmed with FT-IR and ^{1}H NMR. The FT-IR spectra of poly(VIm), in Fig. 5-1, exhibits the characteristic peaks of VIm, C=C-H and N=C-H stretching at 3111cm^{-1} and 1494 cm^{-1}, C=N stretching at 1660 cm^{-1}, ring vibrations at 1282 and 1230 cm^{-1}, CH out-of-plane bending at 914 cm^{-1}, ring torsion at 662 cm^{-1} and C=C-H and N=C-H wagging at 634 cm^{-1}. Moreover, the characteristic peaks of poly(BuA) are also shown in Fig. 5-1, with these ranging from 3011-2827 cm^{-1}, at 1451cm^{-1} and 1381cm^{-1}, representing the C-H of methyl and methylene group symmetric and asymmetric stretching. The peaks at 1727 cm^{-1}and 1154 cm^{-1} are related to stretching vibrations of C=O and C-O-C in the acrylate group. The poly(VIm-co-BuA) FT-IR spectra shows peaks from both poly(VIm) and poly(BuA), though their intensity (originating from VIm) is generally weaker than for the poly(BuA) peaks. The hygroscopicity of PVIm [80] results in traces of water being observed in both poly(VIm) and poly(VIm-co-BuA) IR spectra, even though the samples were dried prior to analysis.

Table 5-1 Feed ratios and polymer compositions of the prepared polymers.

	Poly(VIm)	Poly(VIm-co-BuA)	Poly(VIm-co-BuA)	Poly(VIm-co-BuA)	Poly(BuA)
Feed ratio (mol%)	100:0	70:30	50:50	30:70	0:100
Copolymer composition (mol%)	100:0	63:37	48:52	24:76	0:100

The molar composition of the copolymer was calculated from ^{1}H NMR, where the molar fraction of VIm was determined from the integration of the imidazole protons at δ_H 7.4-6.4 ppm relative to the methylene protons (δ_H 4.1-3.5 ppm) in BuA (as shown in Fig. 5-2). For instance, the molar fraction of VIm in poly(VIm-co-BuA), prepared from a feed composition of 50:50 VIm:BuA, is 48 mol%.

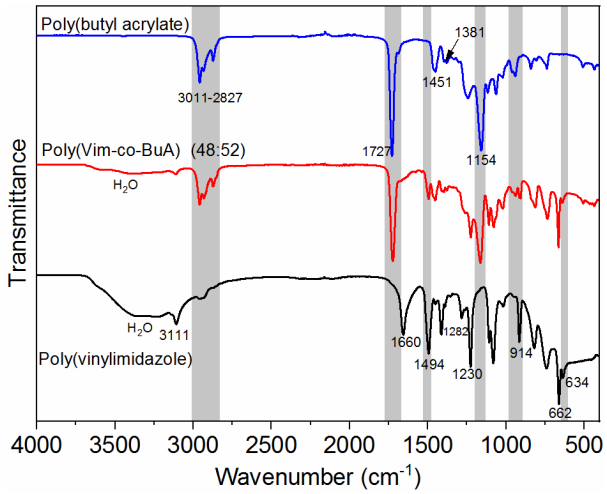

Fig. 5-1 The FT-IR spectra of poly(VIm), poly(VIm-co-BuA) (48:52) and poly(BuA).

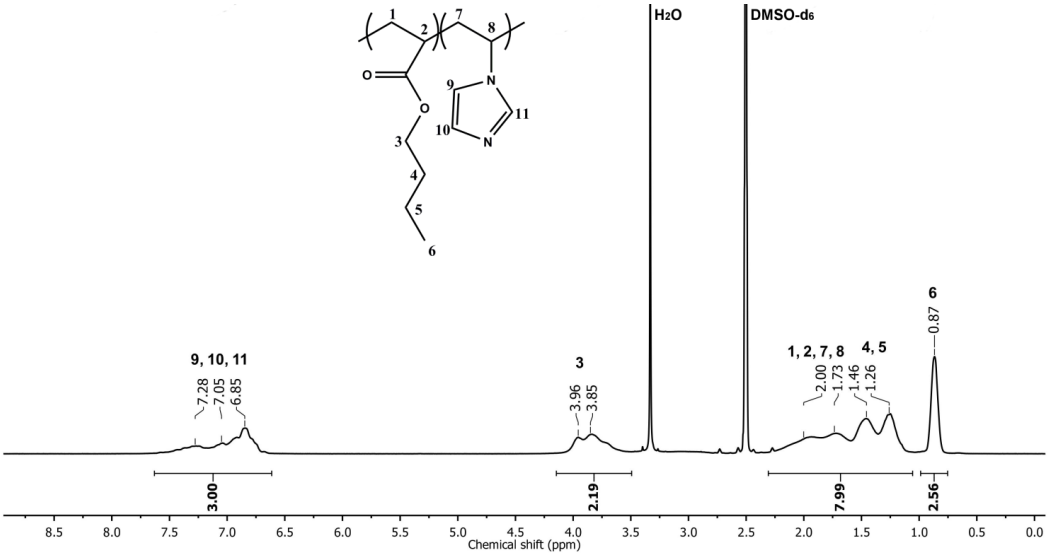

Fig. 5-2 ^{1}H NMR spectrum of poly(VIm-co-BuA) (48:52) run in DMSO-d_6.

The reactivity ratios, which illustrate the polymerisation kinetics of the monomers, were determined based on a series of copolymerisations of BuA and VIm with 10, 30, 50, 70 and 90 mol% BuA, which were terminated at low conversion to ensure constant feed composition. From the ^{1}H NMR of the initially formed poly(VIm-co-BuA) products, the copolymer content of BuA (F_1) and VIm

(F_2) could be determined. Based on a non-linear least squares (NLLSQ) fit and the method of Kelen and Tüdos,[81][82] the copolymer reactivity ratios were calculated as shown in Fig. 5-3.

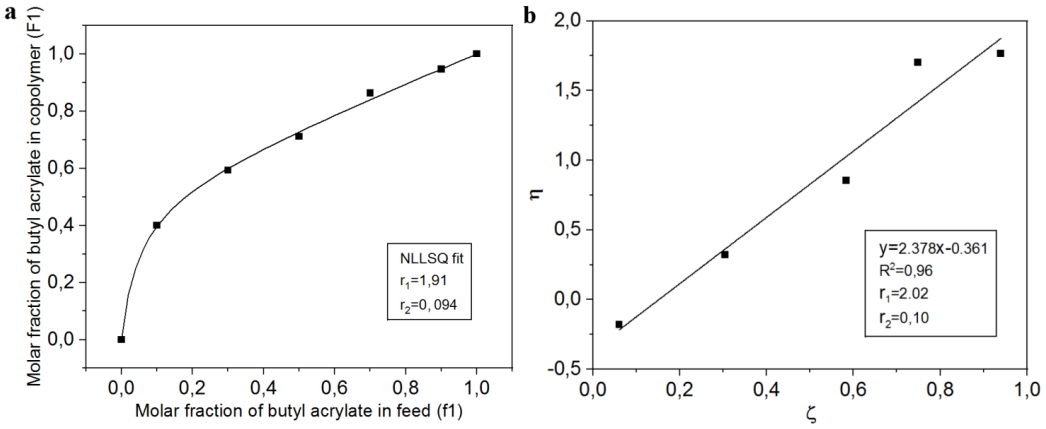

Fig. 5-3: a) Poly(VIm-co-BuA) composition diagram and NLLSQ fit. b) Kelen-Tüdos plot of poly(VIm-co-BuA).

The molar fraction of BuA in the feed (f_1) versus that in the copolymer (F_1) (shown in Fig. 5-3 (a)) shows a clear deviation from ideal copolymerisation. The initially formed copolymer will have a higher content of BuA relative to VIm compared to the feed ratio. This is directly reflected in the reactivity ratios determined by the NLLSQ fit (r_{BuA}=1.91 and r_{VIm}=0.094) and by the method of Kelen and Tüdos (r_{BuA}=2.02 and r_{VIm}=0.10) for BuA and VIm, respectively. Even though these reactivity ratios deviate from ideal copolymerisation, it is possible to obtain copolymers containing both repeating units, and therefore to use them for cross-linking into membranes.

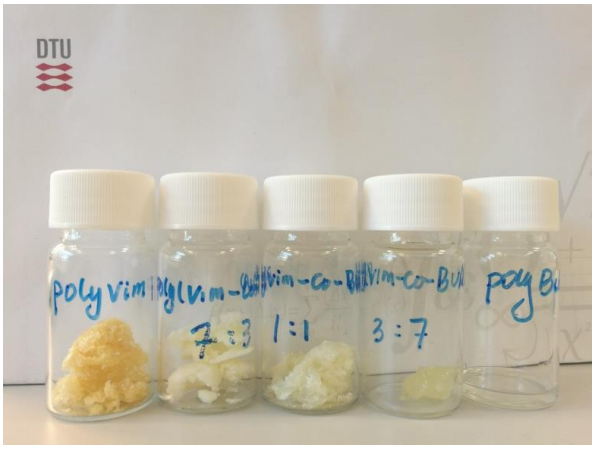

Fig. 5-4 The appearance of the prepared polymers.

A range of different VIm and BuA copolymers was therefore prepared to determine the optimal copolymer compositions for preparing free-standing membranes with a high VIm content and sufficient flexibility. The physical appearance of the prepared polymers is shown in Fig 5-4. The polymers are amphiphilic, which unfortunately prevents SEC analysis of any compositions with more than 24 mol% VIm in the copolymer (SEC in both THF and salted DMF has been tried). The SEC of the 24 mol% VIm copolymer displays only a single peak, corroborating the idea that true copolymerisation took place (SI-Fig 9 in Appendix 1.2). Thermal characterisation of the copolymers was conducted by TGA and DSC (see Figure 5-5).

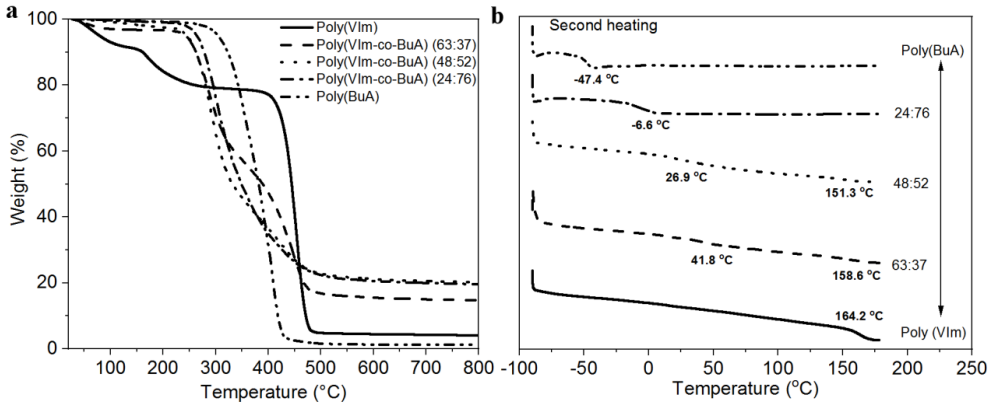

Fig. 5-5 Thermogravimetric analysis (a) and DSC thermograms showing the second heating cycle (b) of poly(VIm), poly(BuA) and copolymers with different compositions.

The TGA analysis (shown in Fig. 5-5 (a)) illustrates the hygroscopic nature of poly(VIm), and we see a very clear weight loss in terms of water in the initial phase of the analysis for the Poly(VIm) homopolymer. By incorporating BuA into the copolymers, however, this issue is reduced, although there is a minor weight loss observed, in line with the amount of VIm in the copolymers. The thermal degradation of all the copolymers takes place in a two-step behaviour, reflecting the content of the two monomers, and for all of the copolymers it is initiated at a lower temperature compared to the pure homopolymers (Poly(VIm) or Poly(BuA)), though this is still sufficiently high to permit application in gas membranes.

The introduction of BuA provided the required flexibility for the copolymers (see DSC thermograms in Figure 5-5 (b)). An interesting detail can be seen from the first heating curve in the DSC analysis, where the absorbed water results in water evaporation, after which one glass transition (T_g) is observed for the homopolymers (-47.2^{o}C for Poly(BuA) and 164^{o}C for Poly(VIm)),

while the copolymers show intermediate glass transition temperatures. For the two systems with a high content of VIm (48 and 63 mol%), two thermal transitions can be observed at 26.9°C and 151.3°C as well as at 41.8°C and 158.6°C, respectively. This could indicate the formation of free Poly(VIm) or of a tapered copolymer (though this cannot be confirmed without SEC analysis). From all of the prepared copolymers, poly(VIm-co-BuA) at ratio of 24:76 has the most interesting combination of a sufficiently high content of VIm while still exhibiting a low glass transition temperature, ultimately resulting in a flexible material that can be used for membrane preparation.

5.2 Preparation of free-standing poly(VIm-co-BuA) membranes

Poly(RTIL) membranes were prepared from the 24:76 VIm:BuA copolymer (poly(VIm-co-BuA)) by direct one-pot solvent casting in a Teflon petri dish (shown in Fig. 5-6) and cross-linking using mixtures of 1, 6-dibromohexane and 1-bromobutane (as shown in Scheme 5-1).

Fig. 5-6 Teflon petri dish used for membrane casting.

The simultaneous cross-linking and functionalisation reaction resulted in free-standing membranes, whereby the reaction of the VIm repeating units leads to the highest possible amount of poly(RTILs) in each membrane. Three kinds of cross-linked membranes were prepared in this work, the so-called 20%, 50% and 100% cross-linked membranes, using a 1:8, 1:2 or a 1:0 ratio of 1, 6-dibromohexane to 1-bromobutane. By varying the ratio between the cross-linker (1,6-bromohexane) and blocking agent (1-bromobutane), membranes with different cross-linking degrees were obtained while maintaining a similar RTIL character.

Any unreacted blocking agent or cross-linker was removed in a vacuum oven after cross-linking, resulting in membranes with a low soluble fraction (<10%) and very high gel fractions (> 90%), as shown in Table 5-2. Free RTILs in membranes are known to increase the permeability of CO_2, and the addition of free RTILs into the one-pot process was therefore also tested. It was possible to add up to 16 wt% free RTILs in the one-pot process, using 100% cross-linker. Free RTILs hindered the cross-linking reaction, and it was therefore only possible to add free RTILs to this membrane composition, while membranes with higher free RTIL content could not be prepared.

There is no obvious difference observed in the FT-IR spectra of membranes with different cross-linking degrees (shown in Fig. 5-7 (a)), since these membranes are effectively chemically equivalent. Fig. 5-7 (b) shows the FT-IR spectra of the 100% cross-linked membrane, 100% cross-linked membrane with free RTIL [BMIM][Tf_2N] and the RTIL, [BMIM][Tf_2N]. It is notable that the peaks of the 100% cross-linked membrane with free ionic liquid are a combination of [BMIM][Tf_2N] and the 100% cross-linked membrane. Additionally, there is no shift in the peaks, indicating that there are no chemical interactions between the membrane network and the free RTIL.

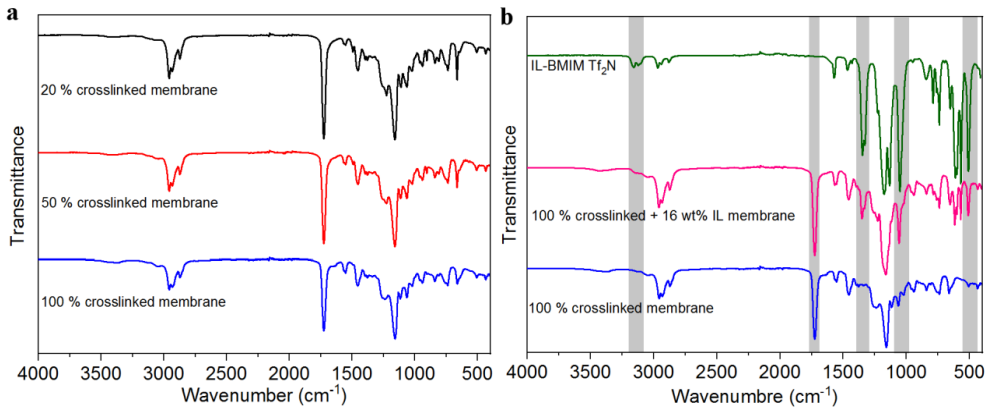

Fig. 5-7 FT-IR spectra of all the prepared membranes with 20, 50 and 100% cross-linker (a) as well as the 100% cross-linked membrane with free ionic liquid and the ionic liquid [BMIM][Tf_2N] (b).

5.3 Thermal properties

Thermogravimetric analysis of the membranes (see Figure 5-8) shows an even earlier onset of decomposition for the membranes compared to poly(VIm-co-BuA), which decreased from 268°C to 220°C after cross-linking. This is attributed to the presence of the imidazolium salts in the polymer backbone, which is the only change of the material after crosslinking. For the membranes, the first

stage of weight loss is observed between 220-350°C, corresponding to decomposition of the cross-linker and the acrylate part of the polymer backbone, while the second degradation between 350 and 530°C is attributed to decomposition of the imidazole ring and the polymer backbone, as has also been observed in other imidazole systems.[83] The residue after thermal degradation is constant for all the membranes, indicating that this relates to copolymer composition and not to the cross-linker/butyl bromide ratio. In the case of additional free RTILs, this residue is reduced, corresponding to the 16 wt% of RTIL. The thermal stability of all membranes is concluded to be sufficient for applying these materials to gas separation membranes, where flue gas between 25 and 75°C of representative flue gas are expected.[84]

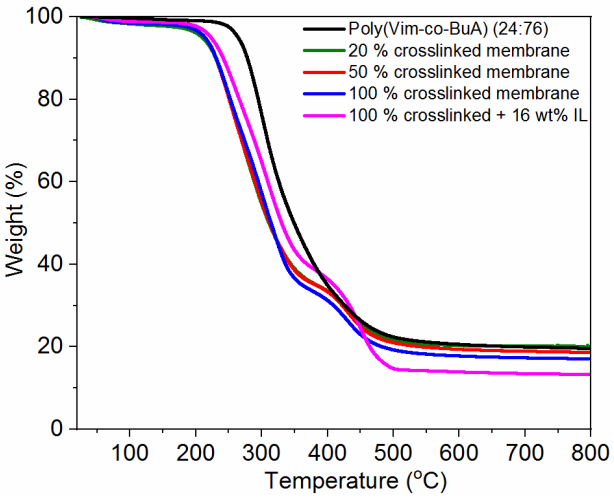

Fig. 5-8 TGA of poly(VIm-co-BuA) (24:76) and all the prepared membranes.

The thermal properties of the cross-linked membranes were also investigated by DSC. From the first heating curve in the DSC analysis, water evaporation can be seen in all of the membranes, which is attributed to the hygroscopic nature of systems containing VIm and the hydrophilic property of RTILs with halogen as counterions. However, on the second heating curve, it is not possible to identify glass transition temperatures for any of the membranes. Cross-linking of the membranes was expected to result in a minor increase in glass transition temperature compared to the original copolymer, as is well-known from other curing reactions.[85] All of the membranes appear soft and flexible, which indicates that the apparent glass transition temperatures are below RT (as shown in Fig. 5-9). This can be a result of either an actual low glass transition temperature or water plasticising the cross-linked membranes.

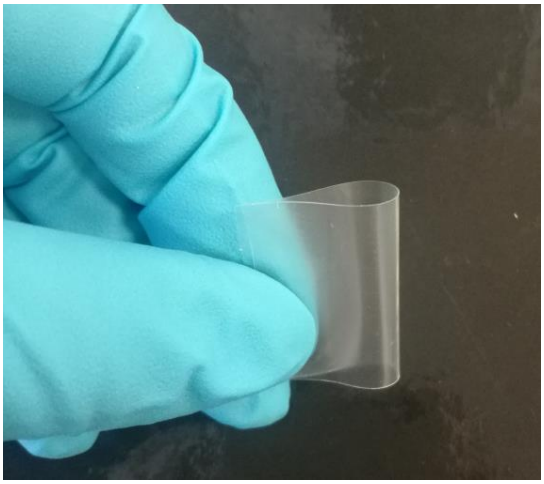

Fig. 5-9 The appearance of a 100% cross-linked membrane.

5.4 Mechanical properties of the cross-linked poly(VIm-co-BuA) membrane

The mechanical properties of the membranes were evaluated by tensile testing. The stress-strain curve of the membranes is shown Fig. 5-10. Young's modulus (MPa), tensile strength (MPa) and elongation at break (%) for the membranes are summarised in Table 5-2.

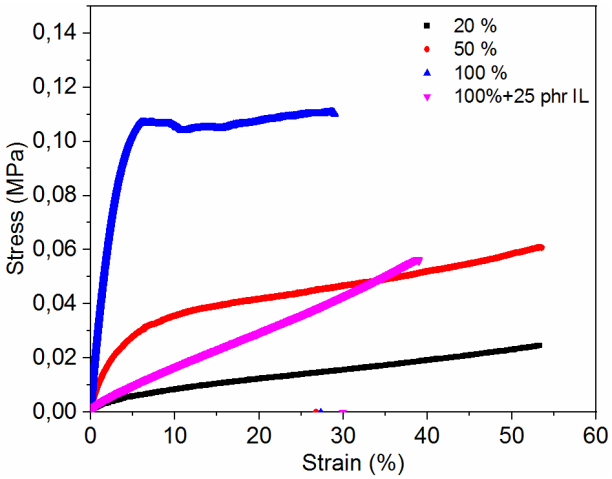

Fig. 5-10 Strain-stress curve of different membranes.

Table 5-2 Gel fraction and mechanical properties of the membranes.

	Gel fraction (%)	Young's modulus (MPa)	Tensile strength (MPa)	Elongation at break (%)
20%	95.77 ± 0.1	0.15	0.024	>53
50%	97.39 ± 0.39	1.35	0.061	>53
100%	98.41 ± 0.03	3.95	0.11	29.8
100% + 16 wt% RTIL	85.35 ± 0.18	0.34	0.056	39.2

Young's modulus was determined from the slope of the stress-strain curve, and it clearly increases with the increasing degree of cross-linking. In addition, the Young's modulus of the membrane with RTIL is observed to be between that of the 20% and 50% cross-linked membranes, because of the plasticising effect. The 100% cross-linked membrane and the 100% cross-linked membrane with 16 wt% RTIL showed elongations at break of 29.8% and 39.2%, respectively. However, the less cross-linked systems could not be extended to their breaking points, due to instrument limitations, resulting in extensions at break above 53%. All of the membranes exhibited mechanical properties that would enable them to be used for gas-phase membranes.

5.5 Gas permeation properties

The membrane prepared in this thesis was tested with single gas apparatus. The single gas permeability (P) and diffusivity coefficient (D) of all membranes were measured using time-lag apparatus. All of the measurements in this study took place at room temperature along with an upstream pressure of 2 bar and a downstream pressure of approximately 0.04 mbar.

The permeability of CO_2, N_2 and CH_4 and permselectivities of CO_2/N_2 and CO_2/CH_4 are listed in Table 5-3. In another study by Gabriel Zarca et al.,[86] the CO_2 permeability of a supported poly[C_4VIm][Tf_2N^-] membrane was observed to be 5.2 Barrers with CO_2/N_2 permselectivities of 17.3. The CO_2 permeability of membranes prepared in this work ranged from 33.71 to 54.38, which increased by about 6.5 to 10.5 times, and CO_2/N_2 permselectivities of more than 20, even though Tf_2N^- counterions are known to have significantly higher CO_2-philicity than halogen ions. This increased CO_2 permeability is attributed to the introduction of BuA, which leads to a much lower glass transition temperature of membranes. At the same time, it also resulted in higher fractional free volume, which is known to be beneficial for gas transportation.[87][58] Additionally, the

oxygen in the acrylate ester group, and its ability to interact with CO_2,[88] could also be an explanation for the improvement in CO_2 permeability.

Table 5-3 The permeability of CO_2, N_2 and CH_4, and the permselectivities of CO_2/N_2 and CO_2/CH_4.

Membrane	Permeability (Barrer)			Permselectivity	
	CO_2	N_2	CH_4	α_{CO_2/N_2}	α_{CO_2/CH_4}
20%	54.38	11.79	6.16	4.61	8.83
50%	44.35	2.05	5.16	21.63	8.59
100%	33.71	1.62	3.64	20.81	9.19
100% + 16 wt% RTIL	38.77	1.39	4.18	27.82	9.28

Table 5-3 also shows that gas permeability increases with decreasing of degree of crosslinking. From the reducing the degree of crosslinking from 100% to 50%, the permeability of CO_2 increased from 33.71 to 44.35 Barrers, without compromising permselectivity. This may be explained by the lower degree of cross-linking providing increasing free volume for the transportation of gases, which is consistent with results of other systems.[89] Additionally, the increase of CO_2 permeability is higher than that of N_2 and CH_4, which illustrates that the poly(RTIL) membranes have better affinity to CO_2. The observed difference in mechanical properties and the lower degree of cross-linking in the 20% cross-linked membrane leads to a considerably more open structure, resulting in increased permeability and diffusivity of N_2, as shown in Tables 5-3 and 5-4, respectively.

Table 5-4 The diffusivity and solubility of CO_2, N_2 and CH_4 in the cross-linked poly(VIm-co-BuA) membranes.

Membrane	Diffusivity ($\times 10^7$ cm^2 s^{-1})			Solubility (cm^3(STP) cm^{-3} atm^{-1})		
	CO_2	N_2	CH_4	CO_2	N_2	CH_4
20%	1.95	2.42	1.91	2.12	0.37	0.25
50%	1.82	1.90	2.21	1.85	0.082	0.18
100%	1.44	N/A	1.49	1.78	N/A	0.19
100% + 16 wt% RTIL	1.95	N/A	1.57	1.51	N/A	0.20

N/A: time-lag could not be determined accurately, due to a very slow permeation rate.

5.6 Composite membrane with free RTILs

Based on previous investigations, introducing free ionic liquid is an efficient way to improve the CO_2 separation performance of poly(RTIL) membranes.[33][11] In this work, 16 wt% [BMIM][Tf-

$_2$N] was added to a 100% cross-linked membrane. Tables 5-3 and 5-4 highlight the gas separation behaviours of membranes before and after the addition of free RTIL. The gas permeability and permselectivity of the membrane with free RTIL increased as expected. At the same time, the diffusivity coefficient increased from 1.44 to 1.95 $\times 10^7$ cm^2 s^{-1}, and the solubility coefficient decreased from 1.78 to 1.51 cm^3 (STP) cm^{-3} atm^{-1}. This was an unexpected result, which illustrates that increased permeability is a result of the added RTIL acting as a poly(RTIL) membrane plasticiser (diffusivity), and apparently it cannot be attributed to the high CO_2 solubility of free RTIL.

5.7 Concluding remarks

A series of copolymers of VIm and BuA were synthesised herein. Poly(VIm-co-BuA) (24:76) was found to be the best compromise between VIm content and thermal properties (T_g=-6.6 ^oC), and it was therefore used for preparing free-standing poly(RTIL) membranes. This was achieved by cross-linking poly(VIm-co-BuA) with a combination of 1, 6-dibromohexane (cross linker) and 1-bromobutane (blocker). Gas separation performance was directly correlated to the degree of cross-linking, where CO_2 permeability was increased from 33.7 Barrers for the 100% cross-linked membrane to 54.4 Barrers for the 20% cross-linked membrane. However, the more flexible 20% cross-linked membrane also showed significantly increased N_2 permeability. An optimal balance between permeability and selectivity was observed for the 50% cross-linked membrane, which showed both high CO_2 permeability (44.4 Barrers) as well as good CO_2 permselectivity over N_2 of 21.6. An ion gel was also prepared in this work by introducing 16 wt% free RTIL [BMIM][Tf_2N] into the 100% cross-linked membrane, resulting in increased CO_2 permeability from 33.71 to 38.77 Barrers and increased CO_2/N_2 permselectivity from 20.81 to 27.82. The results showed that the prepared membranes have the potential to separate CO_2 from flue gas and natural gas. Compared to the analogous neat poly(RTIL) membranes, both the permeability of CO_2 and the permselectivity of CO_2/N_2 increased.

6 Poly(vinylimidazole-co-butyl acrylate) membranes used for CO_2 conversion

Poly(VIm-co-BuA) membranes were noted to have high CO_2 affinity as a bulk property. As mentioned previously, poly(VIm-co-BuA) was obtained by copolymerising VIm and BuA to a ratio of 24:76 and cross-linked with 1, 6-dibromohexane to form poly(RTIL) membranes. In another application, poly(RTILs) are widely used as heterogeneous catalysts of the synthesis of cyclic carbonates via the insertion of CO_2 to epoxides.[1][90][91] Poly(RTILs)' inherence and CO_2 grabbing ability make poly(VIm-co-BuA) membranes potential candidates for catalysing this reaction. It was therefore decided to use them as both CO_2 separation membranes and CO_2 fixation catalysts, as shown in Scheme 6-1. The catalytic performance of poly(VIm-co-BuA) membranes is evaluated in this chapter, the experimental details for which are shown in Chapter 9.3.

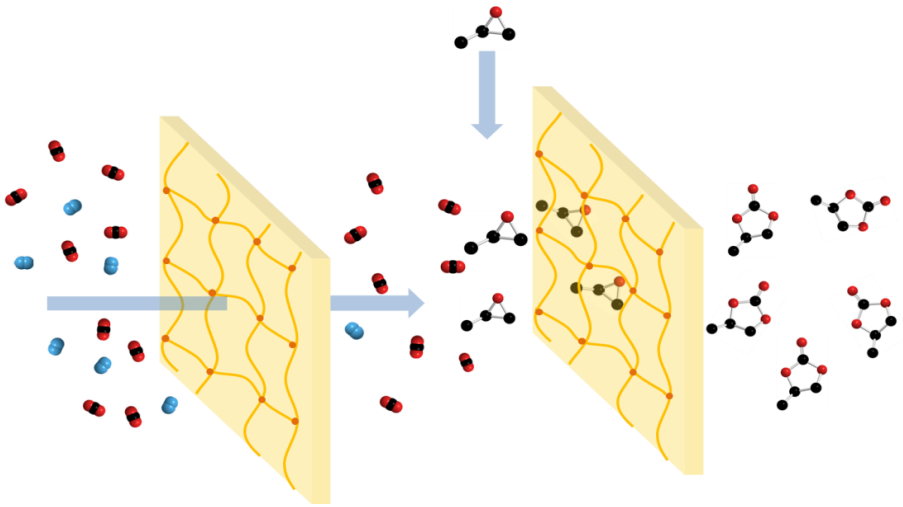

Scheme 6-1 Poly(VIm-co-BuA) membrane used as both a CO_2 separation membrane and a CO_2 fixation catalyst.

6.1 Background to the insertion of CO_2 to epoxides

As concentrations of CO_2 in the atmosphere continue to rise, researchers are paying increasingly more attention to developing effective CCS technology. What is more, CO_2 is considered the most common, nontoxic and renewable carbon resource, which makes it worthwhile finding ways to utilise it. It has been reported that CO_2 acts as feedstock for many kinds of valuable chemicals (seen in Fig. 6-1). Among them, the synthesis of cyclic carbonates, namely the insertion of CO_2 to

epoxides (shown in Scheme 6-2), is conducted in mild conditions alongside an appropriate catalyst and has been applied commercially since the 1950s.[92][93] Cyclic carbonates are widely employed as solvents in chemical processes (even on an industrial scale), including in organic synthesis[94], polymerisation[95], Li-ion batteries[96] and the synthesis of ionic liquids,[95] because of advantages such as low price, low toxicity and biodegradability.[95]

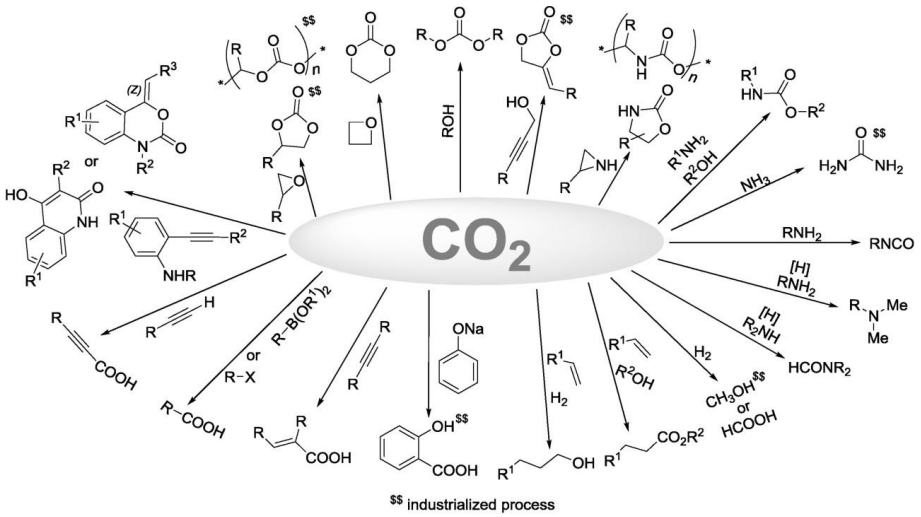

Fig. 6-1 Utilisation of CO_2.[97] (Reproduced with permission of Elsevier B.V, Inc.)

However, the chemically inert nature of CO_2 makes it critical to improve the performance of catalysts used to convert the gas into other chemicals; otherwise, very aggressive reaction conditions, such as high temperatures and pressure, will be required.[98] In order to prepare cyclic carbonates, several kinds of catalysts are being used to activate CO_2 (see Scheme 6-2).

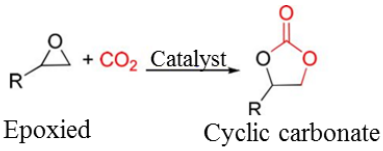

Scheme 6-2. Synthesis of cyclic carbonates from epoxides and carbon dioxide.

It is still essential to improve the performance of such catalysts, due to the extensive applications and economic potential of cyclic carbonates. During the past several decades, both homogeneous and heterogeneous catalysts have been widely developed for CO_2 insertion into epoxides to

parepare such cyclic carbonates,[99][100] which includes ionic liquids,[101] alkali metal salts,[102] metal complexes,[103][104] porous polymers,[105][106] metal oxide frameworks (MOFs)[107][108] and molecular sieves[109]. Among them, RTILs, as non-metallic catalysts, have been widely investigated and used for both homogeneous and heterogeneous catalysts, due to their high CO_2 affinity,[110] environmental friendliness[111] and highly tunable properties.[112] It is well-known that homogeneous catalysts possess higher catalytic properties compared to heterogeneous catalysts, though they can suffer from cumbersome recycling problems. Moreover, the price of RTILs limits the industrial application of large amounts of them as homogeneous catalysts, so numerous RTIL-based heterogeneous catalysts have been reported, including porous material-supported RTILs and poly(RTILs).[113][114] In order to lower reaction temperature, CO_2 pressure and reaction time, researchers have focused on increasing the surface area and amount of effective active catalyst sites, in order to expand the contact opportunities available to CO_2 and epoxide.[114] However, the performance of heterogeneous catalysts is still unacceptable. In 2016, Gao et al. devised for the first time a cross-linked poly(RTILs) catalyst in the reaction of ethylene carbonate with an aniline with a swelling property, which combined the advantages of both homogeneous and heterogeneous catalysts.[115] The heterogeneous catalyst with swelling property has comparable catalytic performance to homogeneous catalysts, which makes such swellable materials attractive candidates as catalysts. Until now, there have been very few studies on the application of swellable catalysts. In our previous work, cross-linked poly(RTIL) membranes, based on cross-linked poly(VIm-co-BuA), were prepared for CO_2 separation. Here, the CO_2 separation membrane was used as a catalyst in the insertion of CO_2 into cyclic epoxides, which was investigated at low CO_2 pressure, relatively low temperature and solvent-, metal- and cocatalyst-free conditions. To the best of our knowledge, this is the first time a CO_2 separation membrane material has been used as a catalyst in a CO_2 conversion reaction.

6.2 Catalyst preparation

In the last chapter, VIm and BuA copolymers were polymerised as poly(VIm-co-BuA) at ratios of 63:27, 48:52 and 24:76 (as shown in Scheme 6-3). Here, catalysts based on all of these copolymers were prepared by cross-linking with 1, 6-dibromohexane according to the same procedure used for preparing the poly(VIm-co-BuA) membranes described in the last chapter. In order to broaden the contact area of the catalyst and reactants, the prepared membranes, the thickness of which was around 100 μm, were ground into small particles, between 100 and 200 μm in diameter, in liquid nitrogen (as shown in Fig. 6-2). Catalysts where all of the VIm in the copolymer poly(VIm-co-BuA)

was cross-linked were named as follows: poly(VIm-co-BuA)-63:37-100% (1a in Scheme 6-3), poly(VIm-co-BuA)-48:52-100% (2a in Scheme 6-3) and poly(VIm-co-BuA)-24:76-100% (3a in Scheme 6-3). Additionally, six kinds of catalysts based on poly(VIm-co-BuA) (24:76) were prepared. Catalysts where 50% and 20% of VIm in poly(VIm-co-BuA) (24:76) was cross-linked with 1, 6-dibromohexane were named poly(VIm-co-BuA)-24:76-50% (3b in Scheme 6-3) and poly(VIm-co-BuA)-24:76-20% (3d in Scheme 6-3), respectively. The catalysts named poly(VIm-co-BuA)-24:76-50%-B (3c in Scheme 6-3) and poly(VIm-co-BuA)-24:76-20%-B (3e in Scheme 6-3) indicate that any remaining VIm that was not cross-linked was occupied with blocking agent 1-bromobutane. In poly(VIm-co-BuA)-24:76-OH (3f in Scheme 6-3), one-third of the VIm is cross-linked, another third is blocked with 1-bromoethonal and the remaining third stays unreacted. Except for the mentioned cross-linked poly(VIm-co-BuA) catalysts, poly(RTILs), namely poly(1-vinyl-3-butylimidazole Br) (Poly[VBIM][Br]) and homopolymer Poly(BuA), were also prepared as references.

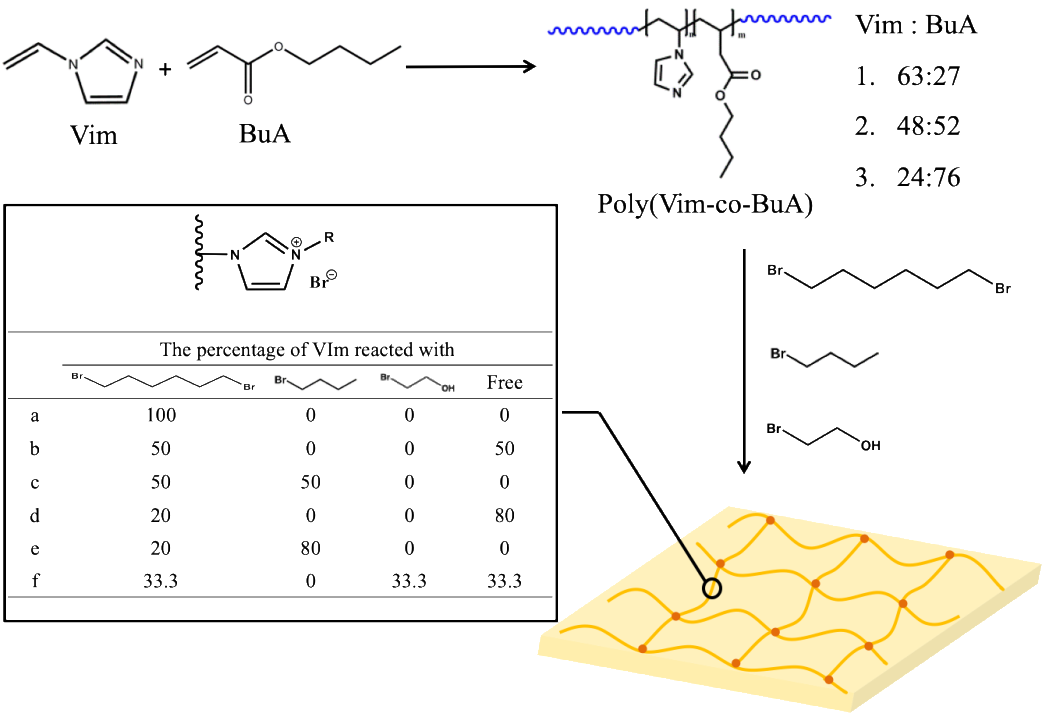

	The percentage of VIm reacted with			
	Br–(CH2)6–Br	Br–(CH2)3–CH3	Br–(CH2)2–OH	Free
a	100	0	0	0
b	50	0	0	50
c	50	50	0	0
d	20	0	0	80
e	20	80	0	0
f	33.3	0	33.3	33.3

Scheme 6-3 Catalyst preparation.

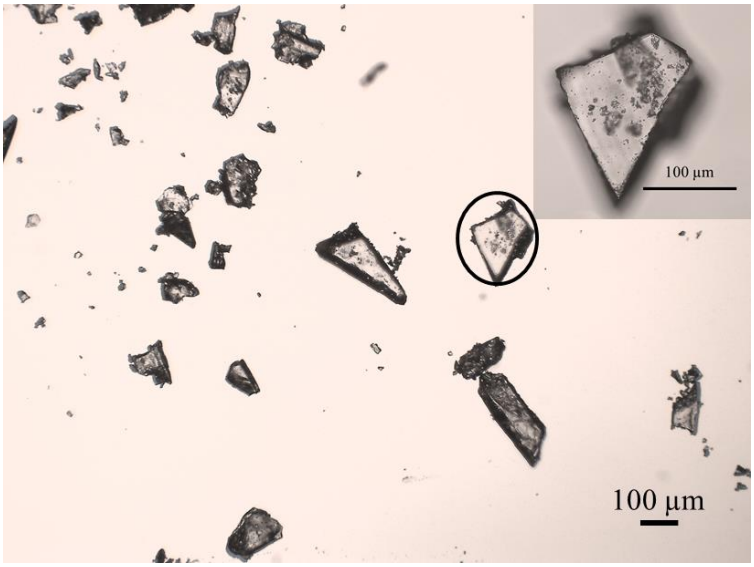

Fig. 6-2 Microscope image of poly(VIm-co-BuA)-24:76-OH particles.

6.3 Swelling behaviour of the poly(VIm-co-BuA) membranes

Eight kinds of cross-linked poly(VIm-co-BuA) particles used as CO_2 fixation catalysts were prepared in this study as shown in Scheme 6-3. However, it is impossible to test the swelling ratio of such small particles. Therefore, the swelling ratio of the cross-linked poly(VIm-co-BuA) membrane, which is the precursor of the poly(VIm-co-BuA) particles, was tested, so that the trend in different catalyst swelling ratios could be obtained (shown in Fig. 6-3). The swelling ratio was tested in ethanol instead of epoxide, the latter of which was considered too toxic for such a study.

For catalyst 1a, 2a and 3a, 100% of VIm in the copolymer was cross-linked, but the entire cross-linking degree was decreased by reducing the molar ratio of VIm in the copolymer. Therefore, the swelling properties increased step by step and line with the decreased cross-linking degree from 1a to 3a as expected. Membranes based on poly(VIm-co-BuA) (24:76), for which the swelling properties increased by decreasing the percentage of cross-linked VIm. Among them, 3c and 3e possessed the same cross-linking percentage as 3b and 3d, respectively. The results show that the swelling ratio of 3c and 3e is lower than that of 3b and 3d, since the blocking agent occupied some of the space for the solvent, which is ethanol herein.

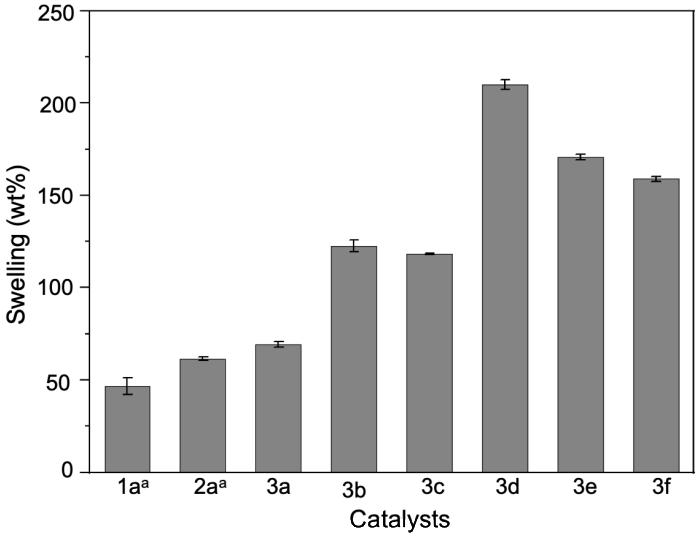

Fig. 6-3 Swelling properties of catalysts in ethanol. (a: swelling time is 15 min and that of others is 5 min).

6.4 Catalytic performance evaluation

6.4.1 Catalyst screening

The catalytic activity of the series of cross-linked poly(VIm-co-BuA)-based poly(RTILs) acting as metal-, solvent- and cocatalyst-free heterogeneous catalysts was tested, and the results of CO_2 insertion to epichlorohydrin are listed in Table 6-1. The experiment was conducted at 50°C and with a CO_2 pressure of 1 bar (balloon) for 12 h. Catalyst loading is based on the molar percentage of bromide versus epoxide, since bromide ions act as nucleophilic counterions, which can open the epoxide ring through a nucleophilic attack, as shown in Scheme 6-4.[92][101][116] It is notable that analogous to neat poly(RTILs) (Entry I), poly[VBIM][Br] (as shown in Fig. 6-4) showed extremely low catalytic activity with a conversion yield down to 2% under the applied experimental conditions. On the other hand, cross-linked poly(VIm-co-BuA) (Entry 1a-3f) had much higher catalytic activity, due to the swelling nature of the cross-linked poly(VIm-co-BuA), since epoxide swelled in the cross-linked poly(VIm-co-BuA) matrix, which possesses excellent CO_2 affinity and provides a good environment between the catalyst, the epoxide and CO_2. As a heterogeneous catalyst, the sufficient contact of catalyst and substrates makes their catalytic performance comparable with homogeneous catalysts.[115] It can be confirmed by the swelling property (shown in Fig. 6-3) and catalytic performance (shown in Table 6-1) of prepared catalysts that those with a higher swelling ratio

possess higher catalytic activity. For instance, comparing the catalytic performance of catalysts based on different copolymers (Entries 1a-2a), in which all of the VIm was cross-linked, the conversion yield increased from 19% to 52% by increasing the swelling from 46.5 wt% to 69.4 wt%. Therefore, the copolymer poly(VIm-co-BuA) (24:76) was used for systematic investigation. Compared to Entry 3a, catalysts with lower cross-linking degrees showed relatively better catalytic performance. For those catalysts with the same degree of cross-linking (Entries 3b and 3c; Entries 3d and 3e), the catalytic activity of catalysts with a blocking agent (Entries 3c and 3e) were lower than that of Entries 3b and 3d, respectively. This finding is attributed to the steric hindrance of the blocking agent on the cation, resulting in a decrease in activity.[117] In order to exclude the effect of the introduced BuA, the catalytic performance of poly(BuA) (Entry II) was also tested, and it transpired that it possess absolutely no catalytic activity, which further confirmed that the swelling property plays a crucial role in any improvement to catalytic performance. According to previous investigations, hydrogen bond donors, such as hydroxyl and carboxyl, could possibly promote the activation of CO_2 and dramatically improve catalytic efficiency. Inspired by the tunable methodology of the synthetic pathway, a free hydroxyl group was introduced into the cross-linked poly(VIm-co-BuA) by replacing the blocking agent 1-bromobutane with 1-bromoethanol, and this was named as poly(VIm-co-BuA)-24:76-OH (Entry 3f). Overall, Entry 3f showed the best conversion yield of 82% under the reaction conditions. Therefore, poly(VIm-co-BuA)-24:76-OH was chosen for further condition optimisation. Entry 3f-membrane is the pristine membrane form of poly(VIm-co-BuA)-24:76-OH, which has a catalytic activity of 51%. This confirms that ground particles form catalysts that enlarge the contact surface area of catalysts and reactants, resulting in much better catalytic performance.

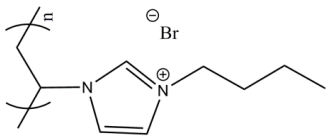

Fig. 6-4 Poly[VBIM][Br] structure.

Table 6-1 Catalyst screening for CO_2 insertion to epichlorohydrin.

Entry	Catalysts	Time (h)	Yield[b] (%)
I	Poly[VBIM][Br]	12	2%
II	Poly(BuA)	12	0
1a	Poly(VIm-co-BuA)-63:37-100%	12	19%
2a	Poly(VIm-co-BuA)-48:52-100%	12	39%
3a	Poly(VIm-co-BuA)-24:76-100%	12	52%
3b	Poly(VIm-co-BuA)-24:76-50%	12	68%
3c	Poly(VIm-co-BuA)-24:76-50%-B	12	54%
3d	Poly(VIm-co-BuA)-24:76-20%	12	59%
3e	Poly(VIm-co-BuA)-24:76-20%-B	12	50%
3f	Poly(VIm-co-BuA)-24:76-OH	12	82%
3f-membrane	Poly(VIm-co-BuA)-24:76-OH (membrane)	12	51%

[a]Reaction conditions: epichlorohydrin: 0.5 ml; Catalyst: 2 mol% per bromide unit; CO_2: 1 bar, 99.99%, balloon, Temperature: 50 °C; [b]Determined by ^{1}H NMR.

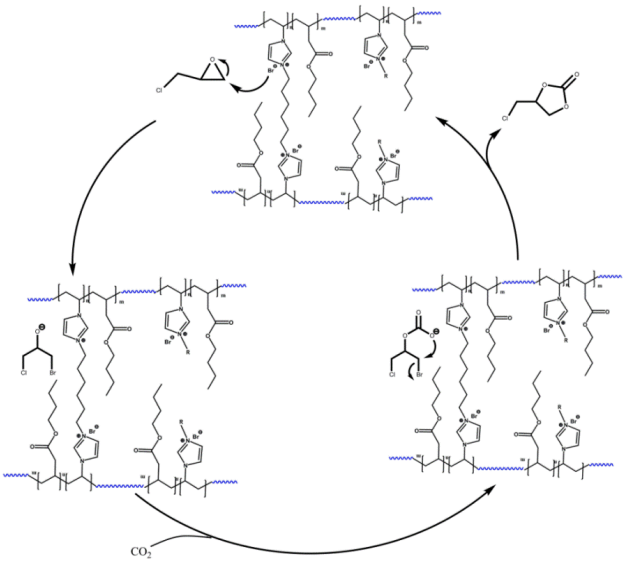

Scheme 6-4 Catalytic mechanism of cross-linked poly(VIm-co-BuA) catalyst to CO_2 insertion to epichlorohydrin.

6.4.2 Experimental conditions' influence

Several reaction parameters affect reaction conversion yield, including catalyst loading, reaction temperature, reaction time and CO_2 pressure. To optimise reaction conditions, the influence of the mentioned parameters, except CO_2 pressure, which is already ambient pressure, were investigated by using poly(VIm-co-BuA)-24:76-OH. First, catalyst loading was optimised as shown in Fig. 6-5, illustrating that the catalytic activity of poly(VIm-co-BuA)-24:76-OH depended significantly on catalyst loading. The conversion yield strongly increased by increasing catalyst loading from 0.5 to 2.0 mol%. However, catalytic activity decreased slightly if catalyst loading was increased further from 2.0 to 3.0 mol%, which could be attributed to the high amount of catalyst hindering CO_2 absorption of the epoxide and CO_2 transportation in the system.

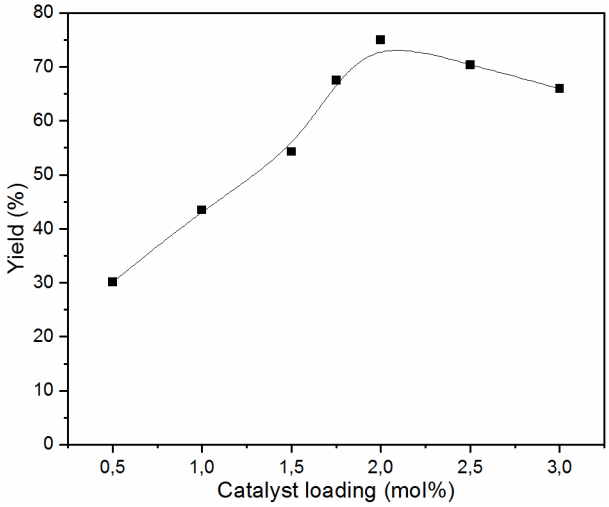

Fig. 6-5 Effects of catalyst loading (epichlorohydrin: 0.5 ml; CO_2: 1 bar, 99.99%, balloon; Temperature: 50°C; Reaction time: 12 h).

The dependence of conversion yield on reaction time was examined at 50°C, 1 bar of CO_2 pressure and with a catalyst loading of 2 mol% per bromide unit. Fig. 6-6 shows that the epichlorohydrin conversion yield increased rapidly and linearly until the reaction time of 9 h at 76.8%. The epichlorohydrin conversion yield increased slowly after 9 h and reached 90% by 24 h, and then remained constant after 27 h at 92.5%.

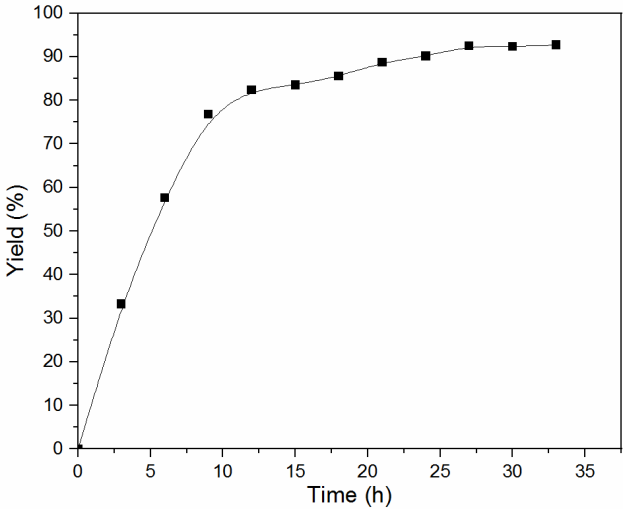

Fig. 6-6 Effects of reaction time (Epichlorohydrin: 1 ml; CO_2: 1 bar, 99.99%, balloon; Temperature: 50°C; Catalyst: 2 mol% per bromide unit).

As well as catalyst loading and reaction time, reaction temperature is another significant parameter that plays a crucial role on the reaction of CO_2 insertion to epoxides. Therefore, in order to establish the influence of temperature on the catalytic activity of poly(VIm-co-BuA)-24:76-OH, the reactions were conducted at different temperatures, namely 30, 35, 40, 45 and 50°C, at 1 bar CO_2 pressure, 2 mol% per bromide unit and a reaction time of 9 h. It was found that the epichlorohydrin conversion yield depended dramatically on reaction temperature, as shown in Fig. 6-7, so much so that it increased linearly with an increase in temperature. This also illustrates that catalyst poly(VIm-co-BuA)-24:76-OH possessed a certain catalytic activity at lower temperatures.

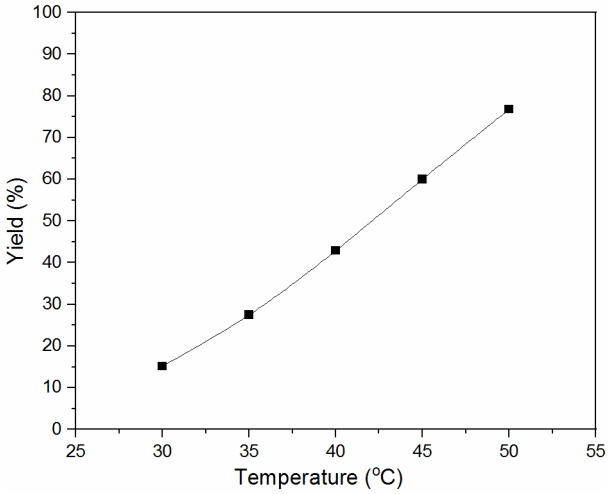

Fig. 6-7 Effects of reaction temperature (Epichlorohydrin: 0.5 ml; CO_2: 1 bar, 99.99%, balloon; Catalyst: 2 mol% per bromide unit; reaction time: 9 h).

6.5 Concluding remarks

Poly(VIm-co-BuA) copolymers with different VIm and BuA ratios of 63:37, 48:52 and 24:76 were cross-linked with 1, 6-dibromohexane-forming poly(RTIL) membranes. The cross-linking degree of the membranes was tunable by changing the amount of cross-linker (1, 6-dibromohexane). Cross-linked poly(VIm-co-BuA) with a different blocking agent, i.e. 1-bromobutane and 1-bromoethanol, was also prepared. The swelling ratio of catalysts with a lower degree of cross-linking was higher than that of membranes with a higher cross-linking persuasion. The cross-linked poly(VIm-co-BuA) membranes showed outstanding catalytic activity in relation to the reaction of CO_2 insertion to epichlorohydrin as heterogeneous catalysts. In addition, the epichlorohydrin conversion yield and the swelling ratio were positively proportional. Among the prepared catalysts, poly(VIm-co-BuA)-24:76-OH had the best catalytic performance, through which the experimental conditions, including catalyst loading, reaction time and temperature, were optimised. It turned out that the conversion yield of catalyst poly(VIm-co-BuA)-24:76-OH moved beyond 90% with a reaction time of 24 h, a catalyst loading of 2 mol% per bromide unit and 1 bar of CO_2 pressure at 50°C.

7 Conclusion

Increasing CO_2 emissions into the atmosphere require improvements in CCU technology. In this thesis, we focus on both CO_2 separation and conversion with RTIL-based membrane material, including MMMs, poly(RTILs)-modified commercial PSf membranes and free-standing cross-linked poly(VIm-co-BuA) membranes.

At first, we attempted to prepare MMMs with PVDF or poly(RTILs) as a polymer matrix ,and magnetic porous particles ZIF-8@SiO_2@Fe_3O_4 as a filler, and the ordered channel of the gap of porous particles would be formed under magnetic field. Unfortunately, neither the magnetic particles nor the polymer membrane matrix could be obtained. Next, the commercial PSf membrane was modified with poly(VIm) and imidazole-based poly(RTILs) via ATRP. The water flux of the original PSf membrane and the modified PSf membranes was tested, and the influence of ATRP reaction time to the water flux of the modified PSf membranes was investigated. It transpired that the membranes with a shorter ATRP reaction time possessed a relatively higher water flux. The hydrophilic functional groups of poly(RTILs) increased the water flux of the modified PSf membrane further. The protein rejection performance of modified PSf membranes was also investigated, which showed they had the potential for use as protein rejection membranes. Finally, VIm and BuA were copolymerised as poly(VIm-co-BuA). Free-standing poly(RTIL) membranes were forming by quarternising poly(VIm-co-BuA)(24:76) with the cross-linker 1, 6-dibromohexane and blocking agent 1-bromobutane. Membranes with different cross-linking degrees were obtained by ranging the ratio of cross-linker and blocking agent. The gas separation performance of the prepared membranes was tested with a single gas apparatus, with the gas separation performance of poly(VIm-co-BuA) increasing compared to that of analogous neat poly(RTILs). According to the previous investigations, poly(RTILs) exhibited the potential for use as catalysts for the CO_2 insertion to epoxide reaction. As a free-standing cross-linked poly(RTIL) membrane with CO_2 capture capability and swelling property, cross-linked poly(VIm-co-BuA) membranes, which were ground down into small particles, showed excellent catalytic activity. Especially, poly(VIm-co-BuA)-24:76-OH possessed the best catalytic performance.

In this thesis, several kinds of membranes were prepared with different membrane formation methods, such as solution casting, knife coating and commercial membrane modification. The application of the prepared membranes varied from CO_2 separation and water treatment, to CO_2

conversion. The influential factors behind the performance of these membranes in terms of different applications were studied, which provided the opportunity to improve membrane properties further.

8 Outlook

In this thesis, membranes have been prepared through a range of methods. Modified PSf membranes can be used as protein rejection membranes, while cross-linked poly(VIm-co-BuA) membranes can be used as CO_2 separation membranes and CO_2 conversion catalysts. Several factors affect membrane performance in terms of different applications, but considering the experience gained through this PhD project, there is still a great potential to improve the performance of such systems even further.

For instance, the water flux of the PSf membrane modified with poly(VIm) and poly(RTILs) increased by up to 3.5 times. It was discovered herein that one of the influencing factors of water flux was a functional group of poly(RTILs). Therefore, it is possible to improve further the performance of modified membranes by introducing different hydrophilic functional groups of poly(RTILs), or more hydrophilic monomers to copolymerise with poly(RTILs) (as shown in Scheme 8-1). The improved hydrophilicity that would be anticipated from preparing such membranes makes them potentially useful as protein rejection membranes.

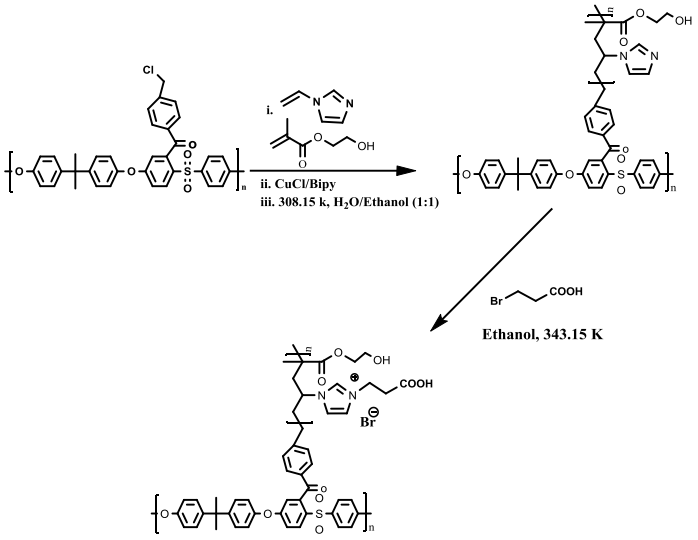

Scheme 8-1 PSf modification possibilities of future work.

For the free standing membranes, vinylimidazole and butyl acrylate were copolymerised as poly(VIm-co-BuA), which in turn was quarternised with the simple cross-linker 1,6-dibromohexane

and the blocking agent 1-bromobutane. Inspired by the highly tunable methodology, it could also be particularly interesting to replace the simple cross-linker and blocking agent with ones with higher CO_2 affinity having functional groups, such as ether and the amino group (such as shown in Scheme 8-2), thus making the transportation of CO_2 much easier. On the other hand, the introduction of a CO_2 affinity co-monomer instead of butyl acrylate, to provide softness, is another option for improving the CO_2 separation performance further.

Finally, the cross-linked poly(VIm-co-BuA) membranes have been seen to be outstanding catalysts for the CO_2 insertion into epoxides. The widely tunable possibility of RTILs gives many possibilities to increase the catalytic activity of poly(VIm-co-BuA)-based materials even further. In addition, since cross-linked materials, which possess strong swelling ratios, showed excellent catalytic activity, different kinds of cross-linked polymers could also be interesting to prepare and test as catalysts.

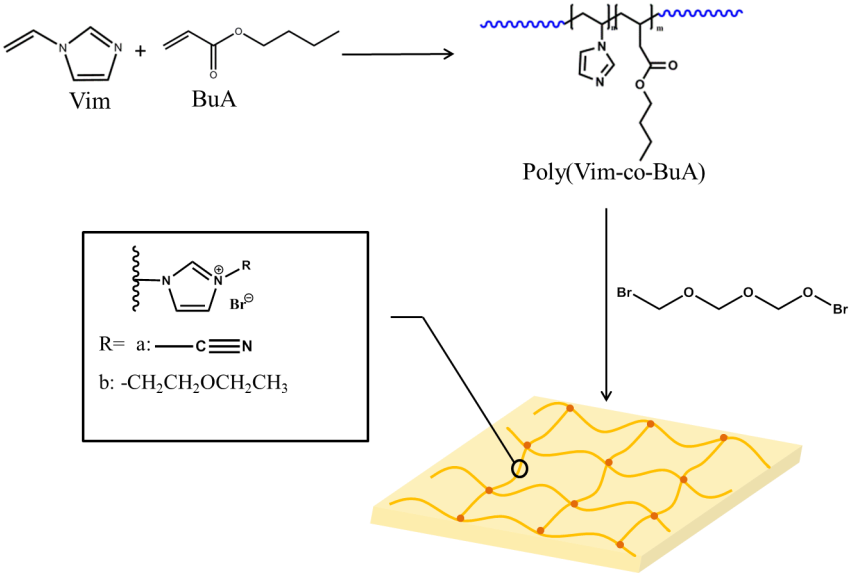

Scheme 8-2 Poly(VIm-co-BuA)-based membrane possibilities of future work.

9 Experimental section

9.1 Preparation of mixed matrix membranes

9.1.1 Materials and instruments

Zinc nitrate hexahydrate ($Zn(NO_3)_2 \cdot 6H_2O \geqslant 98\%$), 2-methylimidazole (99%), Fe_3O_4 nanopowder (97%), 1-vinylimidazole (≥ 99%), tetraethoxysilane (TEOS, ≥ 99%), 1-bromobutane (99%) and 2-bromoethanol (95%) ammonia were purchased from Sigma-Aldrich. Methanol and ethanol (≥ 99.8%) were purchased from the Beijing Chemical Company.

The ZIF-8 crystal was observed with a transmission electron microscope (TEM, JEOL-2010 operated at an accelerating voltage of 200 kV), and its surface area was tested with the Brunauer Emmett Teller (BET). The FTIR spectra were recorded on a Thermo Nicolet 380 spectroscope. The crystal structure of ZIF-8 was tested with a Rigaku Smartlab X-ray diffractometer, using a Cu Ka radiation source (λ=1.5406 Å). RTIL monomers were characterised via a nuclear-magnetic resonance spectrometer (NMR, Bruker 600).

9.1.2 Synthesis of ZIF-8@SiO_2@Fe_3O_4

ZIF-8 nanocrystals were synthesised following the literature.[46] In detail, 4.41 g of zinc nitrate hexahydrate was dissolved in 300 mL methanol (called ‘solution A’), and 4.87 g of 2-methylimidazole was dissolved in another 300 mL methanol (named ‘solution B’). Subsequently, solution B was poured rapidly into solution A under vigorous stirring with the final molar ratio of 1:4:1000 (Zn: Hmim: methanol) and then reacted for 1 h. Next, the reactant was centrifuged and washed three times with methanol. The preparation of SiO_2@Fe_3O_4 was based on a previous investigation,[59] whereby Fe_3O_4 nanopowder (0.3 g) was dispersed in a mixed solution of ethanol (160 mL), deionised water (40 mL) and ammonia (2.0 mL). Tetraethoxysilane (TEOS, 0.3 mL) was introduced into the solution after ultrasonic treatement for 30 min and vigorously stirred for 6 h. The sample was dried in a vacuum at 60°C thereafter. The preparation of ZIF-8@SiO_2@Fe_3O_4 catalysts was obtained by adding 2-methylimidazole solution to the $Zn(NO_3)_2 \cdot 6H_2O$ and SiO_2@Fe_3O_4 solution, and the grey powder was separated by an external magnet after vigorous stirring for 60 min. The obtained product was washed three times with ethanol and then dried in a vacuum oven at 60°C.

9.1.3 Preparation of the PVDF membrane

Pure PVDF membrane can be produced in two ways, namely solution casting and knife casting. For solution casting, a PVDF acetone solution was poured onto a glass plate (12*12 cm) and the solvent was evaporated and further dried in a vacuum oven for 8 h at 70°C. For knife casting, a membrane solution was poured onto the edge of a larger glass plate and scraped with a membrane knife at an appropriate height. The solvent was evaporated thereafter and then further dried in a vacuum oven for 8 h at 70°C.

9.1.4 Synthesis of ionic liquid monomers

Nineteen millilitres of 1-Bromobutane (176 mmol) was poured dropwise into 10 ml 1-vinylimidazole (110 mmol) in a 100 ml round-bottomed flask equipped with a stirrer and refluxed for 24 h under 70°C. A dark-yellow viscous liquid was obtained. The resulting viscous liquid was washed several times with ethyl acetate, following which the ionic liquid [VBIM] [Br^-] was dried in a vacuum oven at 50°C until mass-constant. The method used to synthesise [VHIM] [Br^-] was the same as the one used for [VBIM] [Br^-].

^{1}H NMR (δ_H, ppm, $CDCl_3$-d): 11.53 (s, 1H), 7.64 (s, 1H), 7.52 (m, 1H), 7.37 (s, 1H), 5.92 (dd,1H), 5.38 (dd,1H), 4.39 (t, 2H), 1.92 (m, 2H), 1.4 (m, 2H), 0.96 (t, 3H).

9.2 Modification of the polysulfone membrane

9.2.1 Materials and membrane characterisation

A PSf ultrafiltration membrane (GR40PP, 100 KDa MWCO) was purchased from Alfa Laval, ethanol (≥ 99.8%) was from VWR and diethyl ether (≥ 99.7%), n-butyllithium (n-BuLi, 2.5 M in hexane), 1-vinylimidazole (≥ 99%), 1-bromohexane (98%), 1-bromobutane (99%), Copper(I) chloride (CuCl, 99%), 2,2'-bipyridine (98%) and 2-bromoethanol (95%) were purchased from Sigma-Aldrich. 4-(Chloromethyl)benzoyl chloride (≥ 98%) was obtained from TCI. All of the chemicals were used as received.

Fourier transform infrared (FT-IR) was performed with a Niclet is50 ATR spectrometer with a diamond crystal from Thermo Scientific in the range of 4000-400 cm^{-1}. Advancing and receding water contact angles (WCAs) of the PSf membrane surfaces were determined by using a Dataphysics Contact Angle System OCA20.

9.2.2 PSf membrane activation (chlorination of the PSf membrane)

The PSf membrane was activated according to the previous work of our group.[77] PSf membranes (12 pieces, diameter: 4.5 cm) were merged in ethanol for 2 h and then in diethyl ether for another 30 min. The pretreated membranes were transferred into a big round-bottomed flask with diethyl ether (300 ml) and a stirrer. Subsequently, the flask was sealed with a vacuum gel. The ether was bubbled for 60 min with N_2 to replace the air. Afterwards, a 1-Buthyllithium solution (6 ml, 7.5 mmol, 2.5 M in hexanes) was poured dropwise into the system and reacted for 2 h. The colour of the membranes turned orange. The system was then cooled down to 0°C. 4-(chloromethyl)benzoyl chloride (3 g, 15.9 mmol), which was dissolved in diethyl ether in advance, was introduced to the system and reacted for 1 h. The colour of the membrane turned light yellow. Finally, the reaction was quenched with ethanol and the membranes were thoroughly rinsed with ethanol. The membranes were stored in a mixture of ethanol and water (50/50) for further usage.

9.2.3 PSf membrane modification via ATRP

The modification procedure was reported by our group.[77] CuCl (1.15 g, 11.6 mmol) and 2,2'-Bipyridyl (3.72 g, 23.8 mmol) were introduced in another 250 ml round-bottomed flask, which was evacuated and back-filled three times with N_2. Ethanol/H_2O (85.5 ml) mixture, which was bubbled with N_2 for 1 h in a sealed round-bottomed flask, and 1- vinylimidazole (64.2 ml, 0.71 mol) were introduced into the round-bottomed flask, and bubbled with N_2 for 1 h. The as-prepared solution was introduced into a vacuumed 250 ml round-bottomed flask equipped with a stirrer and chloridised PSf membrane (12 pieces, diameter: 4.5 cm) in an N_2 atmosphere. The flask was then heated to 35°C, and the polymerisation process lasted for 5 min and 45 min in this work. After the reaction, the membranes were rinsed with water and stored in a mixture of water and ethanol (50/50) for the next step.

9.2.4 Quarternisation of poly(VIm) on the surface of the PSf membrane into poly(RTILs)

The poly(VIm)-modified PSf membrane (three pieces), ethanol (60 ml) and 1-Bromobutane (5 ml) (or 3.3 ml bromoethanol or 2.86 ml methyl iodine) were introduced into a 100 ml round-bottomed flask equipped with a stirrer. The reaction was reflux at 60°C for 10 h. Thereafter, the membranes were rinsed with water and stored in a mixture of water and ethanol (50/50) for further usage.

9.2.5 Water flux and BSA rejection measurement

The water flux of the prepared membranes was carried out in a stirred cell (Amicon 8050, Millipore, USA). The measurement was conducted at a stirrer speed of 100 rpm and a constant air pressure of 1 bar. The effective surface area of the membrane was 13.4 cm^2. First, 40 ml of water was placed into the cell with the membrane and a beaker was placed on an electronic balance to monitor the permeate flux. The mass of the permeate water was then collected after 10 ml water permeated under constant air pressure. The water flux was calculated by following eq. 9-1:

$$Flux: J = \frac{V}{tS} \quad 9\text{-}1)$$

where V represents the volume of permeate water in ml (treat water density as 1 g ml^{-1}), t is the flux collection time in h and S is the effective membrane area in m^2.

After the water flux tests, the stirred cell was refilled rapidly with BSA solution (C_f =150 mg/L). The BSA solution flux was tested with the same method used for water flux and calculated according to eq. 9-1. BSA concentration in the permeate (C_p) was tested with a UV spectrometer. The rejection (R) of BSA can be calculated according to eq. 9-2:

$$R(\%) = \left(1 - \frac{C_p}{C_f}\right) \times 100\% \quad 9\text{-}1)$$

9.3 Preparation of the poly(VIm-co-BuA) catalyst for CO_2 coupling with epoxide

9.3.1 Materials

Butyl acrylate, N-vinylimidazole, 2,2'-azobis(2-methylpropionitrile) (AIBN), dimethylformamide (DMF), CDCl3, 1, 6-dibromohexane, 1-bromobutane, 1-bromoethanol and epichlorohydrin were purchased from Sigma-Aldrich. Ethanol was from VWR. Inhibitors were removed from the monomers by passing them through neutral alumina prior to use. CO_2 was from AGA Co. Ltd with a purity grade of 99.999%. All other chemicals were used as received.

9.3.2 Synthesis procedure for the polymers

General procedure involved in preparing poly(VIm-co-BuA) 48:52

Poly(VIm-co-BuA) was synthesised according to our previous work.[118] Briefly, AIBN (0.087 g, 0.53 mmol) was dissolved in DMF (10 mL), and monomers 1-vinylimidazole (1.9 g, 20.2 mmol)

and butyl acrylate (2.6 g, 20.3 mmol) were added into the flask. The reaction mixture was bubbled with nitrogen for 20 min to remove all traces of oxygen. The polymerisation mixture was stirred under nitrogen, using a magnetic stirrer for 10 h at 70°C. During polymerisation, the viscosity of the mixture gradually increased. The crude product was purified by precipitation into ether, and it was re-dissolved in EtOH and precipitated into ether again. The copolymer product was then dried *in vacuo* until constant mass was achieved. Other copolymers were also synthesised using the general method.

IR (cm^{-1}): 3111cm-1 (C=C-H), 3012-2844 cm^{-1}, 1451cm^{-1} (-CH2-), 1727 cm^{-1} and 1160 cm^{-1} (C=O and C-O-C in acrylate group), 1494 cm^{-1} (N=C-H), 1267 cm^{-1} and 1223cm^{-1} (ring), 912 cm^{-1} (C-H), 664 cm^{-1} (ring), 632 cm^{-1} (C=C-H and N=C-H);

1H-NMR (^{1}H, ppm, CDCl3): 7.4-6.4 (m, 3H), 4.1-3.5 (m, 2H), 2.27-1.45(m, 6H), 1.46 (m, 2H), 1.26 (m, 2H), 0.87 (m, 3H).

Preparation of poly(VIm-co-BuA) 24:76

Poly(VIm-co-BuA) 24:76 (30:70 in feed) was prepared in accordance with the general polymerisation procedure, using AIBN (0.87 g, 5.3 mmol), Vinylimidazole (11.4g, 121.1 mmol) and butyl acrylate (36.4 g, 284 mmol) in DMF (100 mL). The product polymer was reclaimed as a light-yellow solid after precipitation into water (yield more than 65%, M_n= 9092 g/mol, T_g= -6.6^{o}C).

IR (cm^{-1}): 3111cm^{-1} (C=C-H stretching), 3012-2844 cm^{-1}, 1451cm^{-1} (-CH_2- symmetric and asymmetric stretching), 1722 $cm^{-1}$and 1160 cm^{-1} (stretching vibration C=O and C-O-C in acrylate group), 1494 cm^{-1} (N=C-H stretching), 1267 cm^{-1} and 1223cm^{-1} (ring vibrations), 912 cm^{-1} (C-H out of plane bending), 664 cm^{-1} (ring torsion), 632 cm^{-1} (C=C-H and N=C-H wagging);

^{1}H-NMR ($\delta_{H,}$ ppm, $CDCl_3$): 7.4-6.4 (m, 3H), 3.96 (m, 2H), 2.35-1.62 (m, 6H), 1.52 (m, 2H), 1.27 (m, 2H) 0.86(m, 3H).

Preparation of poly(VIm-co-BuA) 63:37

Poly(VIm-co-BuA) 63:37 (70:30 in feed) was prepared in accordance with the general polymerisation procedure, using AIBN (0.087 g, 0.53 mmol), Vinylimidazole (2.64 g, 28.1 mmol) and butyl acrylate (1.54 g, 12.0 mmol) in DMF (10 mL). The product polymer was reclaimed as a light-yellow solid after precipitation into ether (yield more than 65%, T_g= 26.9/151.3^{o}C).

IR(cm^{-1}): 3112cm^{-1} (C=C-H stretching), 3012-2800 cm^{-1}, 1455cm^{-1} (-CH_2- symmetric and asymmetric stretching), 1722 $cm^{-1}$and 1164 cm^{-1} (stretching vibration C=O and C-O-C in acrylate group). 1663 cm^{-1} (C=N stretching), 1494 cm^{-1} (N=C-H stretching), 1275 cm^{-1} and 1227cm^{-1} (ring vibrations), 912 cm^{-1} (C-H out of plane bending), 664 cm^{-1} (ring torsion), 636 cm^{-1} (C=C-H and N=C-H wagging);

^{1}H-NMR ($\delta_{H,}$ ppm, DMSO-d): 7.52-6.62 (m, 3H), 4.05-3.55 (m, 2H), 2.27-1.45(m, 6H), 1.45 (m, 2H), 1.24 (m, 2H) 0.87(m, 3H).

Preparation of poly(vinylimidazole)

Poly(vinylimidazole) was prepared in accordance with the general polymerisation procedure, using AIBN (0.087 g, 0.53 mmol), 1-vinylimiazole (5 g, 53 mmol) in DMF (10 mL). The product polymer was reclaimed as brown solid after precipitation into acetone (yield more than 65%, Tg= 164.2°C).

IR (cm^{-1}): 3111cm^{-1} (C=C-H stretching), 1660 cm^{-1} (C=N stretching), 1494 cm^{-1} (N=C-H stretching), 1282 cm^{-1} and 1230 cm^{-1} (ring vibrations), 914 cm^{-1} (C-H out of plane bending), 662 cm^{-1} (ring torsion), 634 cm^{-1} (C=C-H and N=C-H wagging);

^{1}H-NMR (^{1}H, ppm, DMSO-d): 7.49-6.62 (m, 3H), 3.24-2.78 (m, 1H), 1.96 (s, 2H)

Poly[VBIM][Br]

Poly(vinylimidazole) was prepared in accordance with the general polymerisation procedure, using AIBN (0.087 g, 0.53 mmol), 1-vinylimiazole (5 g, 53 mmol) in DMF (10 mL). The product polymer was reclaimed as brown solid after precipitation into acetone (yield more than 65%, T_g= 164.2 ^{o}C).

IR (cm^{-1}): 3111cm^{-1} (C=C-H stretching), 1660 cm^{-1} (C=N stretching), 1494 cm^{-1} (N=C-H stretching), 1282 cm^{-1} and 1230cm^{-1} (ring vibrations), 914 cm^{-1} (C-H out of plane bending), 662 cm^{-1} (ring torsion), 634 cm^{-1} (C=C-H and N=C-H wagging);

^{1}H-NMR ($\delta_{H,}$ ppm, DMSO-d): 7.49-6.62 (m, 3H), 3.24-2.78 (m, 1H), 1.96 (s, 2H)

Poly[VBIM][Br] was synthesised by introducing 1-bromobutane (0.64 g, 2.6 mmol) into an ethanol solution of poly(VIm) (0.25 g, 2.6 mmol) and casting the solution in a small Teflon petri dish (5*5

cm). The casting solution was evaporated in ambient conditions in a fume hood and then transferred into a vacuum oven for 12 h at 70°C. The obtained poly[VBIM][Br] was ground into small particles in liquid nitrogen.

Preparation of poly(BuA)

Poly(BuA) was prepared in accordance with the general polymerisation procedure, using AIBN (0.087 g, 0.53 mmol) and butyl acrylate (5.12 g, 40 mmol) in DMF (10 mL). The product polymer was reclaimed as a transparent liquid with high viscosity after precipitation into DI water (yield more than 65%, T_g= -47.4°C).

IR (cm^{-1}): 3011-2827 cm^{-1}, 1451cm^{-1} and 1381cm^{-1} (-CH_2- symmetric and asymmetric stretching), 1727 $cm^{-1}$and 1154 cm^{-1} (stretching vibration C=O and C-O-C in acrylate group).

^{1}H-NMR (δ_H, ppm, $CDCl_3$): 3.96 (m, 2H), 2.39-1.44 (m, 3H), 1.56 (m, 2H), 1.31 (m, 2H) 0.87(m, 3H).

9.3.3 General procedure for preparing cross-linked poly(VIm-co-BuA) particles,

Poly(VIm-co-BuA)-63:37-100%

The particles were obtained following the general procedure for cross-linked poly(VIm-co-BuA) membranes according to our previous work. In short, poly(VIm-co-BuA) (63:37, 1.5 g, n_{VIm}=8.6 mmol) was dissolved in ethanol (12 mL) by stirring overnight. Then, 1,6-dibromohexane (1.28 g, 4.3 mmol) was introduced into the copolymer solution and stirred for an additional 1 h to prepare the membranes. The solution was degassed by ultrasonication for 10 min and solvent-casted in a Teflon petri dish. The casting solution was allowed to evaporate in ambient conditions in a fume hood. To remove entrapped residues of solvent, the cast membrane was dried *in vacuo* at 65°C for 6 h. The obtained membranes were ground into small particles in liquid nitrogen.

Poly(VIm-co-BuA)-48:52-100%

The particles were obtained following the general procedure for cross-linked poly(VIm-co-BuA) membrane. Briefly, poly(VIm-co-BuA) (48:52, 1.5 g, n_{VIm}=6.8 mmol) was dissolved in ethanol (12 mL) by stirring overnight. Then, 1,6-dibromohexane (0.83 g, 3.4 mmol) was introduced into the copolymer solution and stirred for an additional 1 h to prepare the membranes. The obtained membranes were ground into small particles in liquid nitrogen.

Poly(VIm-co-BuA)-24:76-100%

These particles were obtained by following the general procedure for cross-linked poly(VIm-co-BuA) membrane. Briefly, poly(VIm-co-BuA) (24:76, 1.5 g, n_{VIm}=3.0 mmol) was dissolved in ethanol (12 mL) by stirring overnight. Then, 1,6-dibromohexane (0.37 g, 1.5 mmol) was introduced into the copolymer solution and stirred for an additional 1 h to prepare the membranes. The obtained membranes were ground into small particles in liquid nitrogen.

Poly(VIm-co-BuA)-24:76-50%

The particles were obtained following the general procedure used for the cross-linked poly(VIm-co-BuA) membrane. Briefly, poly(VIm-co-BuA) (24:76, 1.5 g, n_{VIm}=3.0 mmol) was dissolved in ethanol (12 mL) by stirring overnight. Then, 1,6-dibromohexane (0.18 g, 0.75 mmol) was introduced into the copolymer solution and stirred for an additional 1 h to prepare the membranes. The obtained membranes were then ground into small particles in liquid nitrogen.

Poly(VIm-co-BuA)-24:76-50%-B

The particles were obtained following the general procedure for the cross-linked poly(VIm-co-BuA) membrane. Briefly, poly(VIm-co-BuA) (24:76, 1.5 g, n_{VIm}=3.0 mmol) was dissolved in ethanol (12 mL) by stirring overnight. Then, 1,6-dibromohexane (0.18 g, 0.75 mmol) and 1-bromobutane (0.2 g, 1.50 mmol) were introduced into the copolymer solution and stirred for an additional 1 h to prepare the membranes. The obtained membranes were then ground into small particles in liquid nitrogen.

Poly(VIm-co-BuA)-24:76-20%

The particles were obtained following the general procedure for the cross-linked poly(VIm-co-BuA) membrane. Briefly, poly(VIm-co-BuA) (24:76, 1.5 g, n_{VIm}=3.0 mmol) was dissolved in ethanol (12 mL) by stirring overnight. Then, 1,6-dibromohexane (0.07 g, 0.3 mmol) was introduced into the copolymer solution and stirred for an additional 1 h to prepare the membranes. The obtained membranes were ground into small particles in liquid nitrogen.

Poly(VIm-co-BuA)-24:76-20%-B

The particles were obtained following the general procedure for the cross-linked poly(VIm-co-BuA) membrane. Briefly, poly(VIm-co-BuA) (24:76, 1.5 g, n_{VIm}=3.0 mmol) was dissolved in ethanol (12 mL) by stirring overnight. Then, 1,6-dibromohexane (0.09 g, 0.37 mmol) and 1-bromobutane (0.33

g, 2.4 mmol) were introduced into the copolymer solution and stirred for an additional 1 h to prepare the membranes. The obtained membranes were ground into small particles in liquid nitrogen.

Poly(VIm-co-BuA)-24:76-OH

The particles were obtained following the general procedure for the cross-linked poly(VIm-co-BuA) membrane. Briefly, poly(VIm-co-BuA) (24:76, 1.5 g, n_{VIm}=3.0 mmol) was dissolved in ethanol (12 mL) by stirring overnight. Then, 1,6-dibromohexane (0.12 g, 0.5 mmol) and 1-bromobutane (0.13 g, 1 mmol) were introduced into the copolymer solution and stirred for an additional 1 h to prepare the membranes. The obtained membranes were ground into small particles in liquid nitrogen.

9.3.4 Swelling ratio measurement

The swelling property was evaluated by calculating the swelling ratio. First, the weights of dry membranes were measured. Second, the prepared membranes were tested by immersing them in the ethanol until the weight was constant: Poly(VIm-co-BuA) (24:76)-based membranes for 5 min and Poly(VIm-co-BuA)-63:37-100% Poly(VIm-co-BuA)-48:52-100% for 15 min. Next, the swelling ratio was calculated by following eq. 9-2:

$$Swelling\ ratio = \frac{W_W - W_d}{W_d} \times 100\% \qquad 9\text{-}2)$$

where W_W and W_d represent the weight of the wet membrane after swelling and the original dry membrane, respectively.

9.3.5 Catalytic activity evaluation – catalytic insertion of CO_2 with epoxides

In general, the cycloaddition reaction was carried out in a 10 mL Shlenck vial equipped with a magnetic stirrer and a balloon providing CO_2 under 1 atm pressure. Desired amounts of epoxides and catalyst (shown in Fig. 9-1) were introduced in the vial and then reacted at 50°C for 12 h. The reactor was then cooled down to room temperature and CO_2 was released slowly. The product was extracted with chloroform and the conversion yield was obtained by ^{1}H NMR. Catalyst loading was optimised at 50°C and 1 bar CO_2 pressure for 12 h by varying the catalyst loading by 0.5, 1, 1.5, 1.75, 2 and 3 mol% of bromide.

Table 9-1 Substrate dosage

	$V_{epoxide}$ (ml)	$n_{epoxide}$ (mmol)	n_{Br-}=2% $n_{epoxide}$ (mmol)	$m_{catalyst}$ (g)
Poly(VIm-co-BuA)-63:37-100%	0.5	6.4	0.128	0.035
Poly(VIm-co-BuA)-48:52-100%	0.5	6.4	0.128	0.045
Poly(VIm-co-BuA)-24:76-100%	0.5	6.4	0.128	0.08
Poly(VIm-co-BuA)-24:76-50%	0.5	6.4	0.128	0.145
Poly(VIm-co-BuA)-24:76-50%-B	0.5	6.4	0.128	0.08
Poly(VIm-co-BuA)-24:76-20%	0.5	6.4	0.128	0.335
Poly(VIm-co-BuA)-24:76-20%-B	0.5	6.4	0.128	0.08
Poly(VIm-co-BuA)-24:76-OH	0.5	6.4	0.128	0.11

Reference

[1] J. Yuan, D. Mecerreyes, M. Antonietti, Poly(ionic liquid)s: An update, Prog. Polym. Sci. 38 (2013) 1009–1036.

[2] M. Armand, F. Endres, D.R. MacFarlane, H. Ohno, B. Scrosati, Ionic-liquid materials for the electrochemical challenges of the future, Nat. Mater. 8 (2009) 621–629.

[3] W. Zhao, Y. Tang, J. Xi, J. Kong, Functionalized graphene sheets with poly(ionic liquid)s and high adsorption capacity of anionic dyes, Appl. Surf. Sci. 326 (2015) 276–284.

[4] J.F. Brennecke, E.J. Maginn, Ionic liquids: Innovative fluids for chemical processing, AIChE J. 47 (2001) 2384–2389.

[5] Z. Li, J. Liu, J. Li, F. Kang, F. Gao, A novel graphite-based dual ion battery using $PP_{14}NTF_2$ ionic liquid for preparing graphene structure, Carbon N. Y. 138 (2018) 52–60.

[6] Y. Bai, R. Yan, W. Tu, J. Qian, H. Gao, X. Zhang, S. Zhang, Selective separation of methacrylic acid and acetic acid from aqueous solution using carboxyl-functionalized ionic liquids, ACS Sustain. Chem. Eng. 6 (2018).

[7] M.F. Rojas, F.L. Bernard, A. Aquino, J. Borges, F.D. Vecchia, S. Menezes, R. Ligabue, S. Einloft, Poly(ionic liquid)s as efficient catalyst in transformation of CO_2 to cyclic carbonate, J. Mol. Catal. A Chem. 392 (2014) 83–88.

[8] P. Li, K.P. Pramoda, T.-S. Chung, CO_2 separation from flue gas using polyvinyl-(room temperature ionic liquid)–room temperature ionic liquid composite membranes, Ind. Eng. Chem. Res. 50 (2011) 9344–9353.

[9] S.C. Lu, A.L. Khan, I.F.J. Vankelecom, Polysulfone-ionic liquid based membranes for CO_2/N_2 separation with tunable porous surface features, J. Memb. Sci. 518 (2016) 10–20.

[10] L.A. Blanchard, Z. Gu, J.F. Brennecke, High-pressure phase behavior of ionic liquid/CO_2 systems, J. Phys. Chem. B. 105 (2001) 2437–2444.

[11] J.E. Bara, D.L. Gin, R.D. Noble, Effect of anion on gas separation performance of polymer−room-temperature ionic liquid composite membranes, Ind. Eng. Chem. Res. 47 (2008) 9919–9924.

[12] C. Cadena, J.L. Anthony, J.K. Shah, T.I. Morrow, J.F. Brennecke, E.J. Maginn, Why is CO_2 so soluble in imidazolium-based ionic liquids?, J. Am. Chem. Soc. 126 (2004) 5300–5308.

[13] W. Ren, B. Sensenich, A.M. Scurto, High-pressure phase equilibria of {carbon dioxide (CO_2) + n-alkyl-imidazolium bis(trifluoromethylsulfonyl)amide} ionic liquids, J. Chem.

Thermodyn. 42 (2010) 305–311.

[14] S. Hasebe, S. Aoyama, M. Tanaka, H. Kawakami, CO_2 separation of polymer membranes containing silica nanoparticles with gas permeable nano-space, J. Memb. Sci. 536 (2017) 148–155.

[15] Z. Dai, L. Ansaloni, D.L. Gin, R.D. Noble, L. Deng, Facile fabrication of CO_2 separation membranes by cross-linking of poly(ethylene glycol) diglycidyl ether with a diamine and a polyamine-based ionic liquid, J. Memb. Sci. 523 (2017) 551–560.

[16] J. Deng, L. Bai, S. Zeng, X. Zhang, Y. Nie, L. Deng, S. Zhang, Ether-functionalized ionic liquid based composite membranes for carbon dioxide separation, RSC Adv. 6 (2016) 45184–45192.

[17] S. Zulfiqar, M.I. Sarwar, D. Mecerreyes, Polymeric ionic liquids for CO_2 capture and separation: potential, progress and challenges, Polym. Chem. 6 (2015) 6435–6451.

[18] J.L. Anthony, J.L. Anderson, E.J. Maginn, J.F. Brennecke, Anion effects on gas solubility in ionic liquids Jennifer, J. Phys. Chem. B. 109 (2005) 6366–6374.

[19] A. Finotello, J.E. Bara, D. Camper, R.D. Noble, Room-temperature ionic liquids: temperature dependence of gas solubility selectivity, Ind. Eng. Chem. Res. 47 (2008) 3453–3459.

[20] S. Yoo, J. Won, S.W. Kang, Y.S. Kang, S. Nagase, CO_2 separation membranes using ionic liquids in a Nafion matrix, J. Memb. Sci. 363 (2010) 72–79.

[21] J.E. Bara, S. Lessmann, C.J. Gabriel, E.S. Hatakeyama, R.D. Noble, D.L. Gin, Synthesis and performance of polymerizable room-temperature ionic liquids as gas separation membranes, Ind. Eng. Chem. Res. 46 (2007) 5397–5404.

[22] A.M. Lopez, M.G. Cowan, D.L. Gin, R.D. Noble, Phosphonium-based poly(ionic liquid)/ionic liquid ion gel membranes: influence of structure and ionic liquid loading on ion conductivity and light gas separation performance, J. Chem. Eng. Data. 63 (2018) 1154–1162.

[23] Y. Zhang, J. Sunarso, S. Liu, R. Wang, Current status and development of membranes for CO_2/CH_4 separation: A review, Int. J. Greenh. Gas Control. 12 (2013) 84–107.

[24] E. Lasseuguette, J.C. Rouch, J.C. Remigy, Formation of continuous dense polymer layer at the surface of hollow fiber using a photografting process, J. Appl. Polym. Sci. 132 (2015)

[25] P. Li, D.R. Paul, T.-S. Chung, High performance membranes based on ionic liquid polymers for CO_2 separation from the flue gas, Green Chem. 14 (2012) 1052.

[26] J. Luo, A.S. Meyer, R. V Mateiu, M. Pinelo, Cascade catalysis in membranes with enzyme

immobilization for multi-enzymatic conversion of CO_2 to methanol., N. Biotechnol. 32 (2015) 319–27.

[27] L. Yang, J. Ge, C. Liu, G. Wang, W. Xing, Approaches to improve the performance of anode methanol oxidation reaction—a short review, Curr. Opin. Electrochem. 4 (2017) 83–88.

[28] D. Cheng, H.H. Ngo, W. Guo, Y. Liu, S.W. Chang, D.D. Nguyen, L.D. Nghiem, J. Zhou, B. Ni, Anaerobic membrane bioreactors for antibiotic wastewater treatment: Performance and membrane fouling issues, Bioresour. Technol. 267 (2018) 714–724.

[29] D.B. Wijayasekara, M.G. Cowan, J.T. Lewis, D.L. Gin, R.D. Noble, T.S. Bailey, Elastic free-standing RTIL composite membranes for CO_2/N_2 separation based on sphere-forming triblock/diblock copolymer blends, J. Memb. Sci. 511 (2016) 170–179.

[30] M.H. Al Marzouqi, M.A. Abdulkarim, S.A. Marzouk, M.H. El-Naas, H.M. Hasanain, Facilitated transport of CO_2 through immobilized liquid membrane, Ind. Eng. Chem. Res. 44 (2005) 9273–9278.

[31] P. Scovazzo, J. Kieft, D.A. Finan, C. Koval, D. DuBois, R. Noble, Gas separations using non-hexafluorophosphate $[PF_6]^-$ anion supported ionic liquid membranes, J. Memb. Sci. 238 (2004) 57–63.

[32] R.M. Teodoro, L.C. Tomé, D. Mantione, D. Mecerreyes, I.M. Marrucho, Mixing poly(ionic liquid)s and ionic liquids with different cyano anions: Membrane forming ability and CO_2/N_2separation properties, J. Memb. Sci. 552 (2018) 341–348.

[33] T.K. Carlisle, E.F. Wiesenauer, G.D. Nicodemus, D.L. Gin, R.D. Noble, Ideal CO_2 /light gas separation performance of poly(vinylimidazolium) membranes and poly(vinylimidazolium)-ionic liquid composite films, Ind. Eng. Chem. Res. 52 (2013).

[34] P. Li, K.P. Pramoda, T. S. Chung, CO_2 separation from flue gas using polyvinyl-(room temperature ionic liquid)–room temperature ionic liquid composite membranes, Ind. Eng. Chem. Res. 50 (2011) 9344–9353.

[35] A.S. Shaplov, S.M. Morozova, E.I. Lozinskaya, P.S. Vlasov, A.S.L. Gouveia, L.C. Tomé, I.M. Marrucho, Y.S. Vygodskii, Turning into poly(ionic liquid)s as a tool for polyimide modification: Synthesis, characterization and CO_2 separation properties, Polym. Chem. 7 (2016) 580–591.

[36] P. Li, Q. Zhao, J.L. Anderson, S. Varanasi, M.R. Coleman, Synthesis of copolyimides based on room temperature ionic liquid diamines, J. Polym. Sci. Part A Polym. Chem. 48 (2010) 4036–4046.

[37] A.S. Rewar, S. V. Shaligram, U.K. Kharul, Polybenzimidazole based polymeric ionic liquids (PILs): Effects of controlled degree of N-quaternization on physical and gas permeation properties, J. Memb. Sci. 497 (2016) 282–288.

[38] R.S. Bhavsar, S.C. Kumbharkar, A.S. Rewar, U.K. Kharul, Polybenzimidazole based film forming polymeric ionic liquids: Synthesis and effects of cation-anion variation on their physical properties, Polym. Chem. 5 (2014) 4083–4096.

[39] M. Lee, U.H. Choi, D. Salas-de la Cruz, A. Mittal, K.I. Winey, R.H. Colby, H.W. Gibson, Imidazolium polyesters: Structure-property relationships in thermal behavior, ionic conductivity, and morphology, Adv. Funct. Mater. 21 (2011) 708–717.

[40] B. Lin, L. Qiu, B. Qiu, Y. Peng, F. Yan, A soluble and conductive polyfluorene ionomer with pendant imidazolium groups for alkaline fuel cell applications, Macromolecules. 44 (2011) 9642–9649.

[41] R. Gao, M. Zhang, S.W. Wang, R.B. Moore, R.H. Colby, T.E. Long, Polyurethanes containing an imidazolium diol-based ionic-liquid chain extender for incorporation of ionic-liquid electrolytes, Macromol. Chem. Phys. 214 (2013) 1027–1036.

[42] T.O. Magalhães, A.S. Aquino, F.D. Vecchia, F.L. Bernard, M. Seferin, S.C. Menezes, R. Ligabue, S. Einloft, Syntheses and characterization of new poly(ionic liquid)s designed for CO2 capture, RSC Adv. 4 (2014) 18164–18170.

[43] J. Xia, S. Liu, T.S. Chung, Effect of end groups and grafting on the CO_2 separation performance of poly(ethylene glycol) based membranes, Macromolecules. 44 (2011) 7727–7736. doi:10.1021/ma201844y.

[44] V. Nafisi, M.-B. Hägg, Development of dual layer of ZIF-8/PEBAX-2533 mixed matrix membrane for CO_2 capture, J. Memb. Sci. 459 (2014) 244–255.

[45] H.Z. Chen, P. Li, T.S. Chung, PVDF/ionic liquid polymer blends with superior separation performance for removing CO_2 from hydrogen and flue gas, Int. J. Hydrogen Energy. 37 (2012) 11796–11804.

[46] M. Fang, C. Wu, Z. Yang, T. Wang, Y. Xia, J. Li, ZIF-8/PDMS mixed matrix membranes for propane/nitrogen mixture separation: Experimental result and permeation model validation, J. Memb. Sci. 474 (2015) 103–113.

[47] T.W. Pechar, S. Kim, B. Vaughan, E. Marand, M. Tsapatsis, H.K. Jeong, C.J. Cornelius, Fabrication and characterization of polyimide-zeolite L mixed matrix membranes for gas separations, J. Memb. Sci. 277 (2006) 195–202.

[48] M. Galizia, W.S. Chi, Z.P. Smith, T.C. Merkel, R.W. Baker, B.D. Freeman, 50th anniversary perspective: Polymers and mixed matrix membranes for gas and vapor Separation: A review and prospective opportunities, Macromolecules. 50 (2017) 7809–7843.

[49] G. Dong, Y. Zhang, J. Hou, J. Shen, V. Chen, Graphene oxide nanosheets based novel facilitated transport membranes for efficient CO_2 capture, Ind. Eng. Chem. Res. 55 (2016) 5403–5414.

[50] M. Rezi Abdul Hamid, H. K. Jeong, Recent advances on mixed-matrix membranes for gas separation: Opportunities and engineering challenges, Korean J. Chem. Eng. 35 (2018) 1577–1600.

[51] B. Sasikumar, G. Arthanareeswaran, A.F. Ismail, Recent progress in ionic liquid membranes for gas separation, J. Mol. Liq. 266 (2018) 330–341.

[52] Y.C. Hudiono, T.K. Carlisle, J.E. Bara, Y. Zhang, D.L. Gin, R.D. Noble, A three-component mixed-matrix membrane with enhanced CO_2 separation properties based on zeolites and ionic liquid materials, J. Memb. Sci. 350 (2010) 117–123.

[53] J.G. Wijmans, R.W. Baker, The solution-diffusion model a review, J. Memb. Sci. 107 (1995) 1–21.

[54] D.R. Paul, Reformulation of the solution-diffusion theory of reverse osmosis, J. Memb. Sci. 241 (2004) 371–386.

[55] L.M. Robeson, Correlation of separation factor versus permeability for polymeric membranes, J. Memb. Sci. 62 (1991) 165–185.

[56] L.M. Robeson, The upper bound revisited, J. Memb. Sci. 320 (2008) 390–400.

[57] M.G. Cowan, D.L. Gin, R.D. Noble, Poly(ionic liquid)/ionic liquid ion-gels with high "free" ionic liquid content: Platform membrane materials for CO_2/light gas separations, Acc. Chem. Res. 49 (2016) 724–732.

[58] H. Lin, E. Van Wagner, R. Raharjo, B.D. Freeman, I. Roman, High-performance polymer membranes for natural-gas sweetening, Adv. Mater. 18 (2006) 39–44.

[59] Q. Li, S. Jiang, S. Ji, M. Ammar, Q. Zhang, J. Yan, Synthesis of magnetically recyclable ZIF-8@SiO_2@Fe_3O_4 catalysts and their catalytic performance for Knoevenagel reaction, J. Solid State Chem. 223 (2015) 65–72.

[60] H. Li, L. Tuo, K. Yang, H.K. Jeong, Y. Dai, G. He, W. Zhao, Simultaneous enhancement of mechanical properties and CO_2 selectivity of ZIF-8 mixed matrix membranes: Interfacial toughening effect of ionic liquid, J. Memb. Sci. 511 (2016) 130–142.

[61] H.Z. Chen, P. Li, T.S. Chung, PVDF/ionic liquid polymer blends with superior separation performance for removing CO_2 from hydrogen and flue gas, Int. J. Hydrogen Energy. 37 (2012) 11796–11804.

[62] H. Koolivand, A. Sharif, M.R. Kashani, M. Karimi, M.K. Salooki, M.A. Semsarzadeh, Functionalized graphene oxide/polyimide nanocomposites as highly CO_2-selective membranes, J. Polym. Res. 21 (2014).

[63] S. Kanehashi, G.Q. Chen, C.A. Scholes, B. Ozcelik, C. Hua, L. Ciddor, P.D. Southon, D.M. D'Alessandro, S.E. Kentish, Enhancing gas permeability in mixed matrix membranes through tuning the nanoparticle properties, J. Memb. Sci. 482 (2015) 49–55.

[64] R.W. Baker, B.T. Low, Gas separation membrane materials: A perspective, macromolecules. 47 (2014) 6999–7013.

[65] A. Abdelrasoul, H. Doan, A. Lohi, C. H. Cheng, Morphology control of polysulfone membranes in filtration processes: A critical review, ChemBioEng Rev. 2 (2015) 22–43.

[66] L. Zhu, H. Song, J. Wang, L. Xue, Polysulfone hemodiafiltration membranes with enhanced anti-fouling and hemocompatibility modified by poly(vinyl pyrrolidone) via in situ cross-linked polymerization, Mater. Sci. Eng. C. 74 (2017) 159–166.

[67] X.-L.W. Qian Li, Joseph Imbrogno, Georges Belfort, Making polymeric membranes antifouling via "grafting from" polymerization of zwitterions, J. Appl. Polym. Sci. (2015) 41781.

[68] D.J. Miller, D.R. Dreyer, C.W. Bielawski, D.R. Paul, B.D. Freeman, Surface modification of water purification membranes, Angew. Chemie Int. Ed. 56 (2017) 4662–4711.

[69] J. Wang, Y. Xu, L. Zhu, J. Li, B. Zhu, Amphiphilic ABA copolymers used for surface modification of polysulfone membranes, Part 1: Molecular design, synthesis, and characterization, Polymer (Guildf). 49 (2008) 3256–3264.

[70] M. Ping, X. Zhang, M. Liu, Z. Wu, Z. Wang, Surface modification of polyvinylidene fluoride membrane by atom-transfer radical-polymerization of quaternary ammonium compound for mitigating biofouling, J. Memb. Sci. 570–571 (2018) 286–293.

[71] J. Wu, H. Song, D. Li, W. Zhao, W. Zhang, L. Kang, F. Ran, C. Zhao, A effective approach for surface modification of polymer membrane via SI-eATRP in an electrochemical cell with a three electrode system, Surfaces and Interfaces. 8 (2017) 119–126.

[72] G.M. Geise, H.-S. Lee, D.J. Miller, B.D. Freeman, J.E. McGrath, D.R. Paul, Water purification by membranes: The role of polymer science, J. Polym. Sci. Part B Polym. Phys.

48 (2010) 1685–1718.

[73] K. Matyjaszewski, J. Xia, Atom transfer radical polymerization, Chem. Rev. 101 (2001) 2921–2990.

[74] J. Xia, K. Matyjaszewski, Controlled/"living" radical polymerization. Atom transfer radical polymerization using multidentate amine ligands, Macromolecules. 30 (1997) 7697–7700.

[75] K. Matyjaszewski, Advanced materials by atom transfer radical polymerization, Adv. Mater. 30 (2018) 1706441.

[76] T. Holm, Association of butyllithium in diethyl ether and in tetrahydrofuran, Acta Chem. Scand. B. 32 (1978) 162–166.

[77] C. Hoffmann, H. Silau, M. Pinelo, J.M. Woodley, A.E. Daugaard, Surface modification of polysulfone membranes applied for a membrane reactor with immobilized alcohol dehydrogenase, Mater. Today Commun. 14 (2018) 160–168.

[78] M.S. Raja Shahrom, C.D. Wilfred, A.K.Z. Taha, CO_2 capture by task specific ionic liquids (TSILs) and polymerized ionic liquids (PILs and AAPILs), J. Mol. Liq. 219 (2016) 306–312.

[79] E. Karjalainen, D.J. Wales, D.H.A.. Gunasekera, J. Dupont, P. Licence, R.D. Wildman, V. Sans, Tunable ionic control of polymeric films for inkjet based 3D printing, ACS Sustain. Chem. Eng. 6 (2018) 3984–3991.

[80] H.M.L. Thijs, C.R. Becer, C. Guerrero-Sanchez, D. Fournier, R. Hoogenboom, U.S. Schubert, Water uptake of hydrophilic polymers determined by a thermal gravimetric analyzer with a controlled humidity chamber, J. Mater. Chem. 17 (2007) 4864–4871.

[81] T. Kelen, F. Tüdös, Analysis of the linear methods for determining copolymerization reactivity ratios. I. A new improved linear graphic method, J. Macromol. Sci. Part A - Chem. 9 (1975) 1–27.

[82] J.P. Kennedy, T. Kelen, F. Tüdös, Analysis of the linear methods for determining copolymerization reactivity ratios. II. A critical reexamination of cationic monomer reactivity ratios, J. Polym. Sci. Polym. Chem. Ed. 13 (1975) 2277–2289.

[83] T. Feng, B. Lin, S. Zhang, N. Yuan, F. Chu, M.A. Hickner, C. Wang, L. Zhu, J. Ding, Imidazolium-based organic–inorganic hybrid anion exchange membranes for fuel cell applications, J. Memb. Sci. 508 (2016) 7–14.

[84] A. Sayari, Y. Belmabkhout, R. Serna-Guerrero, Flue gas treatment via CO_2 adsorption, Chem. Eng. J. 171 (2011) 760–774.

[85] H.D. Nguyen, D. Löf, S. Hvilsted, A.E. Daugaard, Highly branched bio-based unsaturated

polyesters by enzymatic polymerization, Polymers. 8 (2016) 363.

[86] G. Zarca, W.J. Horne, I. Ortiz, A. Urtiaga, J.E. Bara, Synthesis and gas separation properties of poly(ionic liquid)-ionic liquid composite membranes containing a copper salt, J. Memb. Sci. 515 (2016) 109–114.

[87] D.J.C. H. B. Park, C. H. Jung, Y.M. Lee, A. J. Hill, S. J. Pas, S. T. Mudie, E. V. Wagner, B. D. Freeman, Polymers with cavities tuned for fast selective transport of small molecules and ions, Science (80-.). 318 (2007) 254–258.

[88] Z. Ma, Z. Qiao, Z. Wang, X. Cao, Y. He, J. Wang, S. Wang, CO_2 separation enhancement of the membrane by modifying the polymer with a small molecule containing amine and ester groups, RSC Adv. 4 (2014) 21313.

[89] X. Zhou, M.M. Obadia, S.R. Venna, E.A. Roth, A. Serghei, D.R. Luebke, C. Myers, Z. Chang, R. Enick, E. Drockenmuller, H.B. Nulwala, Highly cross-linked polyether-based 1,2,3-triazolium ion conducting membranes with enhanced gas separation properties, Eur. Polym. J. 84 (2016) 65–76.

[90] X. Wang, Y. Zhou, Z. Guo, G. Chen, J. Li, Y. Shi, Y. Liu, J. Wang, Heterogeneous conversion of CO_2 into cyclic carbonates at ambient pressure catalyzed by ionothermal-derived meso-macroporous hierarchical poly(ionic liquid)s, Chem. Sci. 6 (2015) 6916–6924.

[91] Y. Xie, Q. Sun, Y. Fu, L. Song, J. Liang, X. Xu, H. Wang, J. Li, S. Tu, X. Lu, J. Li, Sponge-like quaternary ammonium-based poly(ionic liquid)s for high CO_2 capture and efficient cycloaddition under mild conditions, J. Mater. Chem. A. 5 (2017) 25594–25600.

[92] R.R. Shaikh, S. Pornpraprom, V. D Elia, Catalytic strategies for the cycloaddition of pure, diluted, and Waste CO_2 to epoxides under ambient conditions, ACS Catal. 8 (2018) 419–450.

[93] M. North, Synthesis of cyclic carbonates from epoxides and carbon dioxide using bimetallic aluminium (salen) complexes, Arkivoc. 2012 (2012) 610–628.

[94] S.B. Lawrenson, R. Arav, M. North, The greening of peptide synthesis, Green Chem. 19 (2017) 1685–1691.

[95] B. Schäffner, F. Schäffner, S.P. Verevkin, A. Börner, Organic carbonates as solvents in synthesis and catalysis, Chem. Rev. 110 (2010) 4554–4581.

[96] X. Wei, W. Xu, M. Vijayakumar, L. Cosimbescu, T. Liu, V. Sprenkle, W. Wang, TEMPO-based catholyte for high-energy density nonaqueous redox flow batteries, Adv. Mater. 26 (2014) 7649–7653.

[97] B. Yu, B. Zou, C.W. Hu, Recent applications of polyoxometalates in CO_2 capture and

transformation, J. CO_2 Util. 26 (2018) 314–322.

[98] A.A. Olajire, Synthesis chemistry of metal-organic frameworks for CO_2 capture and conversion for sustainable energy future, Renew. Sustain. Energy Rev. 92 (2018) 570–607.

[99] Z.Z. Yang, L.N. He, J. Gao, A.H. Liu, B. Yu, Carbon dioxide utilization with C-N bond formation: Carbon dioxide capture and subsequent conversion, Energy Environ. Sci. 5 (2012) 6602–6639.

[100] M. Alves, B. Grignard, R. Mereau, C. Jerome, T. Tassaing, C. Detrembleur, Organocatalyzed coupling of carbon dioxide with epoxides for the synthesis of cyclic carbonates: Catalyst design and mechanistic studies, Catal. Sci. Technol. 7 (2017) 2651–2684.

[101] B.H. Xu, J.Q. Wang, J. Sun, Y. Huang, J.P. Zhang, X.P. Zhang, S.J. Zhang, Fixation of CO_2 into cyclic carbonates catalyzed by ionic liquids: A multi-scale approach, Green Chem. 17 (2015) 108–122.

[102] J.W. Huang, M. Shi, Chemical fixation of carbon dioxide by NaI/PPh3/PhOH, J. Org. Chem. 68 (2003) 6705–6709.

[103] J.D.E. Pasquale, Unusual Catalysis with Nickel(Q) Complexes, Chem. Commun. 5 (1973) 157–158.

[104] W.N. Sit, S.M. Ng, K.Y. Kwong, C.P. Lau, Coupling reactions of CO_2 with neat epoxides catalyzed by PPN salts to yield cyclic carbonates, J. Org. Chem. 70 (2005) 8583–8586.

[105] Y. Xie, J. Liang, Y. Fu, M. Huang, X. Xu, H. Wang, S. Tu, J. Li, with high ionic density for e ffi cient CO_2 capture and conversion into cyclic carbonates, J. Mater. Chem. A Mater. Energy Sustain. 6 (2018) 6660–6666.

[106] W. Wang, Y. Wang, C. Li, L. Yan, M. Jiang, Y. Ding, State-of-the-art multifunctional heterogeneous POP catalyst for cooperative transformation of CO_2 to cyclic carbonates, ACS Sustain. Chem. Eng. 5 (2017) 4523–4528.

[107] M. Ding, H.L. Jiang, Incorporation of imidazolium-based poly(ionic liquid)s into a metal-organic framework for CO_2 capture and conversion, ACS Catal. 8 (2018) 3194–3201.

[108] D. De, T.K. Pal, S. Neogi, S. Senthilkumar, D. Das, S. Sen Gupta, P.K. Bharadwaj, A versatile CuII metal-organic framework exhibiting high gas storage capacity with selectivity for CO_2: Conversion of CO_2 to cyclic carbonate and other catalytic abilities, Chem. - A Eur. J. 22 (2016) 3387–3396.

[109] M. Ahmed, A. Sakthivel, Preparation of cyclic carbonate via cycloaddition of CO_2 on epoxide using amine-functionalized SAPO-34 as catalyst, J. CO_2 Util. 22 (2017) 392–399.

[110] Z. Dai, R.D. Noble, D.L. Gin, X. Zhang, L. Deng, Combination of ionic liquids with membrane technology: A new approach for CO_2 separation, J. Memb. Sci. 497 (2016) 1–20.

[111] Q. Su, Y. Qi, X. Yao, W. Cheng, L. Dong, S. Chen, S. Zhang, Ionic liquids tailored and confined by one-step assembly with mesoporous silica for boosting the catalytic conversion of CO_2 into cyclic carbonates, Green Chem. 20 (2018) 3232–3241.

[112] L.C. Tomé, I.M. Marrucho, Ionic liquid-based materials: a platform to design engineered CO_2 separation membranes, Chem. Soc. Rev. 45 (2016) 2785–2824.

[113] Y. Sun, H. Huang, H. Vardhan, B. Aguila, C. Zhong, J.A. Perman, A.M. Al-Enizi, A. Nafady, S. Ma, Facile approach to graft ionic liquid into MOF for improving the efficiency of CO_2 chemical fixation, ACS Appl. Mater. Interfaces. 10 (2018) 27124–27130.

[114] Z. Guo, Q. Jiang, Y. Shi, J. Li, X. Yang, W. Hou, Y. Zhou, J. Wang, Tethering dual hydroxyls into mesoporous poly(ionic liquid)s for chemical fixation of CO_2 at ambient conditions: A combined experimental and theoretical study, ACS Catal. 7 (2017) 6770–6780.

[115] Y. Zhang, B. Wang, E.H.M. Elageed, L. Qin, B. Ni, X. Liu, G. Gao, Swelling poly(ionic liquid)s: Synthesis and application as quasi-homogeneous catalysts in the reaction of ethylene carbonate with aniline, ACS Macro Lett. 5 (2016) 435–438.

[116] M. North, R. Pasquale, C. Young, Synthesis of cyclic carbonates from epoxides and CO_2, Green Chem. 12 (2010) 1514–1539.

[117] M. Liu, L. Liang, X. Li, X. Gao, J. Sun, Novel urea derivative-based ionic liquids with dual-functions: CO_2 capture and conversion under metal- and solvent-free conditions, Green Chem. 18 (2016) 2851–2863.

[118] T. Song, J. Deng, L. Deng, L. Bai, X. Zhang, S. Zhang, P. Szabo, A.E. Daugaard, Poly(vinylimidazole-co-butyl acrylate) membranes for CO_2 separation, Polymer. 160 (2018) 223–230..

Appendix 1

Poly(Vinylimidazole-co-butyl acrylate) Membranes for CO_2 Separation

Ting Song[a, b], Jing Deng[c], Liyuan Deng[c], Lu Bai[b], Xiangping Zhang[b], Suojiang Zhang[b*], Peter Szabo[a] and Anders E. Daugaard[a*]

Published in *Polymer*, 160 (2019) 223–230

Appendix 1.1 - Publication

Polymer 160 (2019) 223–230

Contents lists available at ScienceDirect

Polymer

journal homepage: www.elsevier.com/locate/polymer

Poly(vinylimidazole-co-butyl acrylate) membranes for CO_2 separation

Ting Song[a,b], Jing Deng[c], Liyuan Deng[c], Lu Bai[b], Xiangping Zhang[b], Suojiang Zhang[b,*], Peter Szabo[a], Anders E. Daugaard[a,**]

[a] Danish Polymer Center, Department of Chemical and Biochemical Engineering, Technical University of Denmark, Building 229, 2800 Kgs, Lyngby, Denmark
[b] Beijing Key Laboratory of Ionic Liquids Clean Process, Institute of Process Engineering, Chinese Academy of Sciences, Beijing, 100190, China
[c] Department of Chemical Engineering, Norwegian University of Science and Technology, 7491, Trondheim, Norway

HIGHLIGHTS

- A range of poly(VIm-co-BuA) were prepared from 1-vinylimidazole and butyl acrylate.
- Reactivity ratios of VIm and BuA were determined through NLLSQ and Kelen and Tüdos.
- Poly(RT-IL) membranes were prepared by one-pot quarternization and cross linking.
- Poly(RT-IL) membranes were tested for permeability, CO_2/N_2 and CO_2/CH_4 selectivity.

ARTICLE INFO

Keywords:
N-vinylimidazole
poly(ionic liquid)
Crosslinking free-standing membrane
Gas separation

ABSTRACT

Room temperature ionic liquids (RTILs) are known to exhibit high CO_2 solubility, which makes them interesting candidates for separation and purification of mixed gas streams. Particularly, RTILs based on imidazoles have shown very promising results. However, membranes of the corresponding poly(RT-IL)s are inherently brittle, which makes them too fragile for use in freestanding membranes. Therefore, copolymers of N-vinylimidazole (VIm) and butyl acrylate (BuA) were prepared, showing reactivity ratios of $r_{BuA} = 1.91–2.02$ and $r_{VIm} = 0.094–0.10$. The prepared copolymers of poly(VIm-co-BuA) with a copolymer composition of 24:76 had sufficiently low T_g (−6.6 °C) and were flexible enough to be used for membrane preparation. The copolymer was quarternized and crosslinked in a one-pot reaction into thin film membranes employing a mixture of mono and difunctional alkyl halides. Membranes were prepared using a mixture of 1:8, 1:2 and 1:0 of 1,6-dibromohexane and 1-bromobutane, resulting in different degrees of crosslinking. The one-pot process additionally allows incorporation of up to 16 wt% free RTIL (BMIM Tf_2N) in the 1:0 ratio membranes. All membranes were tested for CO_2 permeability (33.7–54.38 barrer), and for selectivity towards N_2 and CH_4. By varying the crosslinking degree, it was observed that CO_2 permeability increased with decreasing the degree of crosslinking. Finally, films prepared with free RTIL led to an improvement of the gas separation performance, with CO_2 permeability increased from 33.71 to 38.77 barrer and CO_2/N_2 permselectivity increased from 20.81 to 27.82.

1. Introduction

Room temperature ionic liquids (RTILs), which contain large and unsymmetrical organic cations and organic or inorganic anions, are molten salts at temperatures below 100 °C [1,2]. RTILs are popular in many fields, such as for batteries, in extractions, for dispersion, as catalyst and for separation due to their excellent chemical, thermal, and electrochemical stability, nonflammability and negligible volatility [3–6]. Additionally, the high selection of possible counter ions, being cationic or anionic as well as hydrophilic/hydrophobic, endow RTILs tunable properties to match different applications. However, industrial application of RTILs has been limited due to their high viscosity, price and liquid morphology [7]. Therefore, it is attractive to combine RTILs with membrane technology, which presents advantages of lower energy costs, reduced volatility and easy reuse, to overcome the disadvantages of RTILs [8,9]. RTILs, especially imidazole based RTILs, possess better solubility to CO_2 than other light gases, such as N_2 and CH_4 [10]. Therefore, RTILs have been widely exploited to separate CO_2 from natural gas and flue gas over the past two decades. Initially, RTILs were used in supported ionic liquid membrane (SILM), where commercially

* Corresponding author.
** Corresponding author.
E-mail addresses: sjzhang@ipe.ac.cn (S. Zhang), adt@kt.dtu.dk (A.E. Daugaard).

https://doi.org/10.1016/j.polymer.2018.11.058
Received 4 October 2018; Received in revised form 22 November 2018; Accepted 26 November 2018
Available online 27 November 2018
0032-3861/

available membranes have been filled with a range of RTILs, showing CO_2 separation performance with ideal CO_2 permeabilities of more than 1000 Barrers and CO_2/N_2 permselectivity of more than 20 [11]. RTILs were immobilized in porous membranes with weak capillary forces, where loss of RTILs through leakage from the membrane support is significant [12]. This instability of SILMs under high pressure has limited their industrial application, even though SILMs have shown promising CO_2 separation performance [13]. In order to overcome the shortcomings of SILMs, Noble and Gin et al. [13,14] polymerized RTILs monomers with acrylic, styrenic or vinyl imidazole on porous support membranes to form stable poly(RTIL) membranes for gas separation. Poly(RTIL) membranes possess mechanical stability and efficiently immobilize the RTILs in contrast to SILM, but exhibit much lower gas permeability and diffusivity. That is attributed to a lower fractional free volume of the dense poly(RTIL) compared to that of free RTILs [7]. According to previous investigations, combinations of poly(RTIL) and RTILs in composite membranes improved CO_2 permeability by 400% relative to neat poly(RTIL) membrane due to the introduction of free RTILs [15]. However, imidazole-based poly(RTIL) are too brittle to form free-standing membranes and therefore have to be incorporated into porous polymer membranes as support or added into composites together with e.g. nanocellulose [16] or carbon nanotubes [17,18], which provides the necessary flexibility and mechanical stability to the systems. Alternatively, RTILs can also be grafted onto polymers, which possess excellent mechanical properties, such as polyimides [19,20], polybenzimidazoles [21,22], polyesters [23], polyethersulfones [24,25], polyurethane [26] to form novel and mechanically stable poly (ILs) membrane through condensation polymerization or by polymer modification [27]. In this study, we investigated the copolymerization of N-vinylimidazole (VIm) and butyl acrylate, to facilitate preparation of soft copolymers that could act as precursors for poly(RTIL) membranes. By use of a simple one-pot quarternization and crosslinking reaction, these copolymers are used for preparation of soft, flexible, free-standing membranes, which were investigated for gas separation properties.

2. Experimental

2.1. Chemicals

Butyl acrylate, N-vinylimidazole, 2,2′-azobis(2-methylpropionitrile) (AIBN), dimethylformamide (DMF), 1, 6-dibromohexane and 1-bromobutane were purchased from Sigma-Aldrich. Ethanol was from VWR. The ionic liquid 1-butyl-3-methylimidazolium bis(trifluoromethylsulfonyl)imide ([BMIM] [Tf_2N]) was purchased from Iolitec Ionic Liquids Technologies company. Inhibitors were removed from the monomers by passing them through neutral alumina prior to use. All other chemicals were used as received.

CO_2, N_2, and CH_4 gases were purchased from AGA Co. Ltd with a purity grade of 99.999%.

2.2. General synthesis of polymers, exemplified by poly(vinylimidazole-co-butyl acrylate) (exemplified with poly(VIm-co-BuA) 48:52)

AIBN (0.087 g, 0.53 mmol) was dissolved in DMF (10 mL) and monomers, N-vinylimidazole (1.9 g, 20.2 mmol) and butyl acrylate (2.6 g, 20.3 mmol), were added into the flask. The reaction mixture was bubbled with nitrogen for 20 min to remove all traces of oxygen. The polymerization mixture stirred under nitrogen using a magnetic stirrer for 10 h at 70 °C. During the polymerization the viscosity of the mixture gradually increased due to the conversion of monomer. The crude product was purified by precipitation into ether, it was redissolved in EtOH and precipitated into ether again. The product copolymer was then dried in *vacuo* until constant mass. Poly(vinylimidazole) (poly (VIm)) and poly(butyl acrylate) (poly(BuA)) and other copolymers were also synthesized using the general method (see supporting information for experimental and analytical data shown in supporting information SI-Figs. 1–16).

IR (cm^{-1}): 3111cm^{-1} (C=C-H), 3012-2844 cm^{-1}, 1451cm^{-1} (-CH_2-), 1727 cm^{-1} and 1160 cm^{-1} (C=O and C-O-C in acrylate group), 1660 cm^{-1}, 1494 cm^{-1}, 1223 cm^{-1}, 1267 cm^{-1} (N=C and C=C), 914 cm^{-1}, 664 cm^{-1}, 632 cm^{-1} (C=C-H and N=C-H);

^{1}H NMR (δ_H, ppm, $CDCl_3$): 7.4–6.4 (m, 3H), 4.1–3.5 (m, 2H), 2.27–1.45(m, 6H), 1.46 (m, 2H), 1.26 (m, 2H), 0.87 (m, 3H).

2.3. General procedure for preparation of crosslinked poly(VIm-co-BuA) membranes (exemplified with the 20% crosslinked membrane)

Poly(VIm-co-BuA) (24:76, 1.5 g, 3.0 mmol functional group) was dissolved in ethanol (12 mL) by stirring overnight. Then 1,6-dibromohexane (0.09 g, 0.37 mmol) and 1-bromobutane (0.42 g, 3.01 mmol) (The details for the other compositions are showed in the supporting information) were introduced into the copolymer solution to prepare membranes with different crosslinking degree, and the mixture was stirred for additionally 1 h. The solution was degassed by ultrasonication for 10 min and solvent casted in a Teflon petri dish. The casting solution was allowed to evaporate at ambient conditions in a fume hood. To remove entrapped residues of solvent, the casted membrane was dried in *vacuo* at 65 °C for 6 h. Procedures for all membranes can be seen in the supporting information.

2.4. Preparation of 100% cross linked poly(Vim-co-BuA) membrane with 16 wt% IL

The membrane was prepared in accordance with the general procedure using poly(VIm-co-BuA) (24:76, 1.5 g, 3 mmol functional group) was dissolved in ethanol (12 mL) by stirring overnight. Then, 1,6-dibromohexane (0.47 g, 1.92 mmol) and [BMIM] [Tf_2N] (0.38 g, 0.91 mmol)) were introduced in and stirred for extra 1 h. The solution was degassed by ultrasonication for 10 min and casted in a Teflon petri dish after. The casting solution was allowed to evaporation at ambient conditions in a fume hood. To remove entrapped residues of solvent, the casted membrane was dried in *vacuo* at 65 °C for 6 h. Membrane thickness is 122.4 μm.

2.5. Characterization methods

^{1}H Nuclear magnetic resonance (NMR) spectra of the as prepared poly(VIm-co-BuA) were carried out on a Bruker Avance 300 MHz spectrometer using deuterated dimethylsulfoxide or chloroform as solvents. Fourier transform infrared (FT-IR) was performed with a Niclet is50 ATR spectrometer with a diamond crystal from Thermo Scientific in the range of 4000-400 cm^{-1}. Size-exclusion chromatography (SEC) was carried out on Viscotek 200 instrument with PLgel mixed-D columns and refractive index detector. The measurement took place with THF (1 ml/min) as mobile phase at room temperature. Thermo gravimetric analysis (TGA) was performed in a nitrogen atmosphere on a Discovery TGA from TA Instruments. Differential scanning calorimetry (DSC) was performed on a Discovery DSC from TA Instruments. The thermal analyses were performed at a heating and cooling rate of 10 °C/min. Glass transition temperatures (T_g) were measured at the inflection point. The mechanical properties of the membranes were tested with Electroforce (EF) 3200 series from TA instrument with displacement ratio of 2.2 mm/min. The thickness of the membranes were measured with a Digitix II thickness gauge from NSK. At least 10 points were measured for every membrane; the average value was calculated and used as the membrane thickness. The extractables from the crosslinked membranes were measured by Soxhlet extraction with ethanol for 24 h, three times for each sample and calculated by use of eq. (1) [28].

$$X\,(Soxhlet)(\%) = Gel - content = \left(\frac{M_2}{M_1}\right)\cdot 100,\ M_2 \le M_1 \quad (1)$$

2.6. Gas permeation experiment

The single gas permeability (P) and diffusivity coefficient (D) of all the membranes were measured using a time-lag apparatus. A detailed description of the apparatus has been published elsewhere [29]. All the gases were tested after equilibration of the membrane in vacuum for 6 h to remove residual gases and water in the membrane. The single gas permeation was tested in the order of N_2, CH_4 and CO_2. All the measurements took place at room temperature with the upstream pressure of 2 bar and the downstream pressure of approximately 0.04 mbar. The mechanism for gas transporting through polymer membranes is known to follow a solution-diffusion mechanism. P (Barrer = 10^{-10} cm^3 (STP) $cm\ s^{-1}\ cm^{-2}\ cm\ Hg^{-1}$) was calculated by equation (2).

$$P = \frac{dp}{dt} \times \frac{V}{A} \times \frac{T_0}{p_0 T} \times \frac{l}{p_1 - p_2} \quad (2)$$

where dp/dt (Pa s^{-1}) is steady state pressure increase in time t, V (cm^3) is downstream volume, A (cm^2) represents the effective membrane area, T (K) is the temperature, l (cm) refers to the thickness of a membrane, T_0 and p_0 is the temperature and pressure at standard conditions which is 273.15 K and 1.0133×10^5 Pa, respectively.

The relationship of P, D ($cm^2\ s^{-1}$) and solubility (S) (cm^3 (STP) $cm^{-3}\ cm\ Hg^{-1}$) of the gas in the polymer membrane is described in eq. (3) [14].

$$P = S \times D \quad (3)$$

The single gas diffusivity coefficient can be calculated from eq. (4), in which "θ" represents "time-lag".

$$D = \frac{l^2}{6\theta} \quad (4)$$

The ideal selectivity, $\alpha_{i/j}$, was calculated by the ratio of species permeability, shown as eq. (5):

$$\alpha_{i/j} = \frac{P_i}{P_j} \quad (5)$$

3. Result and discussion

3.1. Synthesis of poly(VIm-co-BuA)

Imidazoles are popular for preparation of RTILs, since these are easily converted into a range of ILs by reaction with a broad selection of alkyl halides. Correspondingly, poly(RTILs) can easily be prepared by use of Vim based RTIL monomer, which polymerizes through free radical and controlled radical conditions. Poly(VIm) is a semicrystalline polymer, which is extremely brittle, which limits its application in many fields. It is also not possible to form free standing membranes consisting solely of poly(VIm) due to this brittleness. It was recently shown that direct 3D printing of mixtures of VIm and BuA result in a material with a significantly reduced brittleness [30]. Since, the copolymer composition from free radical copolymerization of BuA and VIm in solution has not been investigated, the copolymer reactivity ratios were determined by preparation of a range of different copolymers from different feed compositions. The structure of the prepared polymers was confirmed with FT-IR and ^{1}H NMR. The FT-IR spectra of poly(VIm), in Fig. 1, exhibits the characteristic peaks of VIm, where the peak at 3111 cm^{-1} is assigned to the C-H stretching in the imidazole ring, while the peaks at 1660 cm^{-1}, 1494 cm^{-1} are assigned to C=N and C-C stretching in the imidazole ring as well as peaks from ring vibrations at 1282 cm^{-1} and 1239 cm^{-1}. Moreover, the characteristic peaks of poly (BuA) are also shown in Fig. 1, the peaks range of 3011-2827 cm^{-1}, at 1451cm^{-1} and 1381cm^{-1} represent the C-H of methyl and methylene groups symmetric and asymmetric stretching. The peaks at 1727 $cm^{-1}$and 1154 cm^{-1} are related to stretching vibration of C=O and C-O-C in acrylate group. The poly(VIm-co-BuA) FT-IR spectra shows peaks from both poly(VIm) and poly(BuA), though the intensity of peaks originating from VIm are generally weaker than the peaks from poly(BuA). The hygroscopicity of PVIm [31] results in traces of water being observed in both poly(VIm) and poly(VIm-co-BuA) IR spectra, even though the samples were dried prior to analysis.

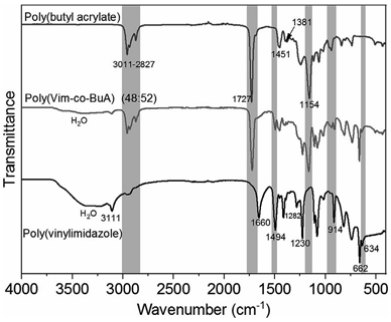

Fig. 1. The FT-IR spectra of poly(VIm), poly(VIm-co-BuA) (48:52) and poly (BuA).

The molar composition of the copolymer was calculated from ^{1}H NMR, where the molar fraction of VIm was determined from the integration of the imidazole protons at δ_H 7.4–6.4 ppm relative to the methylene protons (δ_H 4.1–3.5 ppm) in BuA (as shown in Fig. 2). For instance, the molar fraction of VIm in poly(VIm-co-BuA) prepared from a feed composition of 50:50 VIm:BuA is 48 mol%.

The reactivity ratios, which illustrate the polymerization kinetics of the monomers, were determined based on a series of copolymerizations of BuA and VIm with 10, 30, 50, 70 and 90 mol% BuA, which were terminated at low conversion to ensure constant feed composition. From ^{1}H NMR of the initially formed products of poly(VIm-co-BuA), the copolymer content of BuA (F_1) and VIm (F_2) could be determined. Based on a non-linear least squares (NLLSQ) fit and the method of Kelen and Tüdos [32,33], the copolymer reactivity ratios were calculated as shown in Fig. 3.

The molar fraction of BuA in the feed (f_1) versus that in the copolymer (F_1) (shown in Fig. 3 (a)), shows a clear deviation from ideal copolymerization. The initially formed copolymer will have a higher content of BuA relative to VIm compared to the feed ratio. This is directly reflected in the reactivity ratios determined by the NLLSQ fit (r_{BuA} = 1.91 and r_{VIm} = 0.094) and by the method of Kelen and Tüdos (r_{BuA} = 2.02 and r_{VIm} = 0.10) for BuA and VIm, respectively. Even though these reactivity ratios deviate from ideal copolymerization, it is possible to obtain copolymers containing both repeating units, and therefore to use them for crosslinking into membranes.

A range of different copolymers of Vim and BuA was therefore prepared to determine the optimal copolymer compositions for preparation of free standing membranes with a high VIm content and a sufficient flexibility. The physical appearance of the prepared polymers is shown in the supporting information, SI-Fig 10. The polymers have an amphiphilic nature, which unfortunately prevents SEC analysis of the compositions with more than 24 mol% VIm in the copolymer (SEC in both THF and salted DMF has been tried). SEC of the 24 mol% VIm copolymer displays only a single peak, corroborating that a true copolymerization took place (SI-Fig 9). Thermal characterization of the copolymers was conducted by TGA and DSC (see Fig. 4).

The TGA analysis (shown in Fig. 4(a)) illustrates the hygroscopic nature of poly(Vim), where there is a very clear weight loss of water in the initial phase of the analysis for the homopolymer of Poly(Vim). With incorporation of BuA in the copolymers, this is reduced, though there is a minor weight loss observed, in-line with the amount of VIm in

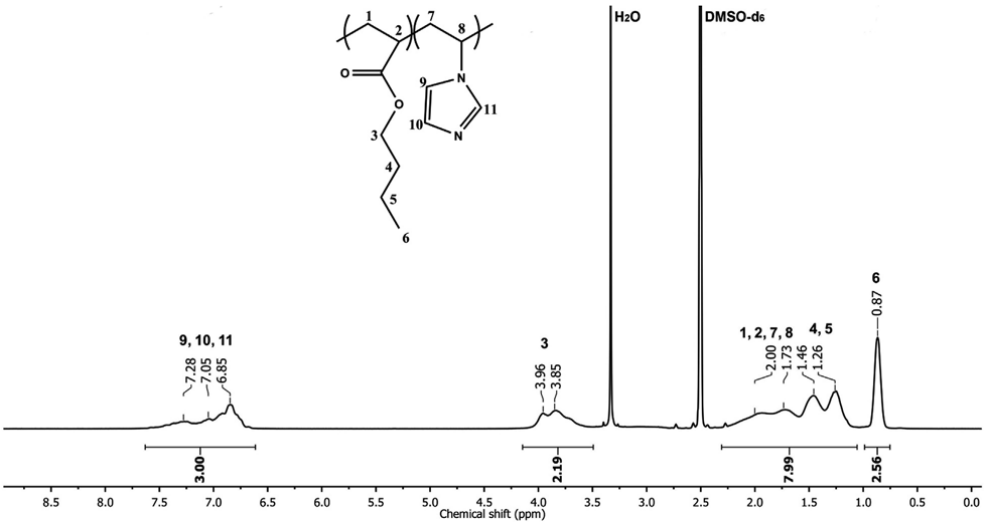

Fig. 2. ^{1}H NMR spectrum of poly(VIm-co-BuA) (48:52) run in DMSO-d_6.

the copolymers. The thermal degradation of all the copolymers takes place in a two-step behaviour, reflecting the content of the two monomers, and for all of the copolymers it is initiated at a lower temperature compared to the pure homopolymers (Poly(Vim) or Poly (BuA)), though this is still sufficiently high to permit application in gas-membranes.

The introduction of BuA provided the required flexibility for the copolymers (see DSC thermograms in Fig. 4(b)). An interesting detail can be seen from the first heating curve in the DSC analysis (SI-Fig 11), where the absorbed water results in an evaporation. After evaporation of the water, one glass transition (T_g) is observed for the homopolymers (−47.2 °C for Poly(BuA) and 164 °C for Poly(VIm)), while the copolymers show intermediate glass transition temperatures. For the two systems with a high content of VIm (48 and 63 mol%), two thermal transitions can be observed 26.9 °C and 151.3 °C as well as 41.8 °C and 158.6 °C, respectively. This could indicate formation of free Poly(Vim) or formation of a tapered copolymer (though this cannot be confirmed without SEC analysis). From all the prepared copolymers, poly(VIm-co-BuA) with ratio of 24:76 has the most interesting combination of a sufficiently high content of VIm, while still exhibiting a low glass transition temperature, ultimately resulting in a flexible material that can be used for membrane preparation.

3.2. Preparation of free-standing poly(VIm-co-BuA) membranes

Poly(RTIL) membranes were prepared from the 24:76 VIm:BuA copolymer (poly(VIm-co-BuA)) by direct one-pot solvent casting and crosslinking using mixtures of 1, 6-dibromohexane and 1-bromobutane as shown in Scheme 1.

The simultaneous crosslinking and functionalization reaction resulted in free-standing membranes, where reaction of the VIm repeating units leads to the highest possible amount of poly(RTIL) in each membrane. Three kinds of crosslinked membranes were prepared in this work, the so-called 20%, 50% and 100% crosslinked membranes have been prepared using a 1:8, 1:2 or a 1:0 ratio of 1, 6-dibromohexane to 1-bromobutane. By varying the ratio between cross-linker (1,6-bromohexane) and blocking agent (1-bromobutane), membranes with different crosslinking degree were obtained, while maintaining a similar IL character.

Any unreacted blocking agent or cross-linker was removed in a

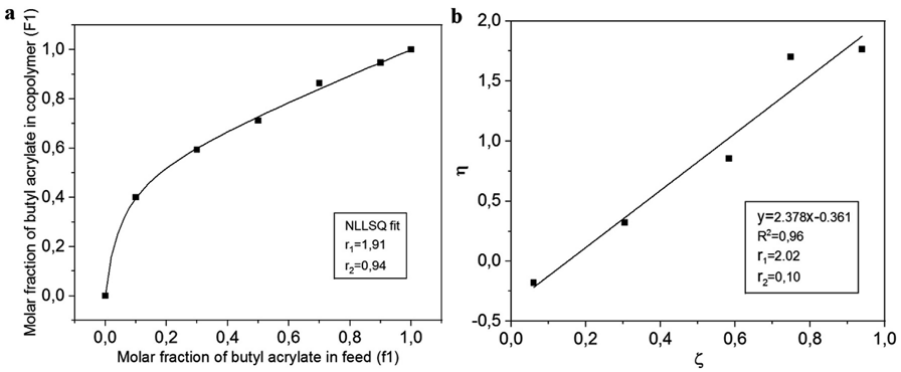

Fig. 3. a) Poly(VIm-co-BuA) composition diagram and NLLSQ fit. b) Kelen-Tüdos plot of poly(VIm-co-BuA).

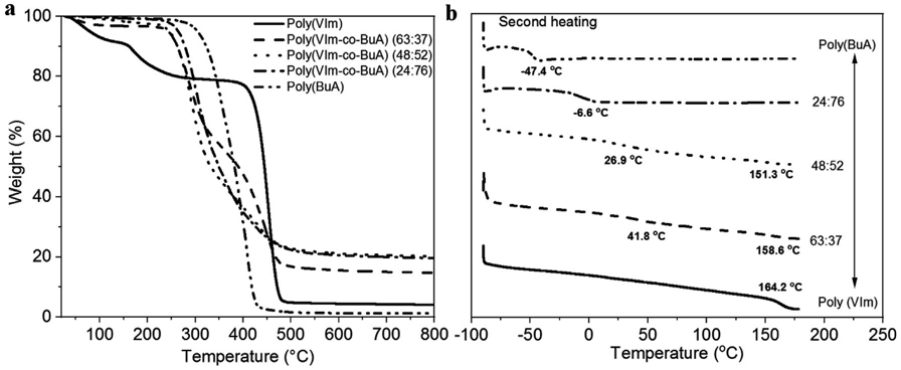

Fig. 4. Thermogravimetric analysis (a) and DSC thermograms showing second heating cycle (b) of poly(VIm), poly(BuA) and copolymers with different composition.

vacuum oven after crosslinking, resulting in membranes with a low soluble fraction (< 10%) and very high gel fractions (> 90%), which was determined through Soxhlet extraction in ethanol, as shown in Table 1. Free IL in membranes is known to increase the permeability of CO_2, and addition of free IL into the one-pot process was therefore also tested. BMIM Tf_2N, which is one of the most commonly used and commercially available RTILs for CO_2 separation [15,34,35], was selected in this work. It was possible to add up to 16 wt% free RTIL Bmim Tf_2N in the one-pot process using 100% cross linker. Free IL hindered the crosslinking reaction, and it was therefore only possible to add free IL to this membrane composition and membranes with higher free IL content could not be prepared.

There is no obvious difference observed in the FT-IR spectra of membranes with different crosslinking degree (shown in Fig. 5 (a)), since these membranes are effectively chemically equivalent. Fig. 5 (b) shows the FT-IR spectra of the 100% crosslinked membrane, 100% crosslinked membrane with free ionic liquid BMIM Tf_2N and the ionic liquid, BMIM Tf_2N. It can be seen that the peaks of 100% crosslinked membrane with free ionic liquid is the combination of that of BMIM Tf_2N and 100% crosslinked membrane. Additionally, there is no shift of the peaks, indicating that there are no chemical interaction between the membrane network and the ionic liquid.

Table 1
Gel fraction and mechanical properties of membranes.

	Gel fraction (%)	Young's modulus (MPa)	Tensile strength (MPa)	Elongation at break (%)
20%	95.77 ± 0.1	0.0015	0.024	> 53
50%	97.39 ± 0.39	0.0135	0.061	> 53
100%	98.41 ± 0.03	0.0395	0.11	29.8
100% + 16 wt% IL	85.35 ± 0.18	0.0034	0.056	39.2

3.3. Thermal properties

Thermogravimetric analysis of the membranes (see Fig. 6) show an even earlier onset of decomposition for the membranes compared to that of poly(VIm-co-BuA), which decreased from 268 °C to 220 °C after crosslinking. This is attributed to the presence of the imidazolium salts in the polymer backbone, which is the only change of the material after crosslinking. For the membranes, the first stage of weight loss is observed between 220 and 350 °C corresponding to decomposition of the cross linker and the acrylate part of the polymer backbone; while the second degradation between 350 and 530 °C is attributed to decomposition of the imidazole ring and the polymer backbone, as has also been observed in other imidazole systems [36]. The residue after

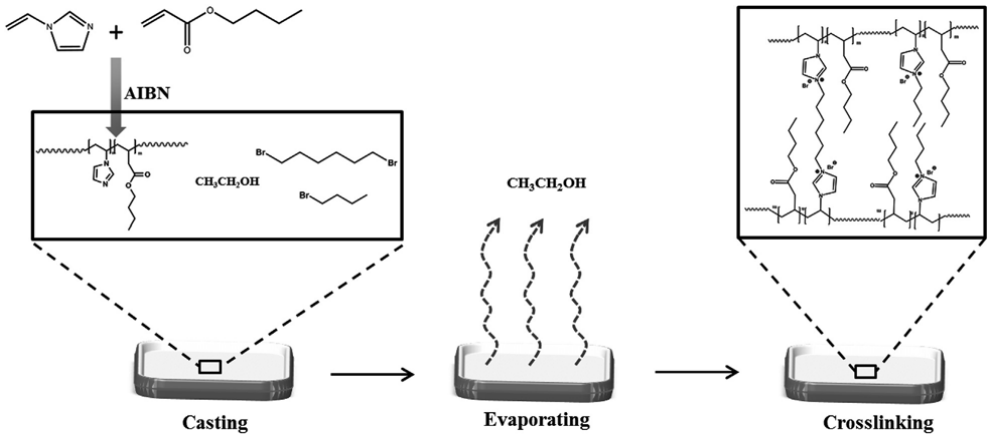

Scheme 1. Copolymer preparation and one-pot casting and crosslinking of membranes.

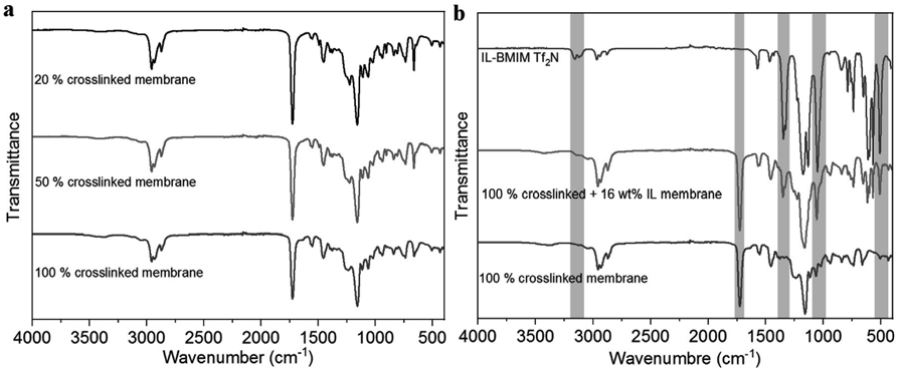

Fig. 5. FT-IR spectra of all the prepared membranes with 20, 50 and 100% cross linker (a) as well as the 100% crosslinked membrane with free ionic liquid and the ionic liquid BMIM Tf_2N (b).

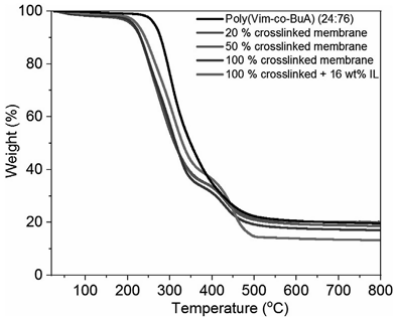

Fig. 6. TGA of poly(VIm-co-BuA) (24:76) and all the prepared membranes.

thermal degradation is constant for all the membranes, indicating that this relates to the copolymer composition and not the cross linker/butyl bromide ratio. In the case of additional free IL, this residue is reduced corresponding to the 16 wt% of IL. The thermal stability of the all membranes is concluded to be sufficient for these materials to be applicable for gas separation membranes, where temperatures between 25 and 75 °C of representative flue gas are expected [37].

The thermal properties of the crosslinked membranes were also investigated by DSC (SI-Fig 17-20). From the first heating curve in the DSC analysis of the membranes, evaporation of water can be seen in all of the membranes, which is attributed to the hygroscopic nature of systems containing Vim and the hydrophilic property of ILs with halogen as counter ion. However, on the second heating curve, it is not possible to identify glass transition temperatures for any of the membranes. Crosslinking of the membranes was expected to result in a minor increase in glass transition temperature compared to the original copolymer, as is well known from other curing reactions [38]. All of the membranes appear soft and flexible, which indicate that the apparent glass transition temperatures is below RT (see picture of films in SI-Fig 21). This can either be a result of an actual low glass transition temperature, or a result of water plasticizing the crosslinked membranes.

3.4. Mechanical property of crosslinked poly(VIm-co-BuA) membrane

The mechanical properties of the membranes were evaluated by tensile testing. The stress-strain curve of the membranes is shown in supporting information SI-Fig 27. Young's modulus (MPa), Tensile strength (MPa) and elongation at break (%) for the membranes are summarized in Table 1.

Young's modulus was determined from the slope of the stress–strain curve, and it clearly increases with increasing degree of crosslinking. In addition, Young's modulus of the membrane with IL is observed to be between that of the 20% and 50% crosslinked membranes, because of the plasticizing effect. The 100% crosslinked membrane and 100% crosslinked membrane with 16 wt% IL showed elongations at break of 29.8% and 39.2%, respectively. However, the less crosslinked systems could not be extended to their breaking points due to instrument limitations, resulting in extensions at break above 53%. All of the membranes exhibit mechanical properties that enable them to be used for gas-phase membranes.

3.5. Gas permeation properties

The gas separation performances of all the membranes were evaluated with a single gas apparatus. The permeability of CO_2, N_2 and CH_4 and permselectivities of CO_2/N_2 and CO_2/CH_4 are shown in Table 2, while solubility and diffiusivity of CO_2, N_2 and CH_4 are shown in Table 3. In a comparable study by Gabriel Zarca et al. [39], of a supported poly[C_4vim] [Tf_2N]$^-$ membrane, they observed a CO_2 permeability of 5.2 barrer with CO_2/N_2 permselectivities of 17.3. The CO_2 permeability of membranes prepared in this work ranges from 33.71 to 54.38, which is an increase of 6.5–10.5 times, with CO_2/N_2 permselectivities of more than 20, even though halogen counterions are known to have significantly lower CO_2-philicity than Tf_2N^- counterions. This increased CO_2 permeability is attributed to the introduction of BuA, which leads to a much lower glass transition temperature of the membranes. At the same time, it also gave higher fractional free volume, which is known to be beneficial for gas transportation [40,41]. Additionally, the oxygen in the acrylate ester group and its ability to interact with CO_2, [42] could also be an explanation for the improvement of CO_2 permeability.

Table 2
The permeability of CO_2, N_2 and CH_4 and permselectivities of CO_2/N_2 and CO_2/CH_4.

Membrane	Permeability (Barrer)			Permselectivity	
	CO_2	N_2	CH_4	α_{CO_2/N_2}	α_{CO_2/CH_4}
20%	54.38	11.79	6.16	4.61	8.83
50%	44.35	2.05	5.16	21.63	8.59
100%	33.71	1.62	3.64	20.81	9.19
100% + 16 wt% IL	38.77	1.39	4.18	27.82	9.28

Table 3
The diffusivity and solubility of CO_2, N_2 and CH_4 in the crosslinked poly(VIm-co-BuA) membranes.

Membrane	Diffusivity ($\times 10^7$ $cm^2 s^{-1}$)			Solubility (cm^3(STP) cm^{-3} atm^{-1})		
	CO_2	N_2	CH_4	CO_2	N_2	CH_4
20%	1.95	2.42	1.91	2.12	0.37	0.25
50%	1.82	1.90	2.21	1.85	0.082	0.18
100%	1.44	N/A	1.49	1.78	N/A	0.19
100% + 16 wt% IL	1.95	N/A	1.57	1.51	N/A	0.20

N/A: time-lag could not be accurately determined due to very slow permeation rate.

Table 2 also shows that the gas permeability increases for membranes prepared with lower amounts of cross linker (50% and 20% mixtures), where the permeability of CO_2 increased from 33.71 to 44.35 barrer without compromising permselctivity. The increase of CO_2 permeability was favored from both CO_2 diffusivity and solubility (as shown in Table 3). The increase in diffusivity, is attributed to the higher fractional free volume of the less crosslinked membranes, which is consistent with results of other systems [43]. Membranes prepared with 20–50% cross linker show an increased solubility of CO_2, which is surprisingly not matched for the membrane with free IL. This leads us to hypothesize that this increase must be due to a greater interaction of CO_2 with the polymer bound RTIL introduced with the blocking agent. Additionally, the increase of CO_2 permeability is higher than that of N_2 and CH_4, which illustrates that the poly(RTIL) membranes have better affinity to CO_2. The observed difference in mechanical properties and lower degree of crosslinking in the membranes with 20% cross linker leads to a considerably more open structure, resulting in an increase in permeability, diffusivity and solubility of N_2 and CH_4 as shown in Tables 2 and 3

3.5.1. Composite membrane with free IL

Based on previous investigations, introduction of free ionic liquid is an efficient way to improve the CO_2 separation performance of poly(IL) membranes [14,35]. In this work, 16 wt% BMIM Tf_2N was added to the 100% crosslinked membrane. Tables 2 and 3 show gas separation behaviors of membranes before and after the addition of free IL. The gas permeability and permselectivity of the membrane with free IL increased as expected. At the same time, the diffusivity coefficient increased from 1.44 to 1.95 $\times 10^7$ $cm^2 s^{-1}$, but the solubility coefficient decreased from 1.78 to 1.51 cm^3 (STP) cm^{-3} atm^{-1}. This was an unexpected result, which illustrates that the increased permeability is a result of the added RTIL acting as a plasticizer of the poly(RTIL) membrane (diffusivity) as observed from the other systems, and apparently cannot be attributed to the high CO_2 solubility of free RTIL.

4. Conclusion

A series of copolymers of VIm and BuA were synthesized in the work. Poly(VIm-co-BuA) (24:76) was found to be the best compromise between content of VIm and thermal properties ($T_g = -6.6$ °C), and it was therefore used for preparation of free-standing poly(RTILs) membranes. Membranes were prepared by crosslinking poly(VIm-co-BuA) with a combination of 1, 6-dibromohexane (cross linker) and 1-bromobutane (blocker). The gas separation performance was directly correlated to the degree of crosslinking, where CO_2 permeability was increased from 33.7 barrer for the membrane prepared with only cross linker to 54.4 barrer for the membrane prepared from a 1:4 mixture of cross linker and blocking agent. However, this more flexible membrane also showed a significantly increased permeability of N_2. An optimal balance between permeability and selectivity was observed for the membrane prepared with 50% cross linker, which showed both a high permeability to CO_2 (44.4 barrer) as well as a good permselectivity of CO_2 over N_2 of 21.6. An ion gel was also prepared in this work by introducing 16 wt% free IL BMIM Tf_2N in the 100% cross linker membrane, showing increased CO_2 permeability from 33.71 to 38.77 barrer and increased permselectivity of CO_2/N_2 from 20.81 to 27.82.

The results showed that the prepared membranes have potential to separate CO_2 from flue gas and natural gas. Compared to the analogous neat poly(RTIL) membranes, both the permeability of CO_2 and the permselectivity of CO_2/N_2 were increased.

Acknowledgement

The Institute of Process Engineering in Beijing and Department of Chemical and Biochemical Engineering at the Technical university of Denmark, the National Key R&D Program of China (2017YFB0603401-03) as well as the National Natural Science Foundation of China (21425625) are greatly acknowledged for funding the project.

Appendix A. Supplementary data

Supplementary data to this article can be found online at https://doi.org/10.1016/j.polymer.2018.11.058.

References

[1] N. Nishimura, H. Ohno, 15th anniversary of polymerised ionic liquids, Polymer 55 (2014) 3289–3297, https://doi.org/10.1016/j.polymer.2014.02.042.
[2] S.P.M. Ventura, F.A. e Silva, M. V Quental, D. Mondal, M.G. Freire, J.A.P. Coutinho, Ionic-liquid-mediated extraction and separation processes for bioactive compounds: past, present, and future trends, Chem. Rev. 117 (2017) 6984–7052, https://doi.org/10.1021/acs.chemrev.6b00550.
[3] M. Armand, F. Endres, D.R. MacFarlane, H. Ohno, B. Scrosati, Ionic-liquid materials for the electrochemical challenges of the future, Nat. Mater. 8 (2009) 621–629, https://doi.org/10.1038/nmat2448.
[4] S.S. Hassoueneh, L. Yu, A.L. Skov, A.E. Daugaard, Soft and flexible conductive PDMS/MWCNT composites, J. Appl. Polym. Sci. 134 (2017), https://doi.org/10.1002/app.44767.
[5] W. Zhao, Y. Tang, J. Xi, J. Kong, Functionalized graphene sheets with poly(ionic liquid)s and high adsorption capacity of anionic dyes, Appl. Surf. Sci. 326 (2015) 276–284, https://doi.org/10.1016/j.apsusc.2014.11.069.
[6] T.P. Lodge, T. Ueki, Mechanically tunable, readily processable ion gels by self-assembly of block copolymers in ionic liquids, Acc. Chem. Res. 49 (2016) 2107–2114, https://doi.org/10.1021/acs.accounts.6b00308.
[7] A.M. Lopez, M.G. Cowan, D.L. Gin, R.D. Noble, Phosphonium-Based Poly(ionic liquid)/ionic liquid ion gel membranes: influence of structure and ionic liquid loading on lon conductivity and light gas Separation Performance, J. Chem. Eng. Data 63 (2018) 1154–1162, https://doi.org/10.1021/acs.jced.7b00541.
[8] D.B. Wijayasekara, M.G. Cowan, J.T. Lewis, D.L. Gin, R.D. Noble, T.S. Bailey, Elastic free-standing RTIL composite membranes for CO_2/N_2 separation based on sphere-forming triblock/diblock copolymer blends, J. Membr. Sci. 511 (2016) 170–179, https://doi.org/10.1016/j.memsci.2016.03.045.
[9] J. Ma, Y. Ying, X. Guo, H. Huang, D. Liu, C. Zhong, Fabrication of mixed-matrix membrane containing metal-organic framework composite with task-specific ionic liquid for efficient CO_2 separation, J. Mater. Chem. A. 4 (2016) 7281–7288, https://doi.org/10.1039/c6ta02611g.
[10] J.L. Anthony, E.J. Maginn, J.F. Brennecke, Solubilities and thermodynamic properties of gases in the ionic liquid 1-n-butyl-3-methylimidazolium hexafluorophosphate, J. Phys. Chem. B 106 (2002) 7315–7320, https://doi.org/10.1021/jp020631a.
[11] P. Scovazzo, J. Kieft, D.A. Finan, C. Koval, D. DuBois, R. Noble, Gas separations using non-hexafluorophosphate [PF6]- anion supported ionic liquid membranes, J. Membr. Sci. 238 (2004) 57–63, https://doi.org/10.1016/j.memsci.2004.02.033.
[12] R.M. Teodoro, L.C. Tomé, D. Mantione, D. Mecerreyes, I.M. Marrucho, Mixing poly (ionic liquid)s and ionic liquids with different cyano anions: membrane forming ability and CO_2/N_2separation properties, J. Membr. Sci. 552 (2018) 341–348, https://doi.org/10.1016/j.memsci.2018.02.019.
[13] J.E. Bara, S. Lessmann, C.J. Gabriel, E.S. Hatakeyama, R.D. Noble, D.L. Gin, Synthesis and performance of polymerizable room-temperature ionic liquids as gas separation membranes, Ind. Eng. Chem. Res. 46 (2007) 5397–5404, https://doi.org/10.1021/ie0704492.
[14] T.K. Carlisle, E.F. Wiesenauer, G.D. Nicodemus, D.L. Gin, R.D. Noble, Ideal CO_2/light gas separation performance of poly(vinylimidazolium) membranes and poly (vinylimidazolium)-ionic liquid composite films, Ind. Eng. Chem. Res. 52 (2013) 1023–1032, https://doi.org/10.1021/ie202305m.
[15] J.E. Bara, R.D. Noble, D.L. Gin, Effect of "free" cation substituent on gas separation performance of polymer – room-temperature ionic liquid composite membranes, Ind. Eng. Chem. Res. 48 (2009) 4607–4610, https://doi.org/10.1021/ie801897r.
[16] C. Vilela, N. Sousa, R.J.B. Pinto, A.J.D. Silvestre, F.M.L. Figueiredo, C.S.R. Freire,

Exploiting poly(ionic liquids) and nanocellulose for the development of bio-based anion-exchange membranes, Biomass Bioenergy 100 (2017) 116–125, https://doi.org/10.1016/j.biombioe.2017.03.016.
[17] D. Gendron, A. Ansaldo, G. Bubak, L. Ceseracciu, G. Vamvounis, D. Ricci, Poly(ionic liquid)-carbon nanotubes self-supported, highly electroconductive composites and their application in electroactive devices, Compos. Sci. Technol. 117 (2015) 364–370, https://doi.org/10.1016/j.compscitech.2015.07.016.
[18] T. Fukushima, A. Kosaka, Y. Yamamoto, T. Aimiya, S. Notazawa, T. Takigawa, T. Inabe, T. Aida, Dramatic effect of dispersed carbon nanotubes on the mechanical and electroconductive properties of polymers derived from ionic liquids, Small 2 (2006) 554–560, https://doi.org/10.1002/smll.200500404.
[19] A.S. Shaplov, S.M. Morozova, E.I. Lozinskaya, P.S. Vlasov, A.S.L. Gouveia, L.C. Tomé, I.M. Marrucho, Y.S. Vygodskii, Turning into poly(ionic liquid)s as a tool for polyimide modification: synthesis, characterization and CO2separation properties, Polym. Chem. 7 (2016) 580–591, https://doi.org/10.1039/c5py01553g.
[20] P. Li, Q. Zhao, J.L. Anderson, S. Varanasi, M.R. Coleman, Synthesis of copolyimides based on room temperature ionic liquid diamines, J. Polym. Sci. Part A Polym. Chem. 48 (2010) 4036–4046, https://doi.org/10.1002/pola.24189.
[21] A.S. Rewar, S.V. Shaligram, U.K. Kharul, Polybenzimidazole based polymeric ionic liquids (PILs): effects of controlled degree of N-quaternization on physical and gas permeation properties, J. Membr. Sci. 497 (2016) 282–288, https://doi.org/10.1016/j.memsci.2015.09.019.
[22] R.S. Bhavsar, S.C. Kumbharkar, A.S. Rewar, U.K. Kharul, Polybenzimidazole based film forming polymeric ionic liquids: synthesis and effects of cation-anion variation on their physical properties, Polym. Chem. 5 (2014) 4083–4096, https://doi.org/10.1039/c3py01709e.
[23] M. Lee, U.H. Choi, D. Salas-de la Cruz, A. Mittal, K.I. Winey, R.H. Colby, H.W. Gibson, Imidazolium Polyesters, Structure-property relationships in thermal behavior, ionic conductivity, and morphology, Adv. Funct. Mater. 21 (2011) 708–717, https://doi.org/10.1002/adfm.201001878.
[24] B. Lin, L. Qiu, B. Qiu, Y. Peng, F. Yan, A soluble and conductive polyfluorene ionomer with pendant imidazolium groups for alkaline fuel cell applications, Macromolecules 44 (2011) 9642–9649, https://doi.org/10.1021/ma202159d.
[25] A. Vollas, T. Chouliaras, V. Deimede, T. Ioannides, J. Kallitsis, A. Vollas, T. Chouliaras, V. Deimede, T. Ioannides, J. Kallitsis, New pyridinium type poly (Ionic Liquids) as membranes for CO_2 separation, Polymers 10 (2018) 912, https://doi.org/10.3390/polym10080912.
[26] R. Gao, M. Zhang, S.W. Wang, R.B. Moore, R.H. Colby, T.E. Long, Polyurethanes containing an imidazolium diol-based ionic-liquid chain extender for incorporation of ionic-liquid electrolytes, Macromol. Chem. Phys. 214 (2013) 1027–1036, https://doi.org/10.1002/macp.201200688.
[27] T.O. Magalhães, A.S. Aquino, F.D. Vecchia, F.L. Bernard, M. Seferin, S.C. Menezes, R. Ligabue, S. Einloft, Syntheses and characterization of new poly(ionic liquid)s designed for CO_2 capture, RSC Adv. 4 (2014) 18164–18170, https://doi.org/10.1039/c4ra00071d.
[28] C. Hirschl, L. Neumaier, S. Puchberger, W. Mühleisen, G. Oreski, G.C. Eder, R. Frank, M. Tranitz, M. Schoppa, M. Wendt, N. Bogdanski, A. Plösch, M. Kraft, Determination of the degree of ethylene vinyl acetate crosslinking via Soxhlet extraction: gold standard or pitfall? Sol. Energy Mater. Sol. Cells 143 (2015) 494–502, https://doi.org/10.1016/j.solmat.2015.07.043.
[29] Z. Dai, L. Ansaloni, D.L. Gin, R.D. Noble, L. Deng, Facile fabrication of CO_2 separation membranes by cross-linking of poly(ethylene glycol) diglycidyl ether with a diamine and a polyamine-based ionic liquid, J. Membr. Sci. 523 (2017) 551–560, https://doi.org/10.1016/j.memsci.2016.10.026.
[30] E. Karjalainen, D.J. Wales, D.H.A. Gunasekera, J. Dupont, P. Licence, R.D. Wildman, V. Sans, Tunable ionic control of polymeric films for inkjet based 3D printing, ACS Sustain. Chem. Eng. 6 (2018) 3984–3991, https://doi.org/10.1021/acssuschemeng.7b04279.
[31] H.M.L. Thijs, C.R. Becer, C. Guerrero-Sanchez, D. Fournier, R. Hoogenboom, U.S. Schubert, Water uptake of hydrophilic polymers determined by a thermal gravimetric analyzer with a controlled humidity chamber, J. Mater. Chem. 17 (2007) 4864–4871, https://doi.org/10.1039/b711990a.
[32] T. Kelen, F. Tüdös, Analysis of the linear methods for determining copolymerization reactivity ratios. I. A new improved linear graphic method, J. Macromol. Sci. Part A - Chem. 9 (1975) 1–27, https://doi.org/10.1080/00222337508068644.
[33] J.P. Kennedy, T. Kelen, F. Tüdös, Analysis of the linear methods for determining copolymerization reactivity ratios. II. A critical reexamination of cationic monomer reactivity ratios, J. Polym. Sci. Polym. Chem. Ed. 13 (1975) 2277–2289, https://doi.org/10.1002/pol.1975.170131010.
[34] J.E. Bara, C.J. Gabriel, S. Lessmann, T.K. Carlisle, A. Finotello, D.L. Gin, R.D. Noble, Enhanced CO_2 separation selectivity in oligo(ethylene glycol) functionalized room-temperature ionic liquids, Ind. Eng. Chem. Res. 46 (2007) 5380–5386, https://doi.org/10.1021/ie070437g.
[35] J.E. Bara, D.L. Gin, R.D. Noble, Effect of anion on gas separation performance of polymer−room-temperature ionic liquid composite membranes, Ind. Eng. Chem. Res. 47 (2008) 9919–9924, https://doi.org/10.1021/ie801019x.
[36] T. Feng, B. Lin, S. Zhang, N. Yuan, F. Chu, M.A. Hickner, C. Wang, L. Zhu, J. Ding, Imidazolium-based organic–inorganic hybrid anion exchange membranes for fuel cell applications, J. Membr. Sci. 508 (2016) 7–14, https://doi.org/10.1016/j.memsci.2016.02.019.
[37] A. Sayari, Y. Belmabkhout, R. Serna-Guerrero, Flue gas treatment via CO_2 adsorption, Chem. Eng. J. 171 (2011) 760–774, https://doi.org/10.1016/j.cej.2011.02.007.
[38] H.D. Nguyen, D. Löf, S. Hvilsted, A.E. Daugaard, Highly branched bio-based unsaturated polyesters by enzymatic polymerization, Polymers 8 (2016) 363, https://doi.org/10.3390/polym8100363.
[39] G. Zarca, W.J. Horne, I. Ortiz, A. Urtiaga, J.E. Bara, Synthesis and gas separation properties of poly(ionic liquid)-ionic liquid composite membranes containing a copper salt, J. Membr. Sci. 515 (2016) 109–114, https://doi.org/10.1016/j.memsci.2016.05.045.
[40] D.J.C.H.B. Park, C.H. Jung, Y.M. Lee, A.J. Hill, S.J. Pas, S.T. Mudie, E.V. Wagner, B.D. Freeman, Polymers with cavities tuned for fast selective transport of small molecules and ions, Science 318 (2007) 254–258, https://doi.org/10.1126/science.1146744.
[41] H. Lin, E. Van Wagner, R. Raharjo, B.D. Freeman, I. Roman, High-performance polymer membranes for natural-gas sweetening, Adv. Mater. 18 (2006) 39–44, https://doi.org/10.1002/adma.200501409.
[42] Z. Ma, Z. Qiao, Z. Wang, X. Cao, Y. He, J. Wang, S. Wang, CO_2 separation enhancement of the membrane by modifying the polymer with a small molecule containing amine and ester groups, RSC Adv. 4 (2014) 21313, https://doi.org/10.1039/c4ra01107d.
[43] X. Zhou, M.M. Obadia, S.R. Venna, E.A. Roth, A. Serghei, D.R. Luebke, C. Myers, Z. Chang, R. Enick, E. Drockenmuller, H.B. Nulwala, Highly cross-linked polyether-based 1,2,3-triazolium ion conducting membranes with enhanced gas separation properties, Eur. Polym. J. 84 (2016) 65–76, https://doi.org/10.1016/j.eurpolymj.2016.09.001.

Appendix 1.2 - Supporting information

Supporting information

Preparation of crosslinked Poly(Vinylimidazole-co-butyl acrylate) membranes for CO_2 separation

Ting Song[a, b], Jing Deng[c], Liyuan Deng[c], Lu Bai[b], Xiangping Zhang[b], Suojiang Zhang[b*], Peter Szabo[a] and Anders E. Daugaard[a*]

[a] *Danish Polymer Center, Department of Chemical and Biochemical Engineering, Technical University of Denmark, Building 229, 2800 Kgs. Lyngby, Denmark*

[b] *Beijing Key Laboratory of Ionic Liquids Clean Process, Institute of Process Engineering, Chinese Academy of Sciences, Beijing, 100190, China*

[c] *Department of Chemical Engineering, Norwegian University of Science and Technology, 7491, Trondheim, Norway*

Contents

Preparation of poly(vinylimidazole)

Poly(vinylimidazole) was prepared in accordance with the general polymerization procedure, using AIBN (0.087 g, 0.53 mmol), 1-vinylimiazole (5 g, 53 mmol) in DMF (10 mL). The product polymer was reclaimed as brown solid after precipitation into acetone (yield more than 65%, T_g= 164.2 ^oC).

IR (cm^{-1}): 3111cm^{-1} (C=C-H stretching), 1660 cm^{-1} (C=N stretching), 1494 cm^{-1} (N=C-H stretching), 1282 cm^{-1} and 1230cm^{-1} (ring vibrations), 914 cm^{-1} (C-H out of plane bending), 662 cm^{-1} (ring torsion), 634 cm^{-1} (C=C-H and N=C-H wagging);

^{1}H-NMR ($\delta_{H,}$ ppm, DMSO-d): 7.49-6.62 (m, 3H), 3.24-2.78 (m, 1H), 1.96 (s, 2H)

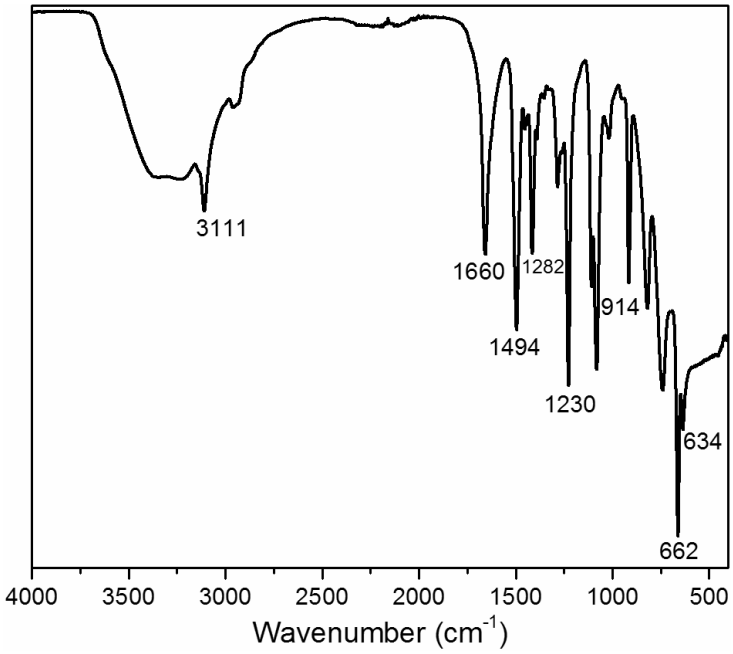

SI-Fig. 1 FT-IR spectra of poly(VIm).

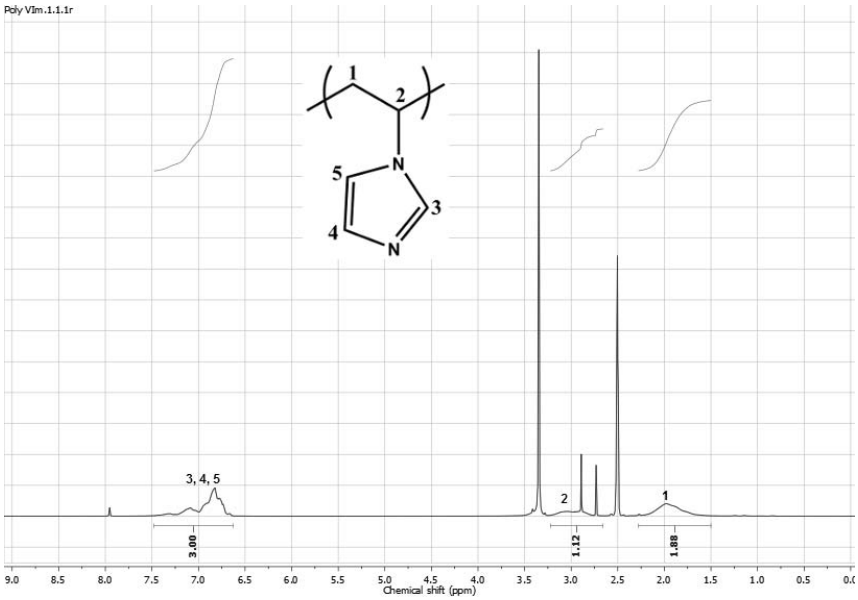

SI-Fig. 2 ^{1}H NMR spectrum of poly(Vim).

Preparation of poly(butyl acrylate)

Poly(butyl acrylate) was prepared in accordance with the general polymerization procedure, using AIBN (0.087 g, 0.53 mmol), butyl acrylate (5.12 g, 40 mmol) in DMF (10 mL). The product polymer was reclaimed as a transparent liquid with high viscosity after precipitation into DI water (yield more than 65 %, T_g= -47.4 ^{o}C).

IR (cm^{-1}): 3011-2827 cm^{-1}, 1451cm^{-1} and 1381cm^{-1} (-CH_2- symmetric and asymmetric stretching), 1727 $cm^{-1}$and 1154 cm^{-1} (stretching vibration C=O and C-O-C in acrylate group).

^{1}H-NMR ($\delta_{H,}$ ppm, $CDCl_3$): 3.96 (m, 2H), 2.39-1.44 (m, 3H), 1.56 (m, 2H), 1.31 (m, 2H) 0.87(m, 3H).

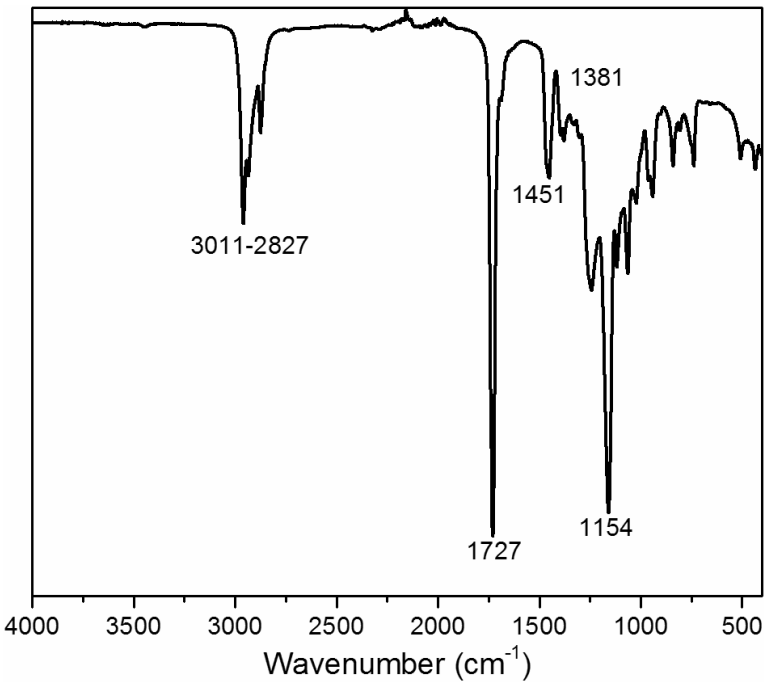

SI-Fig. 3 FT-IR spectra of poly(BuA).

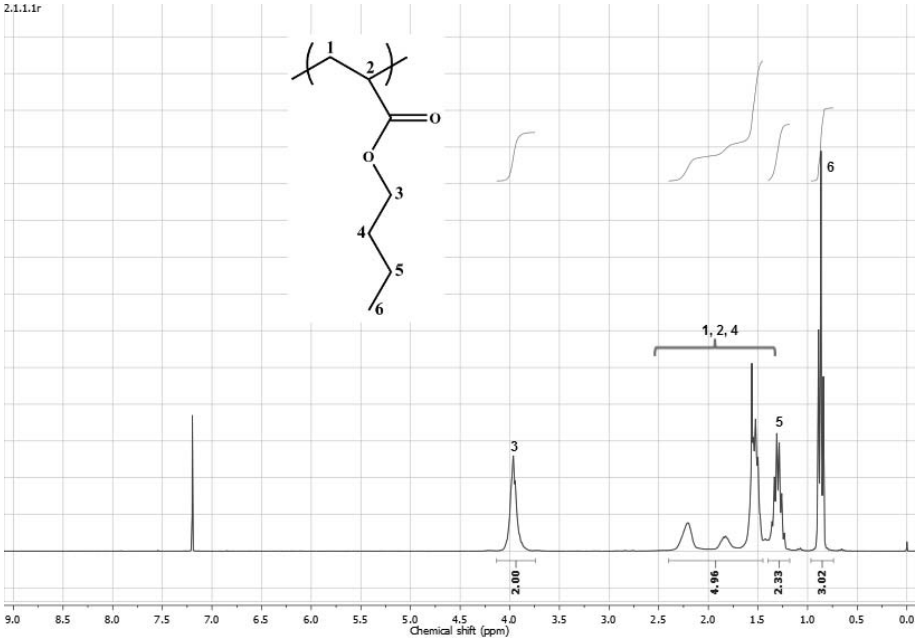

SI-Fig. 4 ^{1}H NMR spectrum of poly(BuA).

Preparation of poly(Vim-co-BuA) 63:37

Poly(Vim-co-BuA) 63:37 (70:30 in feed) was prepared in accordance with the general polymerization procedure, using AIBN (0.087 g, 0.53 mmol), Vinylimidazole (2.64 g, 28.1 mmol) and butyl acrylate (1.54 g, 12.0 mmol) in DMF (10 mL). The product polymer was reclaimed as a light yellow solid after precipitation into ether (yield more than 65 %, T_g= 26.9/151.3 ^{o}C).

IR(cm^{-1}): 3112cm^{-1} (C=C-H stretching), 3012-2800 cm^{-1}, 1455cm^{-1} (-CH_2- symmetric and asymmetric stretching), 1722 $cm^{-1}$and 1164 cm^{-1} (stretching vibration C=O and C-O-C in acrylate group). 1663 cm^{-1} (C=N stretching), 1494 cm^{-1} (N=C-H stretching), 1275 cm^{-1} and 1227cm^{-1} (ring vibrations), 912 cm^{-1} (C-H out of plane bending), 664 cm^{-1} (ring torsion), 636 cm^{-1} (C=C-H and N=C-H wagging);

^{1}H-NMR ($\delta_{H,}$ ppm, DMSO-d): 7.52-6.62 (m, 3H), 4.05-3.55 (m, 2H), 2.27-1.45(m, 6H), 1.45 (m, 2H), 1.24 (m, 2H) 0.87(m, 3H).

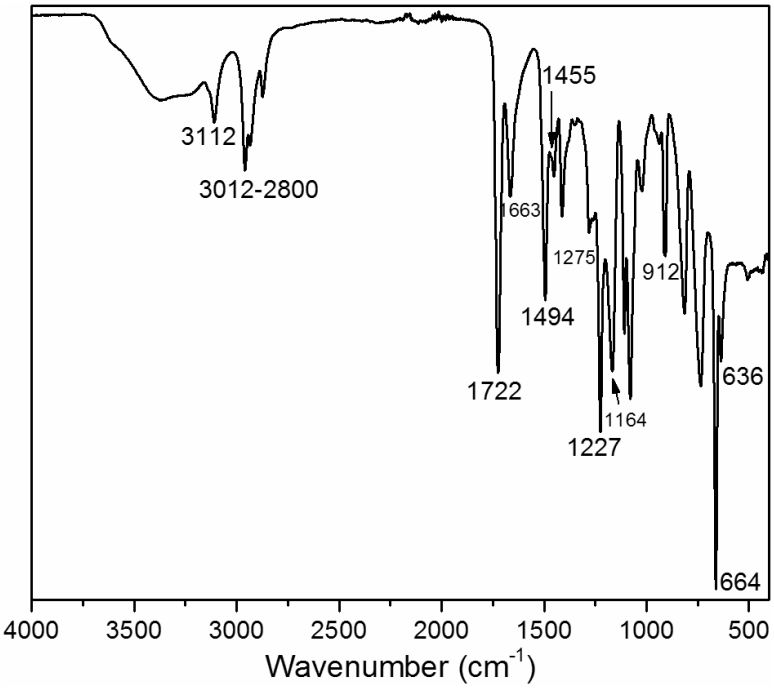

SI-Fig. 5 FT-IR spectrum of poly(Vim-co-BuA) (63:37).

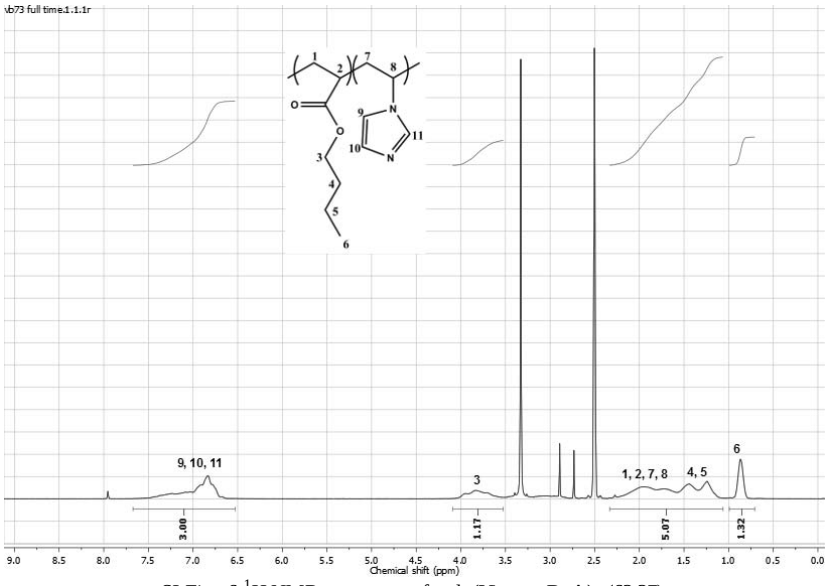

SI-Fig. 6 ^{1}H NMR spectrum of poly(Vim-co-BuA) (63:37).

Preparation of poly(Vim-co-BuA) 24:76

Poly(Vim-co-BuA) 24:76 (30:70 in feed)was prepared in accordance with the general polymerization procedure, using AIBN (0.87 g, 5.3 mmol), Vinylimidazole (11.4g, 121.1 mmol) and butyl acrylate (36.4 g, 284 mmol) in DMF (100 mL). The product polymer was reclaimed as a light yellow solid after precipitation into water (yield more than 65 %, Mn= 9092 g/mol, T_g= -6.6 ^{o}C).

IR (cm^{-1}): 3111cm^{-1} (C=C-H stretching), 3012-2844 cm^{-1}, 1451cm^{-1} (-CH_2- symmetric and asymmetric stretching), 1722 $cm^{-1}$and 1160 cm^{-1} (stretching vibration C=O and C-O-C in acrylate group), 1494 cm^{-1} (N=C-H stretching), 1267 cm^{-1} and 1223cm^{-1} (ring vibrations), 912 cm^{-1} (C-H out of plane bending), 664 cm^{-1} (ring torsion), 632 cm^{-1} (C=C-H and N=C-H wagging);

^{1}H-NMR ($\delta_{H,}$ ppm, $CDCl_3$): 7.4-6.4 (m, 3H), 3.96 (m, 2H), 2.35-1.62 (m, 6H), 1.52 (m, 2H), 1.27 (m, 2H) 0.86(m, 3H).

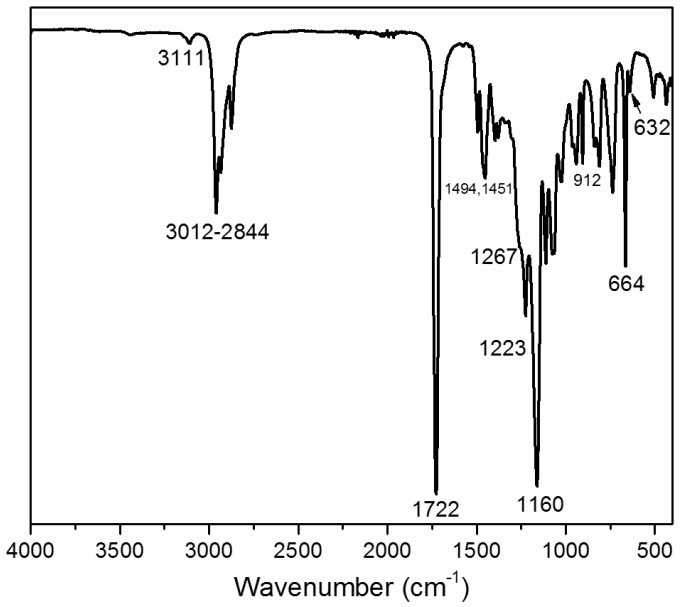

SI-Fig. 7 FT-IR spectrum of poly(Vim-co-BuA) (24:76).

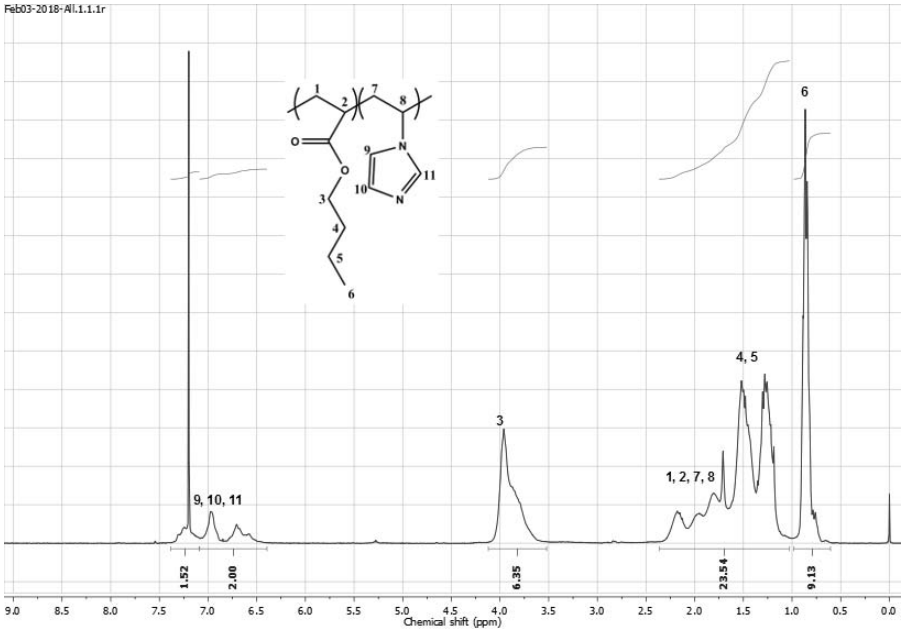

SI-Fig. 8 ^{1}H NMR spectrum of poly(Vim-co-BuA) (24:76).

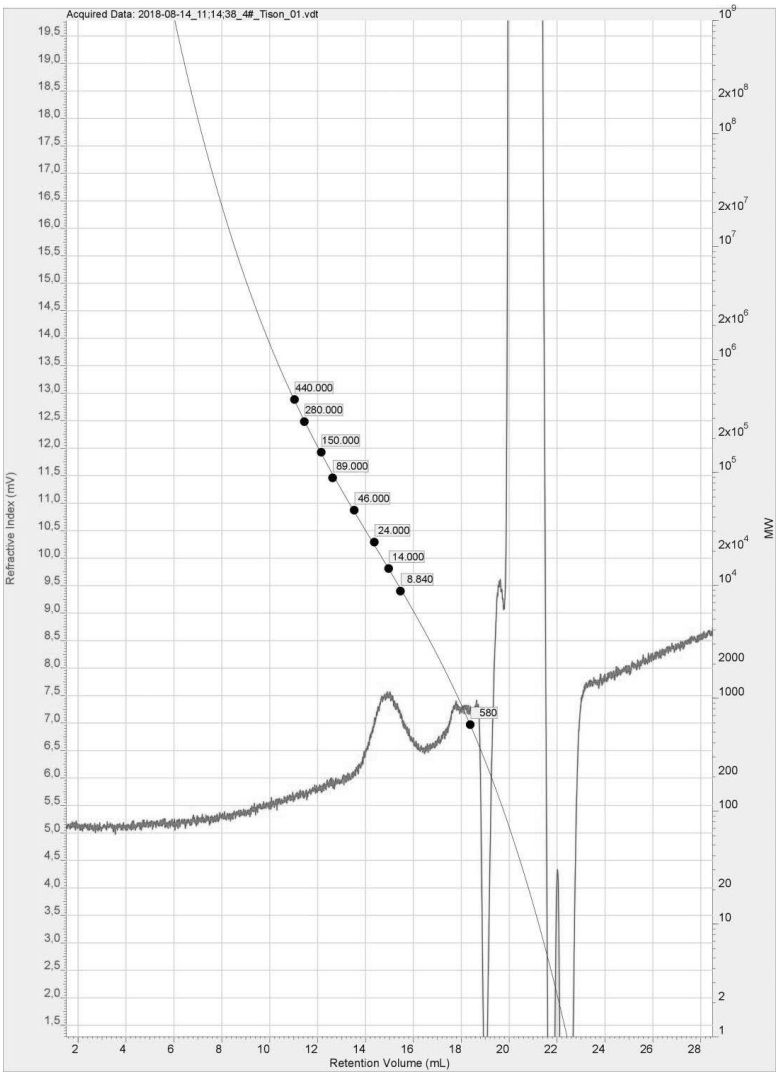

SI-Fig. 9 SEC of poly(Vim-co-BuA) (24:76)

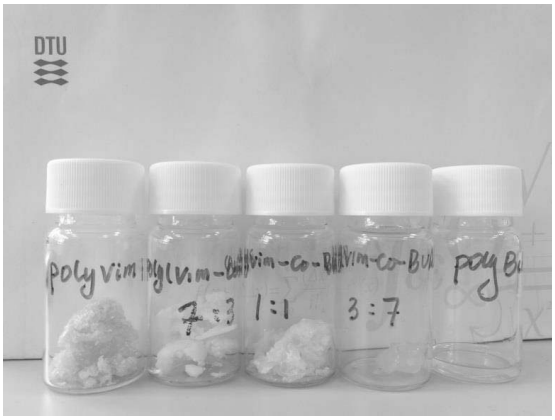

SI-Fig. 10 The appearance of the prepared polymers.

Preparation of 20 % cross linked 24:76 poly(Vim-co-BuA) membrane

The membrane was prepared in accordance with the general procedure using poly(VIm-co-BuA) (24:76, 1.5 g, 3.0 mmol functional group) was dissolved in ethanol (12 mL) by stirring overnight. Then, 1,6-dibromohexane (0.09 g, 0.37 mmol) and 1-bromobutane (0.42 g, 3.01 mmol) were introduced in and stirred for extra 1 h. The solution was degassed by ultrasonication for 10 min and casted in a Teflon petri dish after. The casting solution was allowed to evaporation at ambient conditions in a fume hood. To remove entrapped residues of solvent, the casted membrane was dried *in vacuo* at 65 °C for 6 h. Membrane thickness is 85.4 μm

Preparation of 50 % cross linked 24:76 poly(Vim-co-BuA) membrane

The membrane was prepared in accordance with the general procedure using poly(VIm-co-BuA) (24:76, 1.5 g, 3.0 mol functional group) was dissolved in ethanol (12 mL) by stirring overnight. Then, 1,6-dibromohexane (0.24 g, 0.98 mmol) and 1-bromobutane (0.26 g, 1.90 mol) were introduced in and stirred for extra 1 h. The solution was degassed by ultrasonication for 10 min and casted in a Teflon petri dish after. The casting solution was allowed to evaporation at ambient conditions in a fume hood. To remove entrapped residues of solvent, the casted membrane was dried *in vacuo* at 65 °C for 6 h. Membrane thickness is 100.9 μm.

Preparation of 100% cross linked 24:76 poly(Vim-co-BuA) membrane

The membrane was prepared in accordance with the general procedure using poly(VIm-co-BuA) (24:76, 1.5 g, 3.0 mmol functional group) was dissolved in ethanol (12 mL) by stirring overnight. Then, 1,6-dibromohexane (0.47 g, 1.92 mmol) was introduced in and stirred for extra 1 h. The solution was degassed by ultrasonication for 10 min and casted in a Teflon petri dish after. The casting solution was allowed to evaporation at ambient conditions in a fume hood. To remove entrapped residues of solvent, the casted membrane was dried *in vacuo* at 65 °C for 6 h. . Membrane thickness 94.2 µm.

DSC spectrum of polymers synthesized and membranes prepared

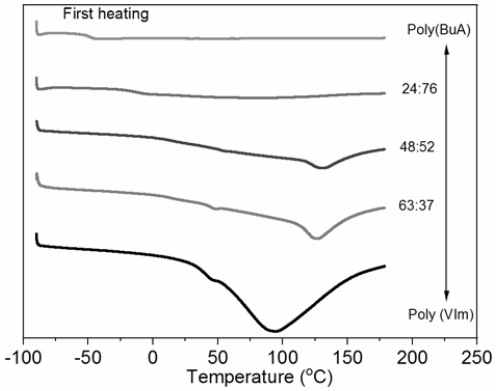

SI-Fig. 11 DSC thermograms showing first heating cycle of poly(VIm), poly(BuA) and copolymers with different ratio.

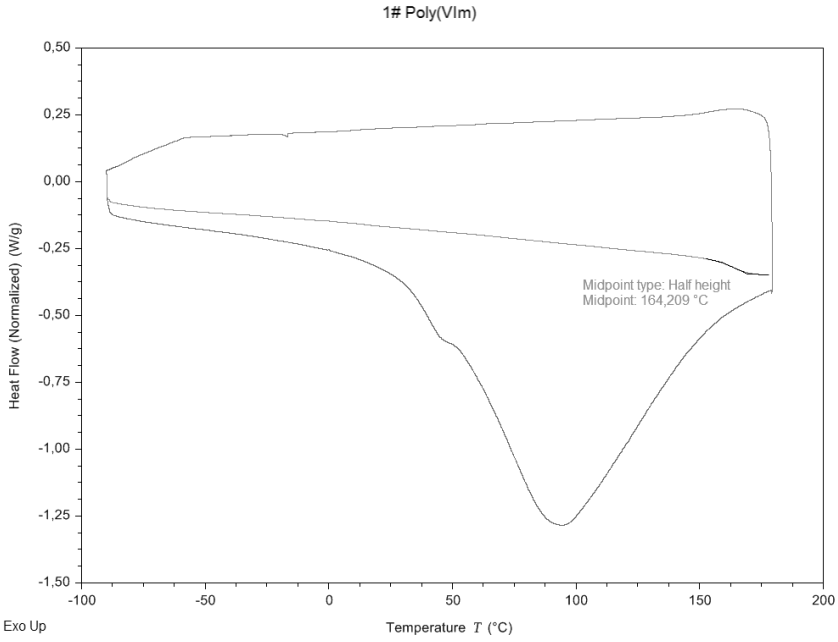

SI-Fig. 12 DSC of Poly(VIm).

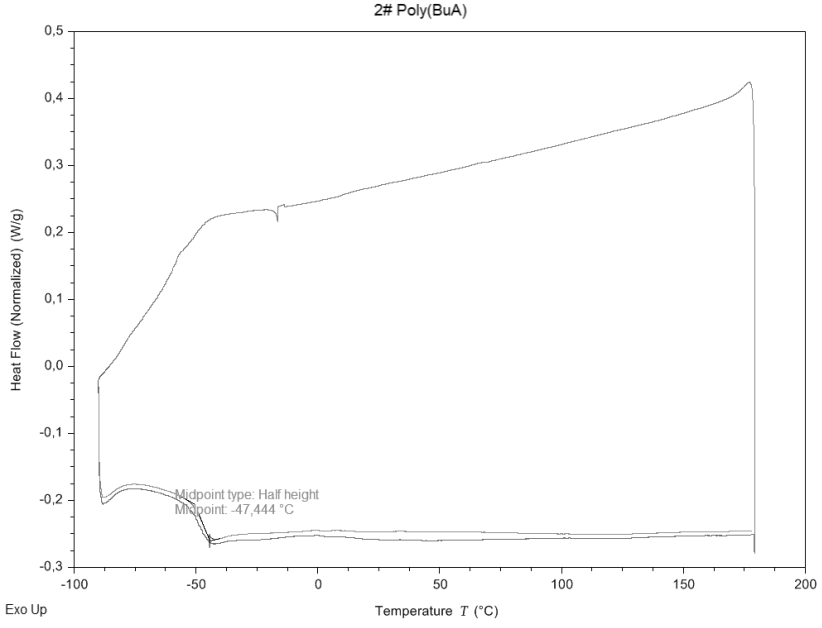

SI-Fig. 13 DSC of poly(BuA).

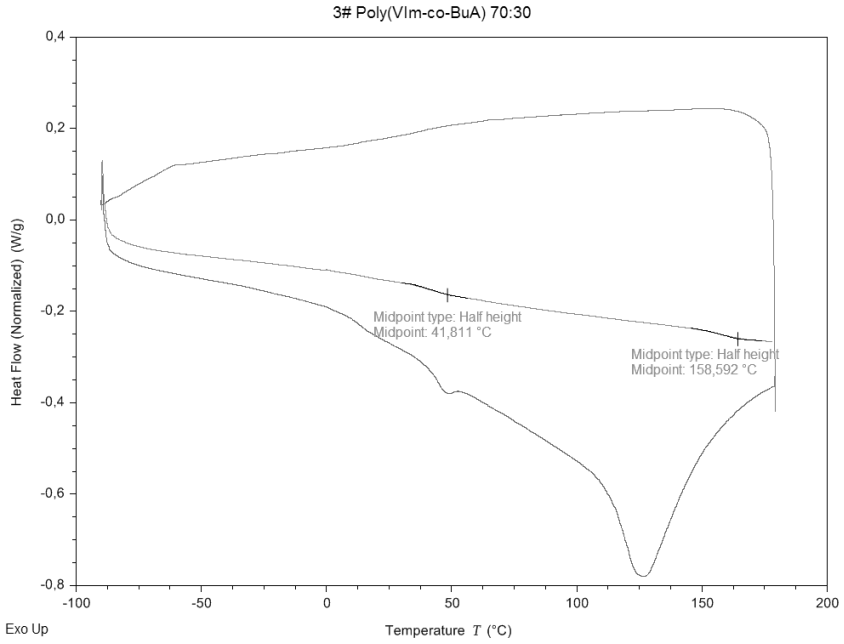

SI-Fig. 14 DSC of poly(VIm-co-BuA)(63:37).

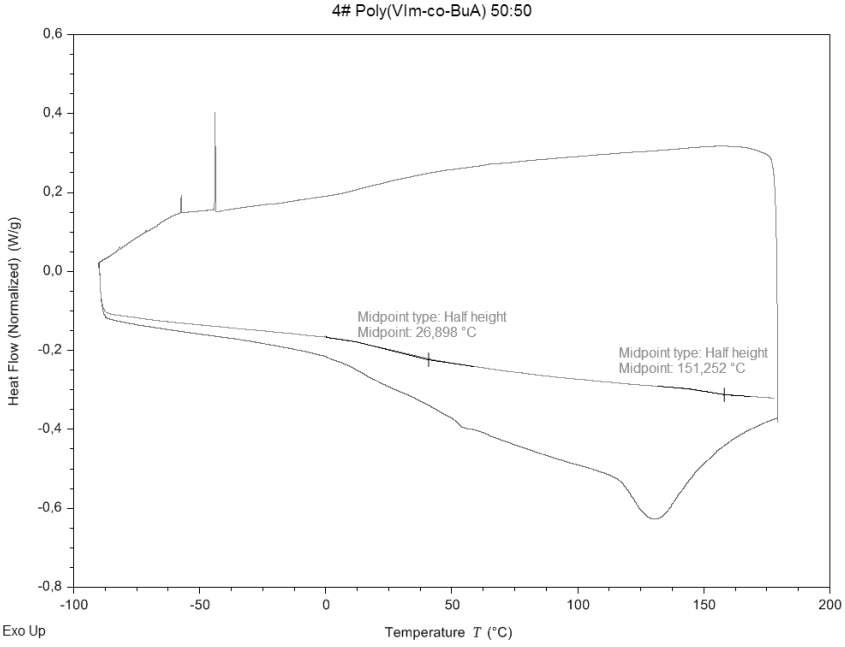

SI-Fig. 15 DSC of poly(VIm-co-BuA)(48:52).

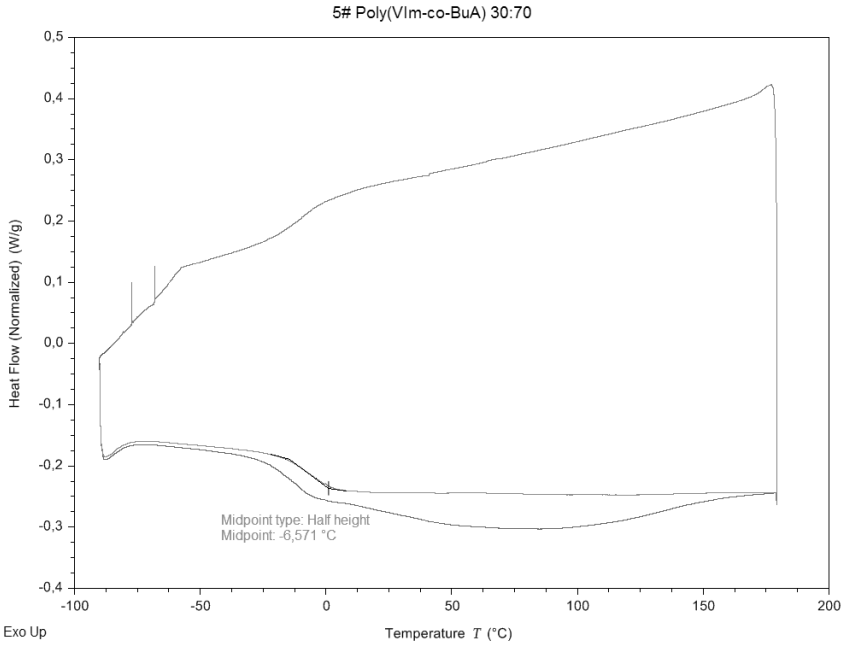

SI-Fig. 16 DSC of poly(VIm-co-BuA)(24:76).

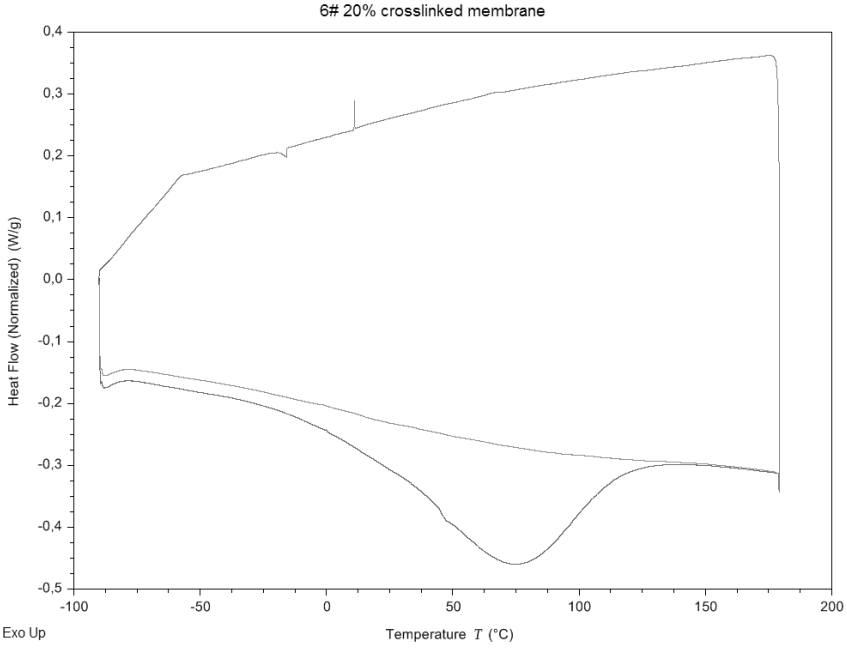

SI-Fig. 17 DSC of 20 % crosslinked membrane.

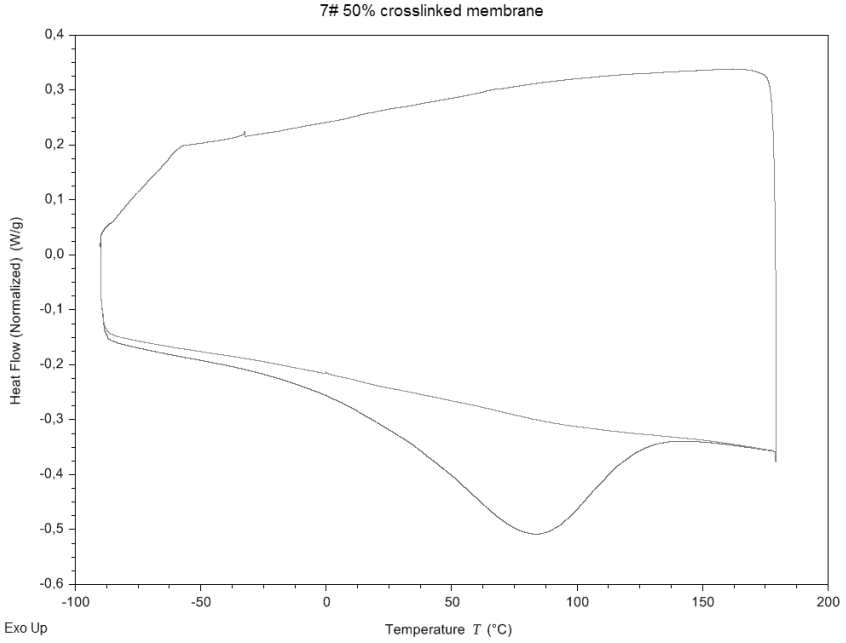

SI-Fig. 18 DSC of 50 % crosslinked membrane.

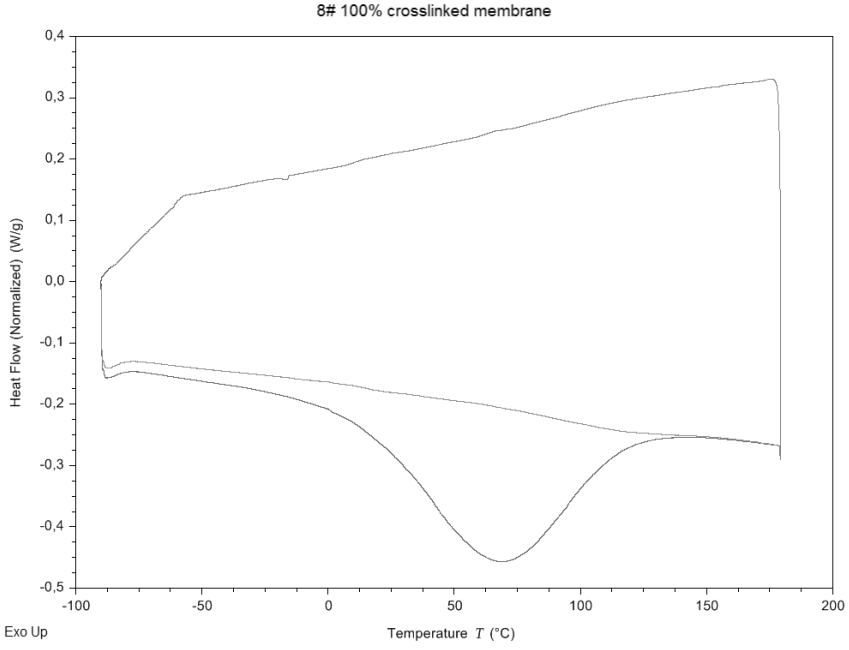

SI-Fig. 19 DSC of 100 % crosslinked membrane.

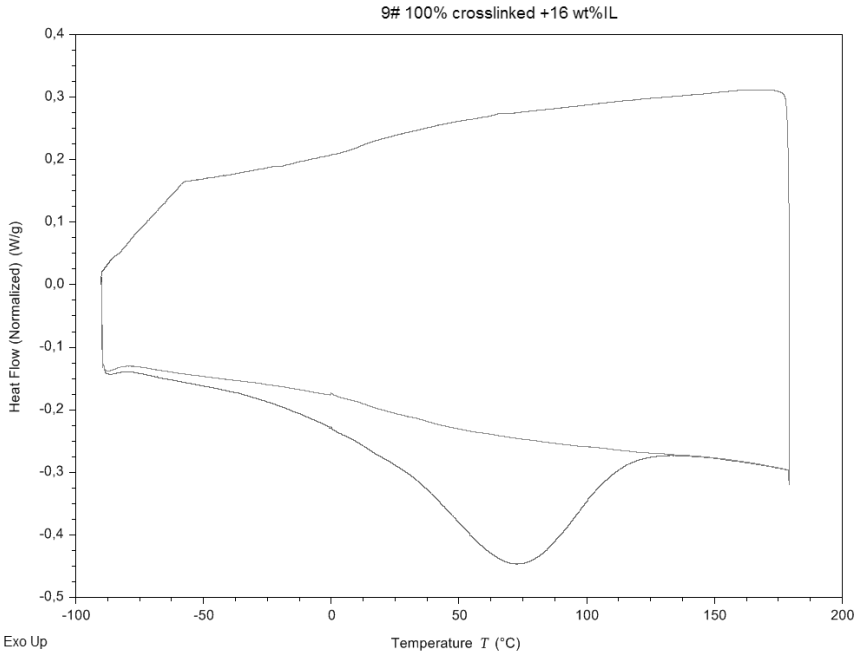

SI-Fig. 20 DSC of 100 % crosslinked membrane with 16 wt% free IL.

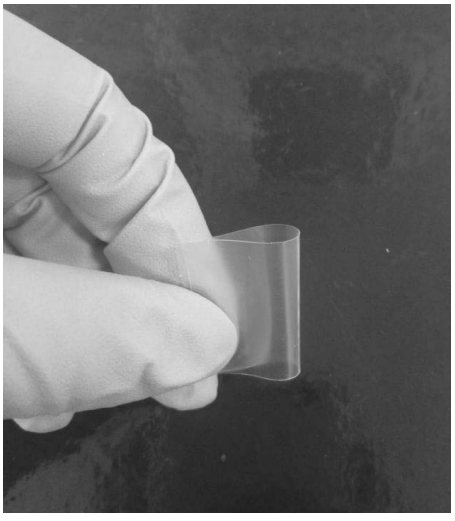

SI-Fig. 21 The appearance of 100 % crosslinked membrane.

TGA spectrum of polymers synthesized and membranes prepared

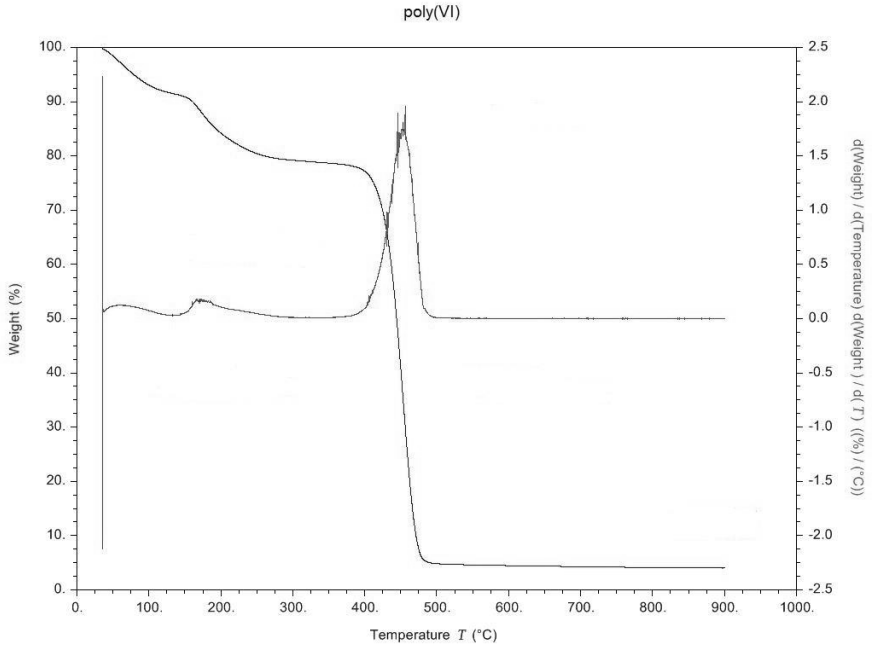

SI-Fig. 22 TGA of poly(VIm)

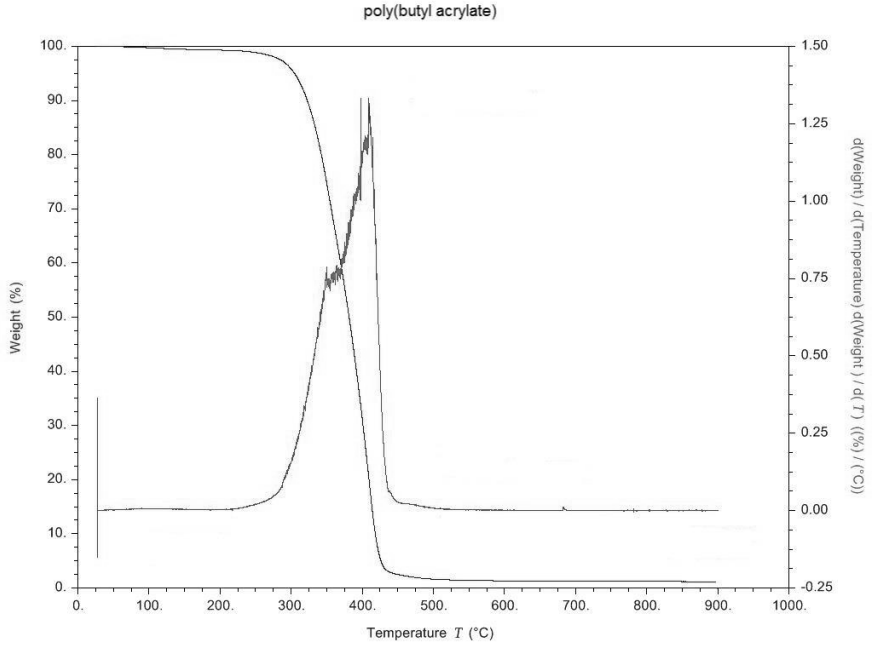

SI-Fig. 23 TGA of poly(BuA)

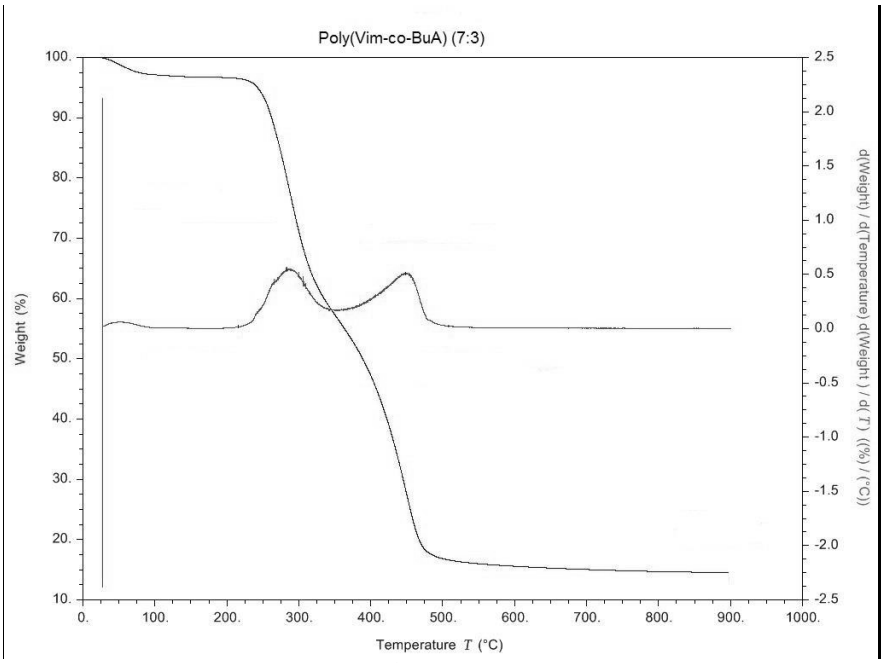

SI-Fig. 24 TGA of poly(VIm-co-BuA)(63:37).

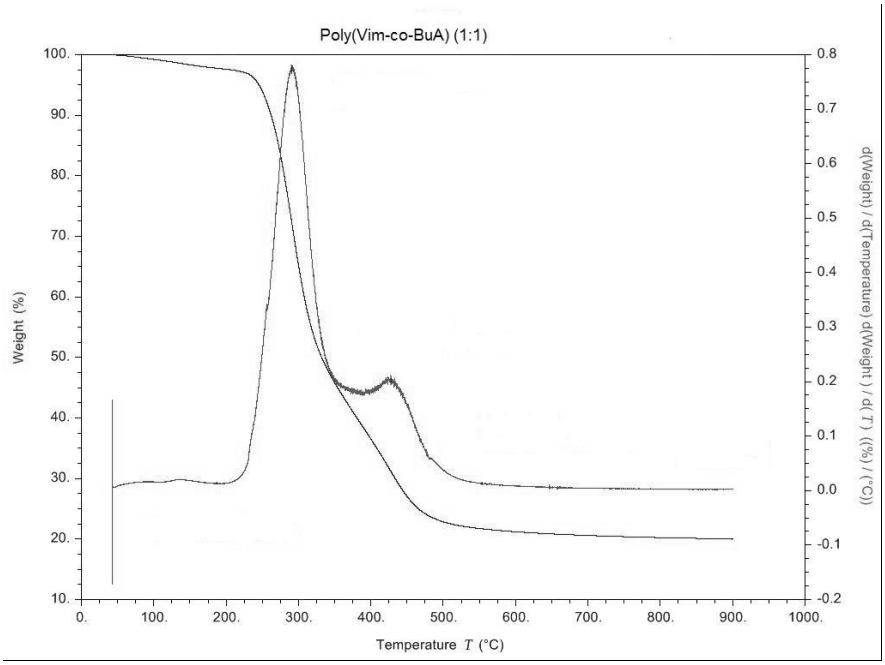

SI-Fig. 25 TGA of poly(VIm-co-BuA)(48:52).

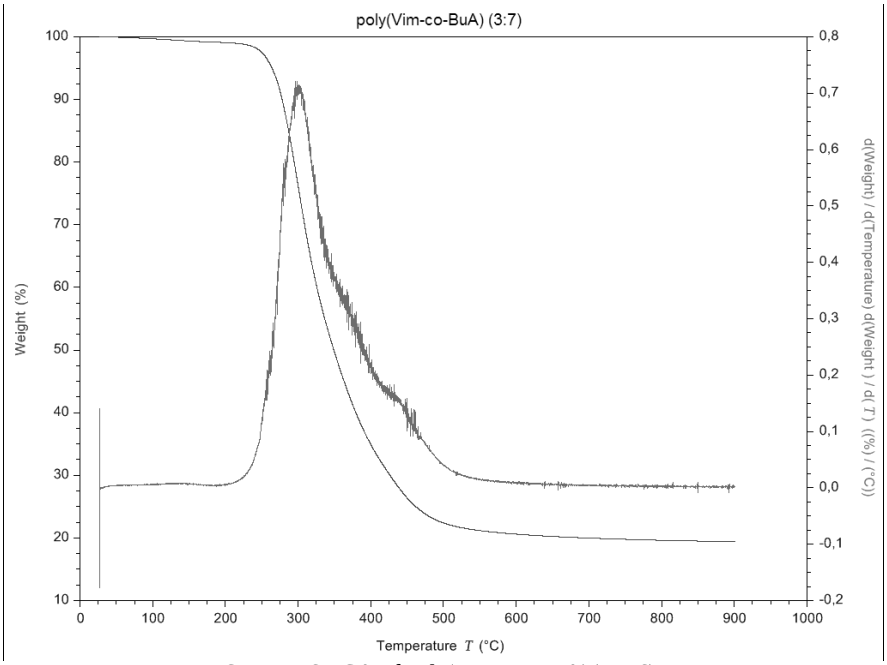

SI-Fig. 26 TGA of poly(VIm-co-BuA)(24:76).

Strain-stress curve of different membranes

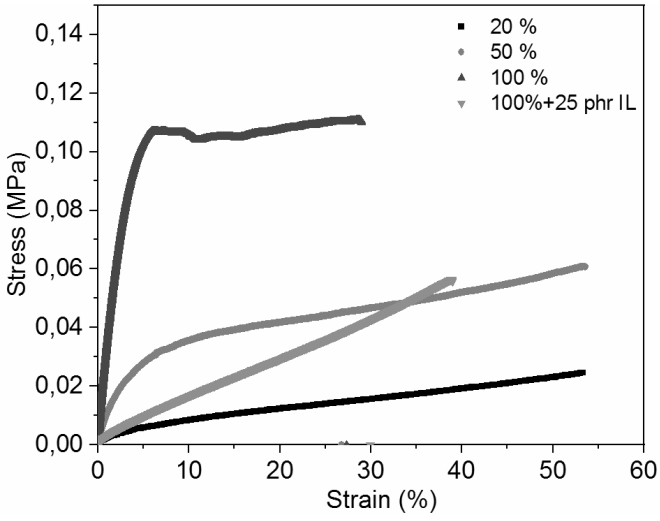

SI-Fig. 27 Strain-stress curve of different membranes.

Department of Chemical and Biochemical Engineering
Technical University of Denmark
Søltofts Plads, Building 229
DK - 2800 Kgs. Lyngby
Denmark

Phone: +45 45 25 28 00
Web: www.kt.dtu.dk/